



Norwegian University of
Science and Technology

Hydrogen Embrittlement of 25Cr duplex stainless steel exposed to well fluid with H₂S - effect of cold working and product form

Svein Ollestad

Materials Science and Engineering

Submission date: July 2017

Supervisor: Roy Johnsen, MTP

Norwegian University of Science and Technology
Department of Mechanical and Industrial Engineering

Hydrogen Embrittlement (HE)/Sulfide Stress Cracking
(SSC) of corrosion resistant alloys in H₂S environment -
the effect of product form and cold working

Svein Ollestad

July 8, 2017

Abstract

It is known that cold deformation may have detrimental effects on resistance against Sulphide Stress Cracking/Stress Corrosion Cracking and Hydrogen Induced Stress Cracking. Though it is clear that cold deformation should be restricted, it is sometimes necessary due to e.g. reeling installation or cold sizing. However, the most common standards relevant for pipe production and fabrication are not specific in how much cold deformation that can be allowed. NACE0175/ISO 15156 and ASME B31.3 allows maximum 5% cold deformation for carbon steel without subsequent heat treatment, but no limits are given for stainless steels (SS). NORSOK M-101 allows up to 10% cold deformation of austenitic stainless steel (SS) and 5% for duplex SS and Ni alloys, but as this is a standard for structural steel fabrication, this limit does not consider H₂S service.

Testing will be carried out on duplex SS and austenitic SS to get a better understanding of limitations on the amount of cold deformation these materials can have in a sour environment. 25% Cr duplex SS (wrought) and 22% Cr duplex SS (wrought) will be tested by constant load in NACE Solution A at an elevated temperature of 80°C and H₂S-partial pressure of 20kPa. As a base case the materials will be cold deformed to minimum 4.8% deformation before the start of constant load testing. The microstructure of the duplex materials will be examined in a Light Optic Microscope (LOM) before and after the initial deformation and before H₂S-exposure, to characterize the ferrite content and the austenite spacing in the materials. If any signs of cracking with the LOM, further investigation with a Scanning Electron Microscope will be done.

Preface and Acknowledgements

This thesis was written for a master's degree in Materials Science and Engineering with specialization in Material Development and Properties at The Norwegian University of Science and Technology in Trondheim (NTNU). The thesis was proposed by my co-supervisor at DNV-GL in Høvik, and has been carried out at DNV-GL's lab in Bergen. The work has been carried out with close cooperation from ATI Metals and OneSubsea, who have both contributed with financial support for materials as well as expenses for travel and accommodation.

I would like to thank my supervisor Professor Roy Johnsen at NTNU in the IPM department and my other co-supervisor, Erling Skavås from DNV-GL in Høvik.

In addition I would like to thank employees of DNV-GL's materials department in Bergen for their help and advice throughout the project. Lastly, thank you to Einar Strans, John J. Dunn and Njall Stefansson in ATI Metlas and Christopher Nwakwuo in OneSubsea.

Contents

1	Introduction	1
1.1	Background	1
1.2	Objective	2
2	Theoretical Background	3
2.1	Environmentally Assisted Cracking	3
2.1.1	Hydrogen Embrittlement	3
2.1.2	Stress Corrosion Cracking	3
2.1.3	Sulfide Stress Cracking	4
2.2	Corrosion Resistant Alloys	5
2.2.1	Martensitic Stainless Steels	5
2.2.2	Duplex Stainless Steels	6
2.2.3	Austenitic Stainless Steels	8
2.2.4	Ni-based alloys	8
2.3	Fracture Mechanics	9
2.3.1	Fracture Mechanics	9
2.3.2	Fractography	9
2.4	H ₂ S-Containing Corrosive Environments	10
2.4.1	Pipeline containing well fluid	10
2.5	Corrosion Kinetics in Cl ⁻ -H ₂ S-Environments	11
2.5.1	H ₂ S-Corrosion	11
2.5.2	Influence of H ₂ S on passivation	12
2.6	Influence of Environmental Conditions	13
2.6.1	pH	13
2.6.2	Temperature	13
2.6.3	Elemental Sulfur	14
2.7	Non-environmental parameters	14
2.7.1	Microstructure	14
2.7.2	Plastic Deformation	16
2.7.3	Hydrostatic Stress	16
2.8	Environmental Limits	16
2.8.1	Duplex Steels	16
2.8.2	Ni-Base Alloys	18

2.8.3	Martensitic Steels	19
2.9	Material Selection and Qualification	19
2.9.1	Laboratory Test Methods for SSC/SCC Resistance	19
2.9.2	Test Solution	21
3	Experimental Method	23
3.1	Material	23
3.1.1	Material data	23
3.1.2	Additional material deformation of Duplex SS	23
3.1.3	Machining	24
3.2	Pre-examination	24
3.2.1	Tensile test	24
3.2.2	Hardness Test	25
3.2.3	Pre examination of Duplex SS with LOM	25
3.3	Constant Load in H ₂ S	26
3.3.1	Experimental Setup and General Procedure	26
3.3.2	Test equipment	28
3.3.3	Assembled Test Equipment	30
3.3.4	Step 1: Test Solution	33
3.3.5	Step 2-3: Preparation and Installation of Tensile Test Rods	33
3.3.6	Step 4: Tensioning of Test Samples	33
3.3.7	Step 5: Assemble Equipment	34
3.3.8	Step 6-8:Filling with Test Solution and Purging	34
3.3.9	Step 9-10: Gas and Temperature Adjustments	34
3.3.10	Step 11: Monitoring	35
3.3.11	Step 12: Disconnection	35
3.4	Duplex SS: Revised Test Procedure	36
3.4.1	Initial Test-Procedure	36
3.4.2	Revised Test-Procedure	36
3.5	Post-examination	37
3.5.1	LOM	37
3.5.2	SEM	37
3.6	Safety Precautions	38
3.6.1	H ₂ S-gas	38
3.6.2	Concentrated NaOH	38
3.6.3	Handling of Nace solution A	39
3.6.4	High-pressure/temperature testing	39
4	Results	40
4.1	Pre-exposure tests	40
4.1.1	Tensile Test	40
4.1.2	Hardness Test	41
4.1.3	Duplex SS characterization in LOM	42

4.2	Constant Load in H ₂ S	50
4.3	Post-examination	51
4.3.1	Macroscope	52
4.3.2	LOM of cross sections	59
4.3.3	Sample K: 22Cr Duplex SS, 4.8% Deformation, 20%H ₂ S	59
4.3.4	Sample N: 25Cr Duplex SS, 10% Deformation, 20%H ₂ S	60
5	Discussion	62
5.1	Comparison with other test results	62
5.2	Experimental Parameters	62
5.2.1	Test Temperature	62
5.2.2	Deformation and Microstructure	62
5.2.3	H ₂ S-concentration	63
5.3	Experimental challenges	63
5.3.1	Loading of samples	63
5.3.2	NaOH contamination of test solution	64
5.4	Validity of results	64
6	Conclusion	65
	Bibliography	69
	Appendix	70
A	Risk analysis	70
B	Poster	74
C	Material Certificate - 22Cr	75
D	Material Certificate - 25Cr	79
E	Material Certificate - ATI830	83

Abbreviations

AYS	Actual Yield Strength
CRA	Corrosion Resistant Alloy
CW	Cold Work
DNV-GL	Det Norske Veritas Germanischer Lloyd
DCB	Double Cantilever Beam
DSS	Duplex Stainless Steel
EAC	Environmentally Assisted Cracking
FCC	Face Centered Cubic
HAZ	Heat Affected Zone
HE	Hydrogen Embrittlement
HEDE	Hydrogen Enhanced Decohesion
HELP	Hydrogen Enhanced Localized Plasticity
HIC	Hydrogen Induced Cracking
HIP	Hot Isostatic Pressing
HISC	Hydrogen Induced Stress Cracking
LEL	Lower Explosive Limit
LOM	Light Optic Microscopy
MSS	Martensitic Stainless Steel
NACE	National Association of Corrosion Engineers
NTNU	Norsk Teknisk Naturvitenskaplig Universitet / Norwegian University of Science and Technology
PREN	Pitting Resistance Equivalent Number
ROA	Reduction of Area
RT	Room Temperature
SMSS	Super Martensitic Stainless Steel
SS	Stainless Steel
SSRT	Slow Strain Rate Testing
SCC	Stress Corrosion Cracking
SDSS	Super Duplex Stainless Steel
SEM	Scanning Electron Microscopy
SSC	Sulfide Stress Corrosion
UTS	Ultimate Tensile Strength

Chapter 1

Introduction

1.1 Background

When exposed to an H₂S-environment, corrosion resistant alloys (CRA) may suffer from Hydrogen Embrittlement (HE) or Sulfide Stress Cracking (SSC). As a result of this NACE (the National Association of Corrosion Engineers) published the first edition of NACE MR0175 in 2001. This document gave guidance to which levels of H₂S partial pressure that requires further precautions against SSC. Today limitations for temperature, partial H₂S pressure, Chloride content and pH are given by ISO 15156 which gives requirements and recommendations for selection of a steel for use in an H₂S environment without suffering HE/SSC. These values are for extreme cases, and it is of high interest to acquire more information as other factors such as load, alloy composition, microstructure, product form and environmental conditions can influence the risk of failure.^{1,2}

Within the worldwide shelf little H₂S is found, but it is a common ingredient in oil- and gas reservoirs. However, with an increased demand for oil and gas, wells are becoming deeper and deeper. This poses a challenge as with increasing depths a higher presence of H₂S is found. A direct consequence of this is an increased demand for more knowledge of the environmental limits of current CRAs as well as further development of stronger H₂S-resistant alloys.^{3,4}

1.2 Objective

The main objective of this work is to :

- Establish a theoretical understanding of the mechanisms behind HE/SSC
- Perform a test program for examination of the resistance against HE and SSC for different forms of duplex stainless steels as well as a Ni-based alloy.

A thorough theoretical investigation shall look into the source of hydrogen and the mechanism of hydrogen development in a well fluid containing H_2S . The final test program is to be developed based on “state-of-the-art” knowledge of HE/SSC of corrosion resistant alloys, in addition to current limits set by governing standards. Included in the test program shall a full mechanical characterization be given, prior to the SSC test. This includes tensile test with material properties from stress/strain curve, hardness test and metallurgical inspection (α/γ -content and γ -spacing).

Chapter 2

Theoretical Background

2.1 Environmentally Assisted Cracking

A CRA may suffer several environmentally assisted cracking (EAC) modes. Hydrogen embrittlement (HE), stress corrosion cracking (SCC) and sulfide stress cracking (SSC) are some of the more important modes.⁵

2.1.1 Hydrogen Embrittlement

Hydrogen Embrittlement (HE) has been observed and reported as early as 1875 where the phenomenon was studied in iron and steel by William H. Johnson.⁶ A substantial amount of research has been done in later years as the need for strong corrosion resistant alloys has increased.⁷

An influx of Hydrogen into a metal may lead to loss of ductility, limit the materials toughness and accelerate the growth of a crack within the metal.⁸ This may lead to cases where the presence of hydrogen results in material failure at loads significantly lower compared to that a hydrogen-free metal would be able to sustain. In fact, failure may occur at stresses far lower than the Actual Yield Strength (AYS).^{9,10}

The general understanding of HE mechanism is migration of hydrogen towards internal stress centres such as a crack tip or a notch.¹¹ In addition, it is well known that a steels susceptibility towards suffering HE increases with increasing yield strength.^{8,11,12}

Despite extensive studies, a proper understanding of the mechanisms of HE still remains unclear. Several different models have evolved; Hydrogen-Enhanced Decohesion (HEDE) and Hydrogen-Enhanced Localization Plasticity (HELP) are the most predominant. Neither of these have been experimentally verified, but there are experiments that support the HELP-model.^{7,10}

2.1.2 Stress Corrosion Cracking

Stress Corrosion Cracking (SCC) is one of several types of environmentally assisted cracking modes, which has caused the oil and gas industry an annual cost of £1.37 Billion.¹³ This

is a process where combination of tensile stress and an anodic process of localized corrosion causes cracking. The corrosion process occurs when for instance a steel is exposed to a corrosive environment containing sour gas, hydrogen sulfide, carbon dioxide and free water. Higher presence of chlorides or oxidants as well as increased temperature leads to faster kinetics, thus increasing the likelihood of failure by this mechanism. SCC may occur below yield stress and fracture toughness, and will lead to rapid fracture when exceeded.^{1,13}

In addition to presence of corrosion environment and residual and/or applied stress, a susceptible material is required. Generally, the stronger the metal the higher susceptibility to SCC. Use of thicker steel with lower strength will reduce the risk of failure, but this is not necessarily the best option from an economic perspective.¹³

As SCC may occur under the surface, detection before a potentially catastrophic failure can be challenging. SCC failures has been reported as early in 1965, and several pipeline failures have been reported globally since, some leading to fatalities. The Trans Canada pipeline was exposed to six SCC-related failures in the period of 1985 to 1995, the latter resulting in a major explosion.^{13,14}

The electrochemical reactions involved in SCC are shown in equation 2.1-2.3.¹⁵



Which of the cathodic reactions (equation 2.2 and 2.3) that occur depend on local electrochemical conditions such as pH, concentration of oxygen and potential.¹⁵

2.1.3 Sulfide Stress Cracking

Sulfide Stress Cracking may occur in an aqueous H₂S-environment, and is closely related to the materials HE-susceptibility. As SSC is a form of HE, tensile stress and a susceptible material is required. In addition, a corrosion reaction needs to occur, as this is a process that requires available hydrogen. Generally, it is expected that for a steel in this environment, a protective iron sulfide (FeS) layer will form and adhere to the metal surface, as described by equation 2.9.¹⁶⁻¹⁸

This layer will normally protect against further corrosion, but it does not prevent hydrogen to migrate to interstitial positions in the matrix, especially within plastic regions such as crack tips.¹⁶ Unless the material is fully protected against corrosion, some hydrogen will be developed, which may pose a risk. It is also well known that harder microstructures such as non- or low-tempered martensite and bainite are more susceptible to suffer HE-related fractures. Unwanted harder structures may arise from poor heat treatment procedures or within the heat affected zone of welds.¹⁹

According to Kane¹⁸ the effects of H₂S-corrosion can be divided in two key consequences; Increased corrosion rate and limitation of hydrogen recombination (thus increased hydrogen

absorption). The combination of these two effects is an increase in hydrogen charging compared to a similar environment without H₂S.¹⁸ The corrosion reaction and kinetics related to this is discussed further in section 2.5.1

Testing of SSC susceptibility of different materials have shown that even extremely low concentrations of H₂S may be sufficient to cause SSC failure.¹⁸ It is therefore vital that good knowledge of a materials susceptibility is obtained before chosen as a component in a H₂S-environment.

2.2 Corrosion Resistant Alloys

A CRA is an alloy that has been manufactured and chosen for an environment where extra strong resistance towards a corrosion environment is required, in addition to the need of high material strength. Use of a CRA may also eliminate the use of corrosion inhibitors. Four main categories of CRAs can be distinguished:^{5,18}

- Martensitic stainless steels (MSS)
- Duplex stainless steels (DSS)
- Austenitic stainless steels
- Ni-based alloys

An important application for CRAs have been in production of gas containing hydrogen sulfide (H₂S), also known as “sour gas”. In a production tubing, proof stress (yield strength that gives 0.2% plastic strain) requirements can range from 550MPa to over 1100MPa for shallow and very deep and high-pressurized wells, respectively.⁵

Some of the more common CRAs used in oil and gas industry have been listed in table 2.1.¹⁷

2.2.1 Martensitic Stainless Steels

MSS is produced by quenching the alloy from the austenitic phase, producing a martensitic structure. C and Ni is used to stabilize the austenite phase, and Cr, typically 13%, is added for corrosion protection. Further alloying with 1-3% Mo will increase the resistance against H₂S. Minimum yield strength of a MSS is 550MPa and it has a surface hardness of about 280HV10, though some higher HV-values may be found at welds. The term Super Martensitic Stainless Steels (SMSS) is also used when the alloy has an extra low carbon content, typically around 0.01%. Compared to MSS, SMSS show excellent welding abilities and increased corrosion resistance.^{3,5,20}

2.2.1.1 Corrosion Properties

Pipelines produced with MSS are vulnerable to hydrogen embrittlement mechanisms such as sulfide stress cracking when exposed to a H₂S-containing environment. Some types of MSS has also had 4-6% Ni 1.5-2 Mo added for extra resistance to localized corrosion.

Table 2.1: Some typical CRAs used for production tubing in a oil/gas wells¹⁷

Alloy Group / name	UNS no.	Composition (wt%)					
		Fe	Cr	Ni	Mo	C	Other
Ni-based (γ), <i>CW</i>							
28*	N08028	Bal.	27	31	3.5	0.02	1.0Cu, Ti
825	N08825	Bal.	22	42	3.0	0.03	2.0Cu, 1.0Ti
Ni-based (γ), <i>PH</i>							
Alloy 925*	N09925	32	22	42	3.0	0.02	2.Cu, 2Ti, Al
718*	N07718	19	19	52	3.0	0.02	5Nb, Ti, Al
Duplex SS ($\alpha + \gamma$), <i>CW</i>							
22Cr	S31803	Bal	22	5.5	3.0	0.02	0.14N
25Cr*	S31260	Bal	25	7.0	3.0	0.02	0.5Cu, 0.2W, 0.18N
Martensitic SS							
AISI 410 SS	S41000	Bal	13	-	-	0.15	-
13Cr*	S42000	Bal	13	-	-	0.20	-

* These CRAs have been developed/modified for use in oil and gas wells.

α = ferrite, γ = austenite, CW = cold work strengthening, PH = precipitation hardening.

MSS has a maximum susceptibility to SSC around room temperature. However, resistance to SSC is also dependent on pH, H₂S and Cl⁻. Figure 2.1 illustrates the relationship between temperature and partial H₂S pressure for when a MSS is susceptible to SSC (sour service).^{3,18}

2.2.2 Duplex Stainless Steels

Duplex stainless steels were first developed in the 1940s and 1950s. Due to difficulties with fabrication of this complex microstructure as well as challenges with post-weld precipitation of brittle phases. Use has been limited until recent years, but currently DSS have been found useful in topside and subsea equipment in the oil and gas industry.²¹

Duplex stainless steels are obtained by adding elements that expands the ($\gamma+\alpha$)-phase, producing austenite (γ) islands within a ferritic (α) matrix. This is done using a correct balance of α -formers (Cr, Mo, Ti, Nb, Si, Al) and γ -formers (Ni, Mn, C and N).^{22,23}

The result of this is a steel with a strength potentially twice as strong as ordinary austenitic steels. One of the reasons for this is the grain refinement achieved by the duplex phase structure, which can be further refined by application of a thermomechanical treatment around 900°C to 1000°C. With this treatment a very fine microduplex structure may be achieved, resulting in super-plasticity, that is, very high ductility at extra high tem-

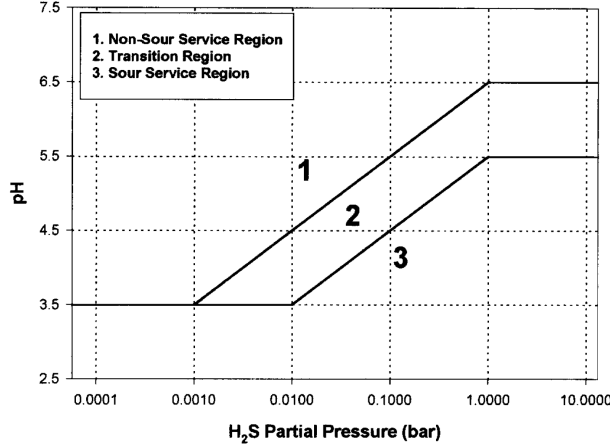


Figure 2.1: Relationship between pH and H₂S-content on sour service of a general MSS or CS.¹⁸

peratures. The result of this is a structure that has a superior corrosion resistance compared to MSS in brine environments containing H₂S and CO₂ gas.^{18,22,23}

2.2.2.1 Corrosion Properties

The ferrite structure in DSS grants a much stronger resistance against transgranular stress corrosion cracking than ordinary austenitic steels, as ferrite is immune to this type of failure. DSS is also considered to be resistant to solidification cracking, particularly with respect to welding.^{22,23}

To quantify the ability of a DSS to withstand from pitting corrosion in a Cl⁻ solution, a PREN-value (Pitting Resistance Equivalent Number) can be obtained. This value is also applicable to a Cl⁻-H₂S-environment. A DSS should have a value over 32, and if the PREN-value is over 40 the steel is denoted as a Super-Duplex Stainless Steel (SDSS). Calculation of PREN-value⁵ is given by equation 2.4. For each listed element in the equation the wt% is used in the calculation. It is worth noting that even though a higher PREN-value provides a higher corrosion resistance, it also leads to an increased risk of detrimental sigma and alpha-prime phases.²² Presence of these phases may lead to loss of impact toughness and decrease risk of cracking resistance. These phases may evolve during the manufacturing process or welding, and are best avoided by increasing the cooling rate.^{2,5,22,23}

$$PREN = Cr + 3.3(Mo + 0.5W) + 16N \quad (2.4)$$

Within a H₂S and CO₂ environment DSS may risk EAC in both high and low temperatures, as the ferritic and austenitic phases show different properties. At lower temperatures, cracking is found in the ferrite phase as a result of typical HE, whereas at higher temperatures the anodic SCC is the more detrimental mechanism.¹⁷ These two factors combined is the result of a maximum susceptibility towards H₂S-related fracture at a temperature area of 60 to 120°C, depending on alloy type and other environmental parameters.^{5,17}

2.2.3 Austenitic Stainless Steels

Austenitic stainless steels typically hold a high level of Ni, Cr, Mo and N, and hold a stable austenitic structure even after strong deformation.¹⁸

2.2.3.1 Corrosion Resistance

Due to a high level of Cr and Mo, this alloy group has an exceptionally good corrosion resistance in an H₂S-brine environment, both against general and localized (pitting) corrosion.¹⁸ The addition of N strengthens the pitting resistance further, however this effect appears to be not as strong in a H₂S-holding environment compared to e.g. oxygen holding seawater.¹⁸

2.2.4 Ni-based alloys

This group can be subdivided into two groups; Cold worked and precipitation hardened alloys. Both alloy categories, which typically only hold 5-15% Fe, show very good properties against SSC and corrosion due to their high amount of Ni, Cr and Mo alloy elements. According to ISO-15156:3,² alloys containing $\geq 30\%$ Ni and $\geq 3\%$ Mo are considered Ni-based.

Cold worked Ni-based alloys can for non-complex structures such as tubes be cold worked to strength levels over 1000MPa. Due to their treatment, cold worked alloys may have a more elongated microstructure, which may show as a variable in some tests. The austenitic structure can be strengthened by precipitation of gamma prime (Ni₃(Ti, Al)) and gamma double prime (Ni₃Nb)

For more complex geometries precipitation hardening alloys is a good alternative. This group is alloyed with Ti and Al, which increases the yield strength by formation of nitrides. These act as crack arrestors, thus strengthening the material.^{5,17,18}

2.2.4.1 Corrosion Resistance

These alloys may show SCC-failure at temperatures greater than 150°C, but failure often requires presence of a severe environment containing very high levels of H₂S.¹⁸

Due to the excellent corrosion resistance most Ni-based CRA's are found in wells with significant H₂S, typically over 10%. For these alloys higher Ni usually means SCC resistance at higher partial H₂S pressures or temperatures. Resistance against SCC also decreases with lower pH and higher salinity. To illustrate the SCC resistance of a Ni based alloy Rhodes suggests the parameter Σ , as shown in equation 2.5. This is only valid for alloys with Mo content ≥ 2.5 .⁵

$$\Sigma = Ni + 2Mo + 0.5Cr \quad (2.5)$$

2.3 Fracture Mechanics

2.3.1 Fracture Mechanics

Two fracture modes can happen in a metal; brittle and ductile fracture. A brittle fracture occurs by rapid crack propagation and shows no visible deformation on a macroscopic scale. Crack propagation will in most brittle crystalline materials occur as a transgranular fracture, also known as cleavage fracture. Cleavage fracture occurs by breaking of atom bonds along a specific crystallographic plane, propagating through the grain. In certain cases, especially where grain boundaries have been weakened, intergranular fracture may occur. In this case, the fracture path propagate in-between the grain boundaries. Weakening of boundaries may be a result of precipitation of brittle phases, hydrogen embrittlement and intergranular corrosion. Figure 2.3 shows an example of a brittle fracture surface of a steel.^{24,25}



Figure 2.2: Ductile Cup-and-cone fracture of an aluminium specimen.²⁴



Figure 2.3: Brittle fracture surface of a mild steel.²⁴

The ductile fracture mode is followed by extensive macroscopic plastic deformation. A tensile ductile fracture will usually include plastic deformation until a region of necking occurs. This will result in a cup-and-cone fracture, whose name is a result of the fracture surfaces forming mating surfaces similar to a cup and a cone. After necking occurs small microvoids will form within the sample. With continued deforming tensile stress these microvoids grow together to form an elliptical crack. The crack will continue to grow perpendicular to the load axis until rapid crack propagation around the outer part of the neck occurs. The crack propagates along shear planes at roughly 45° , which is the angle of maximum shear stress. A ductile cup-and-cone fracture surface is shown in figure 2.2, and the process is illustrated in figure 2.4.^{24,25}

2.3.2 Fractography

For detailed information of the fracture mechanism, microscopic examination by either scanning electron microscopy (SEM) or light optic microscopy (LOM) can be used. SEM is often

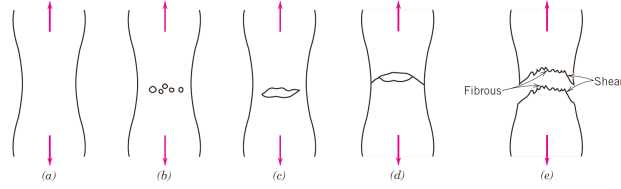


Figure 2.4: Illustration of the different stages in a ductile cup-and-cone fracture.²⁴

preferred as it has a much better resolution and depth of field, which are both needed to investigate a surface with larger topographic features. Investigation of a ductile fracture surface in SEM, as shown in figure 2.5, will illustrate the spherical dimples, which is a characteristic of a ductile fracture from a tensile stress load. A transgranular and intergranular fracture are shown in figure 2.6 and figure 2.7, respectively.²⁴

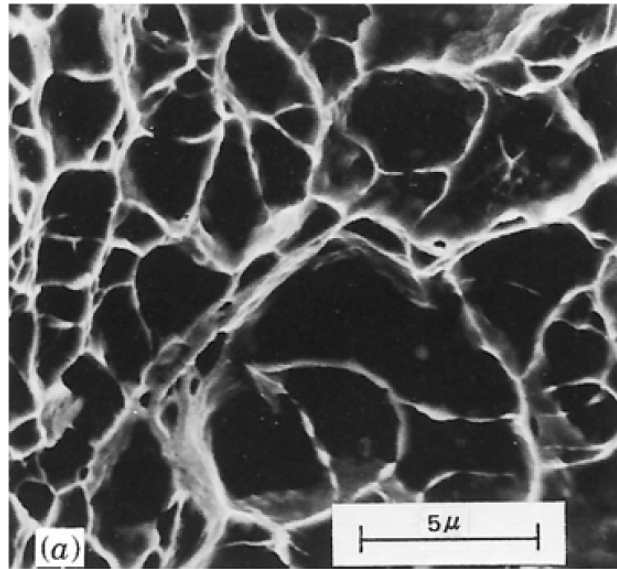


Figure 2.5: SEM photo showing the characteristic spherical dimples of a ductile fracture surface. Magnification 3300X.²⁴

In SSC Fractography low alloy steels may show both intergranular and transgranular fracture, but for high-strength steels with over 700MPa YS it appears that intergranular cracking is the most predominant mechanism.

2.4 H₂S-Containing Corrosive Environments

2.4.1 Pipeline containing well fluid

A unprocessed oil and gas mixture may pose a challenge with regards of detrimental effects as it can contain water, sand, CO₂, H₂S in addition to hydrocarbons (in the form of oil,

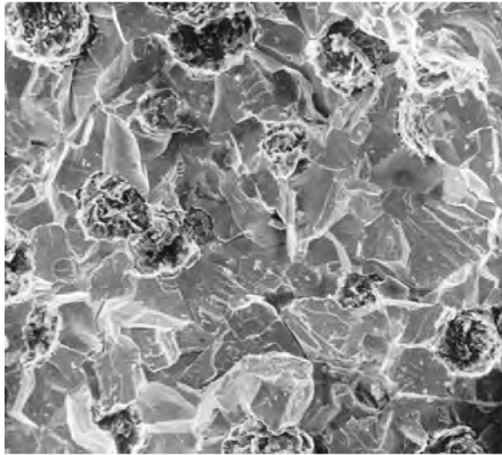


Figure 2.6: SEM of a transgranular brittle fracture. Magnification unknown.²⁴



Figure 2.7: SEM of a intergranular fracture surface. Magnification 50X.²⁴

condensate and gas). The water in the mixture contains a high amount of ions, such as chloride, sodium and calcium. This water, originated from the reservoir has been denoted formation water, whereas water that condenses within the pipeline wall due to cooling of surrounding seawater is denoted condensed water.³

Above 200°C challenges may arise as the hydro carbons may contain naphthenic acids (NAs), which can be corrosive.³ Under this temperature the corrosive risk is due to wetting of the pipe wall, that is, contact between pipewall and a corrosive water film. Some environmental factors that contribute to this mechanism are pH, temperature, chloride content, dissolved CO₂ and H₂S and flow rate. In a typical unprocessed oil and gas mixture pH values are typically calculated to be in the ranges 3.5-4 and 4.5-6 for condensed water and formation water, respectively.³

2.5 Corrosion Kinetics in Cl⁻-H₂S-Environments

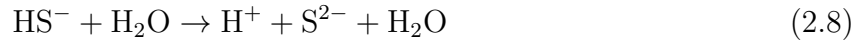
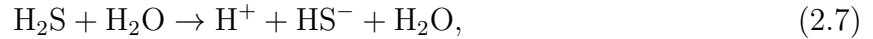
2.5.1 H₂S-Corrosion

The general corrosion reaction of Fe in a H₂S-environment under anaerobic conditions is given by the following reactions:¹⁸

anodic:



cathodic:



net reactions:



where H° is atomic hydrogen, adsorbed on the metal surface.

Depending on environmental conditions such as pH and partial H_2S -pressure, the iron sulfide products may be found in other forms such as FeS_2 . The hydrogen produced in reaction 2.9 is atomic state, and will adsorb to the metal surface at local cathodic sites. The majority of the produced hydrogen will recombine to form molecular hydrogen-gas, and evaporate. Some hydrogen can however be absorbed into the metal and accumulate at interstitial positions and defects in the lattice.

The presence of dissolved H_2S greatly affects the kinetics of hydrogen gas formation, by limiting the amount molecular hydrogen gas that is formed. This leads to an increase in the amount of absorbed hydrogen in the metal. Elements with this effect are termed "hydrogen recombination poisons", and include in addition to sulfur elements such as Sn, Pb, Sb and P. A measurement of the relative amount of hydrogen being absorbed is defined by α , the hydrogen charging efficiency coefficient:¹⁸

$$\alpha = H_A/H_p \quad (2.10)$$

Where H_A and H_p is the amount of absorbed and (corrosion-)produced atomic hydrogen, respectively.

2.5.2 Influence of H_2S on passivation

The main purpose of the Cr-content in a steel is formation of a protective Cr-oxide, however presence of H_2S limits the growth of the oxide layer by adsorption of atomic sulfide, S_{ads} as well as production of sulfides at the metal surface. For a Cr-Ni-Fe alloy, the Cr will react with OH^- to form chromium oxide, whereas Ni together with sulfide produce small Ni-sulfide islands. The metallic-sulfides have strong bonds and will together with the adsorbed atomic sulfide block sites from formation of the passivating Cr-oxide layer. The passivation layer may grow in-between these sites, but will require longer time to grow laterally.^{3,26} This competitive mechanism, suggested by P. Marcus,²⁶ is illustrated in figure 2.8.

Two modes of passivity loss can occur. Either cathodic activation or anodically initiated localized corrosion. The cathodic activation can occur if a sufficient acidic solution is present such that active corrosion can be sustained. An increase in corrosion increases the risk of loss of passivity. High corrosion motivates for higher alloy content as given by the PREN-formula 2.4, which is why SDSS shows a much better resistance than DSS.⁵

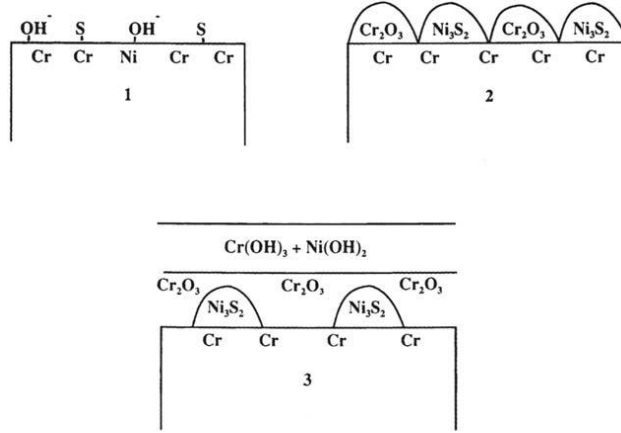


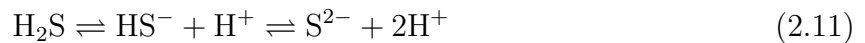
Figure 2.8: Illustration of the "competition" between formation of Cr-oxides and Ni-sulfides on the surface of a Ni-Cr-Fe-alloy.²⁶

2.6 Influence of Environmental Conditions

2.6.1 pH

There is a consensus between studies that an increase of pH leads to a reduction of susceptibility towards SSC and SCC. When pH is sufficiently low the passivity layer can be altered, thus making cracking possible when chlorides are present. Some cracking threshold limits have been proposed, but these depend on chloride content.^{5,18,21}

Depending on pH, the equilibrium reaction (equation 2.11) of H₂S shifts, as shown in figure 2.9.²⁷ This shows how predominant dissolved H₂S is at pH values below 4. As described earlier, H₂S considerably increases the general corrosion of steels, accompanied by hydrogen adsorption.



2.6.2 Temperature

MSS and DSS are most susceptible to SSC around room temperature.¹⁸ According to TM0177 test temperatures above 24°C will reduce the SSC severity in steels, whereas temperatures below will increase the SSC susceptibility of the steel.

For higher temperatures, SCC is the dominating factor, as higher temperature increases the corrosion kinetics of the localized anodic corrosion.^{28,29} Figure 2.10 shows the relationship between time to SSC failure against temperature for a low alloy C-Mn steel.

The combination of SSC and SCC results in a worst-case scenario at intermediate temperatures for DSS. For duplex steels research have shown highest cracking susceptibility around 80-120°C.^{18,29,30}

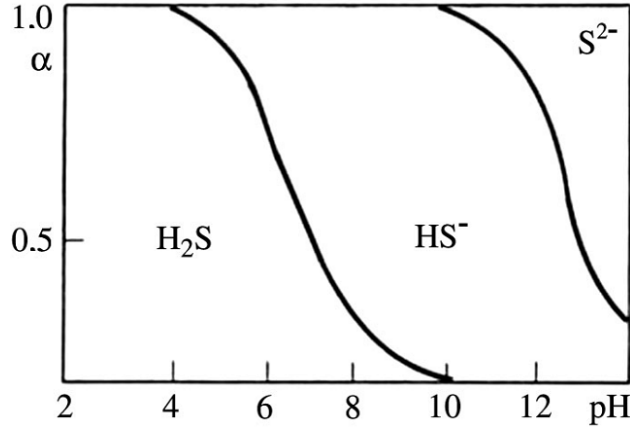


Figure 2.9: Dissociation (α) of H_2S , HS^- and S^{2-} as function of pH.²⁷

2.6.3 Elemental Sulfur

In solutions with high pressure gas and high H_2S content, elemental sulfur (S°) is often found. Especially in wells consisting of over 10% H_2S , S° is expected, but it has also been found in wells with half the amount of H_2S .

In a neutral brine solution, S° increases the acidity as shown in reaction 2.12



The reaction is slow and is not expected to have any effect at room temperature. Studies of UNS S30400 and UNS S31600 at 80°C did however show some H_2S -formation accompanied by a slight pH-drop. This effect was even stronger at higher temperatures. At 200°C the experiment found 100 ppm H_2S in the solution. At higher temperatures, where the solubility of elemental sulfur is higher, corrosiveness promoting pitting and crevice corrosion is found. A study of the Ni-based alloy 825 (UNS N08825) showed a more extensive corrosion.⁵

2.7 Non-environmental parameters

2.7.1 Microstructure

Austenite is not as vulnerable to hydrogen as ferrite, and may in fact under certain conditions act as a crack stopper. As SSC is a type of HE-mechanism, ferritic and martensitic steels show a much higher susceptibility to SSC-failure than austenitic materials. Ferritic/martensitic structures are also insensitive to SCC, with the exception when under applied strain rate equal or greater than yield stress. The increased susceptibility to SSC for a ferritic structure is due to a shorter diffusion path compared to within an austenitic structure.²¹

For austenite the sensitivity is the other way around; Insensitive to SSC and sensitive to SCC. Combined with the effect of temperature sensitivity described in section 2.6.2, DSS may suffer either or both SSC/SCC, given other environmental conditions (such as pH,

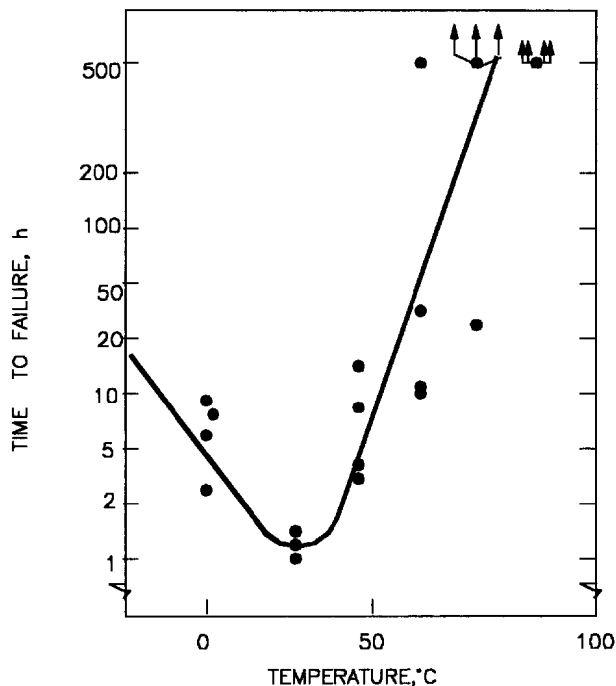


Figure 2.10: Relationship between time to SSC-failure and temperature for a low alloy C-Mn steel.¹⁸

p_{H_2S}) are within their detrimental range.^{21,31} According to Zhao et. al,¹⁶ among the ferritic structures, microstructures with a high amount of acicular ferrite has a better resistance than pure ferritic microstructure. The pearlitic ferrite structure is the weakest microstructure in terms of SSC-resistance.

For a duplex steel it has been shown that the sigma phase significantly increases embrittlement risk of a 22%Cr DSS.²² In addition, grain size refinement plays an important role; The larger the grains, the larger the susceptibility to cracking.²¹ These factors show that poorly performed manufacturing process may lead to higher risk of failure. Little research is done to compare the susceptibility of wrought and HIP-steels to SSC-failure, which makes it hard to compare the effect of microstructure as function of production method.

Lattice diffusion coefficient of Hydrogen for common CRAs are listed in Table 2.2.³²

Table 2.2: Lattice diffusion coefficient (D) for some CRA materials³²

Material	D [cm ² /s]
Martensitic SS	10 ⁻⁶ -10 ⁻⁷
Austenitic SS	10 ⁻¹⁰ -10 ⁻¹²
Duplex SS	10 ⁻¹⁰
Ni Base alloys	10 ⁻¹⁰ -10 ⁻¹¹

2.7.2 Plastic Deformation

It is well known that austenitic structure may be transformed to martensitic either by a sufficiently low temperature, or sufficient plastic deformation. As described in 2.7.1, it is thus natural to expect the possibility of detrimental effects of plastic deformation on unstable austenitic alloys or semi-austenitic alloys such as DSS, when exposed to a HE-mechanism. The direct effect of the martensitic transformation is in fact to raise the start temperature of transformation, M_s .^{20,31}

Research has found that for a pre-strained austenitic alloy, deformation-induced martensite has a very strong effect on hydrogen diffusion in austenitic steels. This is found by a larger hydrogen diffusivity and permeability as a function of increasing martensite amount in these materials. Studies have also shown that a material under strain may enhance hydrogen diffusion in a BCC alloy due to local destruction of protective oxide films.³¹

Studies have shown that hydrogen ingress increases with cold work.²¹ In addition, it has also been shown that for a 22%Cr tubing material the critical chloride content for cracking decreases strongly with an increase in cold work. The direction of stress on a tubing material is also of importance, as the γ -islands tend to elongate along the longitudinal direction due to the manufacturing process. A stress along the transverse direction is therefore more detrimental as there will be a decrease of γ -islands along the crack path. This also means that a DSS with higher α should show a higher risk of failure.²¹

2.7.3 Hydrostatic Stress

It is well known that hydrostatic stress is a large driving force for hydrogen diffusion from bulk material to a crack tip.³² The strain of the material will be highest at the crack tip and slowly decrease with increasing distance, whereas the highest stress field is found a small distance away from the crack (figure 2.11). Due to the dilation of the lattice hydrogen will readily diffuse toward sites with increased hydrostatic stress.³²

2.8 Environmental Limits

2.8.1 Duplex Steels

2.8.1.1 Limit given by ISO 15156:3

For in-situ pH occurring in a production environment, ISO 15156:3 states that any chloride content is acceptable. However, a maximum temperature and maximum H_2S partial pressure has been given. These values are shown in table 2.3. The standard further states that given a maximum chloride content of 50ppm, some duplex materials have been used without any restrictions on temperature, partial H_2S pressure or in situ pH. These are shown in table 2.4.

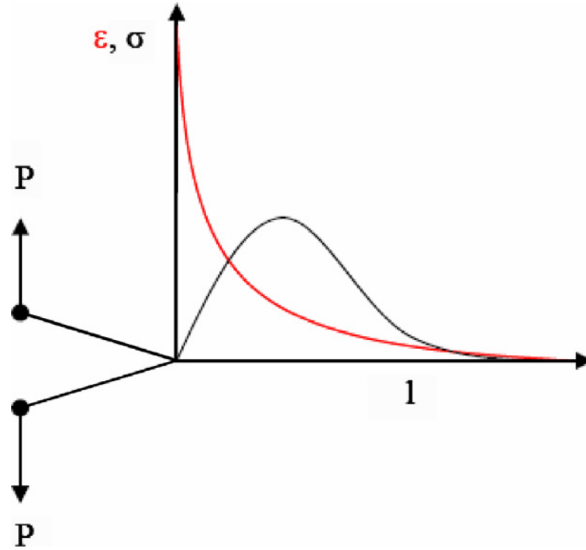


Figure 2.11: Stress and strain fields ahead of a crack.³²

Table 2.3: Temperature, partial H₂S pressure and chloride content limits for DSS used for any equipment or component. *Any in situ pH in a production environment.²

Material	Temperature, max	Partial H ₂ S pressure, max	Chloride content	pH
32 ≤ PREN ≤ 40, Mo ≥ 1.5%	232°C	10kPa	any	any in situ*
S31803 (HIP)	232°C	10kPa	any	any in situ*
40 ≤ PREN ≤ 45	232°C	20kPa	any	any in situ*

2.8.1.2 Limits by experimental work

Several authors have found that a critical temperature for maximum cracking susceptibility for DSS and SDSS to be around 70-80°C.²¹

In a NACE solution at RT the threshold pH limit for cracking appears to be around 3 for 22%Cr and 4 for 25%Cr. However, these threshold limits depend on chloride content.²¹

Maldonado et al.³³ confirmed the partial H₂S limit given in ISO 15156:3 (table 2.3) for duplex S31803 in solution-annealed condition (PREN ≈ 25) by loading triplet samples to 90% AYS for up to 90 days in pH solutions of 3 and 4, 5 with partial H₂S pressures of 10, 34 and 69kPa and a temperature of 80°C.

Not only did the 10kPa samples survive the test, but the samples exposed to 34kPa did not show any signs of cracking. A few of the samples exposed to 69kPa showed failure, but these happened after more than 720 hours, which is the normal test period for TM0177 Method A.²⁸ A concentrated summary of the experiment is summarized in table 2.5³³

In another study, Siegmund et al. investigated the SSC/SCC resistance of a DSS and SDSS with H₂S partial pressures of 0.5bar (50kPa), 0.7bar (70kPa) and 1.0bar (100kPa) at

Table 2.4: Temperatur, partial H₂S pressure limits for DSS used for any equipment or component in production environments with limited chloride content. *Any in situ pH in a production environment.²

Material	Temperature, max	Partial H ₂ S pressure, max	Chloride content	pH
$30 \leq \text{PREN} \leq 40, \text{Mo} \geq 1.5\%$	any	any	$\leq 50\text{ppm}$	any in situ
$40 \leq \text{PREN} \leq 45$	any	any	$\leq 50\text{ppm}$	any in situ

Table 2.5: Summary of test results of several series of a DSS with different environmental parameters.³³

Temperature °C	Cl ppm	H ₂ S kPa	pH	Exposure days	Result
80	1,000	10	3	30	no cracking
80	100,000	10	4.5	90	no cracking
80	1,000	34	3	90	no cracking
80	100,000	34	4.5	90	no cracking
80	1,000	69	3	90	some failures*
80	100,000	69	4.5	90	some failures*

*Cracking in one of three parallels, after 1152 and 1440 hours for pH 3 and 4.5, respectively.

several temperatures ranging from 28.5°C to 180°C . The experiment used tensile tests held at 90% of AYS for 720 hours. No cracking was observed, but there were cases of localized corrosion on some of the samples. This test did however not use the standard test solutions suggested, but a solution resulting in a pH estimated to range from 4.2 to 5.0. This pH value is substantially higher than the lowest expected pH values in a well fluid, as discussed in section 2.4.1.³⁴

2.8.2 Ni-Base Alloys

Studies carried out so far show that Ni-based alloys can show a resistance towards SSC far greater than of duplex steels. For instance, Sarinen found no susceptibility to SSC when exposing a UNS N06625 (HIP) in a SSRT with a temperature of 177°C and partial pressures of up to 21bar H₂S and 25bar CO₂.³⁵

Ni-base alloys are also prone to SCC failure, but this is only expected for temperatures above 150°C . However, this mechanism is limited to severe H₂S levels and high salinity. SCC resistance is increased with increased Ni, Mo and W.¹⁸

2.8.3 Martensitic Steels

ISO 15156:3 states that for a production environment, any combination of temperature and chloride content is acceptable. However, partial H₂S-pressure is limited to max 10kPa, and solution pH must be ≥ 3.5 . The standard also give important minimum requirements for quenching and tempering during production. Any welding performed on the material requires post weld heat treatment.²

At lower pH values lower than what is required for passivation of MSS, the steel shows a poor resistance against SSC. This can be improved by adding Mo, but partial H₂S pressure also plays a vital role. The lower pH limit increases as the partial H₂S pressure increases.³⁶

2.9 Material Selection and Qualification

ISO 15156 gives guidance to selection of materials for use in H₂S-environments in oil and gas production. The standard is divided in three parts; General principles for selection of cracking-resistant materials, selection of carbon and low-alloy steels and selection of CRAs. The limiting values given are based on field experience and/or laboratory testing. This means that no further testing is required on a general basis, when selecting a material. It is however strongly recommended to consider the consequences of failure before deciding to chose a material without further testing Tests can be performed either as fit-for purpose or at levels more detrimental than those expected in the are of use.^{1,2}

The applied stress or strain will not necessarily give an accurate service condition, as actual conditions may rely on manufacturing history and service exposure. EFC-17 recommends a applied stress of either 90% or 100% of the actual yield strength.

For Slow Strain Rate Test (SSRT) a strain rate of $10^{-6}s^{-1}$ is recommended. This strain rate is a result of a compromise: At higher strain rates SSC effects may be lost due to more predominant mechanical effects. Lower rates will lead to a higher time consumption, thus making the tests more demanding. As results from SSRT cannot be compared when performed with different sample sizes and strain rates, using a standardized sample size and strain rate is advisable.²⁹

2.9.1 Laboratory Test Methods for SSC/SCC Resistance

NACE Standard TM0177²⁸ can be used when further investigation of a materials resistance towards EAC in an H₂S is required. The main objective of using a standard as such is to make sure that data performed by different laboratories are done in the same matter, making them comparable. The standard describes four different test methods; Tensile Test, Bent Beam, C-Ring ad Double Cantilever Beam (DCB). All of these are constant load methods, and are intended to verify if a certain alloy fails under a defined load. This load is often related to the AYS. There are however supplementary tests that can be performed, such as SSRT. This chapter will look further into some of the different test methods, including other important aspects such as test solution and key differences between the methods.²⁸

2.9.1.1 Tensile Test

A constant load is applied to a tensile specimen in the desired environment. Tests performed according to NACE Standard TM0177 will be held under constant load for up to 720 hours or until fracture occurs. By repeating this test a threshold stress limit can be achieved. Alternatively this test can also be performed to see if an alloy is fit for a given environment.^{2, 15}

2.9.1.2 Slow Strain Rate Test

The Slow Strain Rate Test, also known as constant extension rate test, applies a load to a tensile specimen such that the strain rate is constant. The test is carried out until the test sample has fractured. Fracture by H₂S assisted SSC/SCC is determined by loss of ductility, reduction in ultimate tensile strength and fracture morphology. If the extension rate is too quick, ductile fracture will occur, as there is not enough time for a H₂S-assisted failure to occur. Due to this, it may be preferable to pre-charge the sample with hydrogen prior to testing. These tests may be preferable over a constant load test, as they usually go over a much shorter period of time. SSRT is in contrast to the constant load methods mentioned in this paper not described in TM0177, but some guidelines are given in EFC-17. This standard suggests use of a strain rate around 10^{-6}s^{-1} .^{15, 29, 37}

Cyclic slow strain rate testing is an alternative SSRT method, where with a constant strain the load is increased and decreased between to set values. The purpose of this can be to simulate the effect of pipe movement.³⁸

2.9.1.3 Double Cantilever Beam

The Double Cantilever Beam test has guidelines given by TM0177 and tests SSC susceptibility of a material by determining a critical stress intensity factor, $K_{I,SSC}$. There has been reports that measured values for $K_{I,SSC}$ may vary strongly with test variables.^{28, 39}

2.9.1.4 Bent-Beam Test

The Bent-beam test, Method B in TM0177, is intended for testing carbon and low-alloy steels. The method evaluates cracking resistance in low-pH solution aqueous environments with H₂S. Samples are deflected with different bending stresses, and any failures are noted. By performing multiple tests of each specimen at each stress level a statistical probability, S_C factor is determined. This factor indicates that for this stress level there is a 50% chance of failure.²⁸

2.9.1.5 Dynamic vs Static loading test

SSRT requires shorter time than a static loading test, and will give a qualitative comparison between different alloys and environmental parameters, which can be used to set a basis for defining important limits. Especially towards SSC conditions, this method can potentially

be too severe, which is a cause of criticism. EFC-17 does however recommend that this test is done as a supplementary test, in addition to a main test with static load.^{5,29}

A drawback of a static loading test is that there is no way to be certain what would happen if the tensile stress was held longer than the initial time span. NACE TM0177 suggests to hold the sample under tensile stress for 720 hours, but failures have been reported for tensile tests held up to 2160 hours. This may give reason to question the certainty of this test.³³

The severity of SSRT compared to a static tensile test is well illustrated in figure 2.12, where failure and no-failure of a MSS as a function of pH and partial H₂S pressure is plotted for different test methods. Results from these methods can be good to complement each other, but cannot necessarily be directly compared.⁵

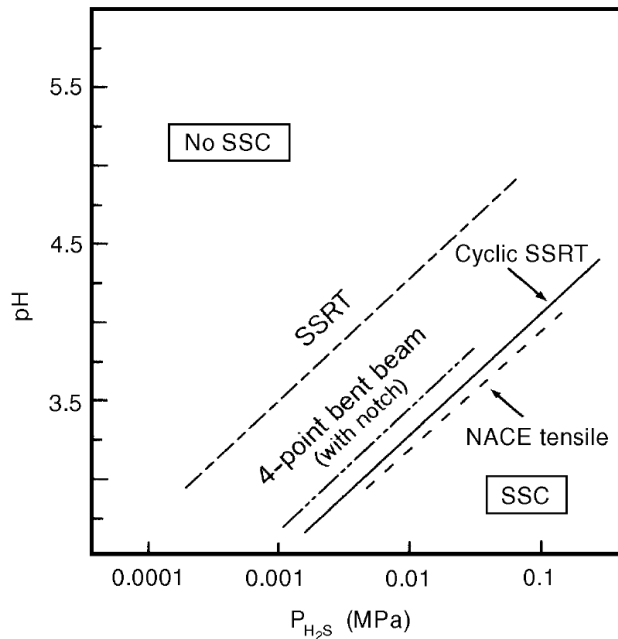


Figure 2.12: Comparison of SSC test results of a M13Cr-95 MSS with different test methods.⁵

2.9.2 Test Solution

Depending on test material and conditions, three different test solutions are suggested by TM0177. Test Solution A and B are both acidified and buffered aqueous brine solutions, saturated with H₂S. The pH for Test Solution A and B is expected to be in the ranges 2.6-2.8 and 3.4-3.6, respectively. Test Solution C is intended when a specific service environment is to be tested. Test of specific environment could for instance be of interest when a company want to do a "fit-for-purpose" test of a material for use in a specific environment.^{28,29}

EFC-17 recommends that when choosing a test environment pH should be less or equal to the lowest expected production environment pH. Partial H₂S pressure and chloride content should be equal or higher than the lowest expected pressure/content in the production environment. Addition of chlorides should generally be done with use of NaCl. If testing

is performed at higher temperature, stress should be applied at ambient temperature before heating to desired temperature.²⁹

In some cases, it can be interesting for a company to test other specific environments. In fact, ATI Metals, the supplier of the Ni-base alloy to be investigated in this work, will do this. The alloy will be tested with conditions according to ISO 15156 Level V.² These test conditions are: Temperature of 150°C , Cl⁻-content of 101 000mg/L and H₂S and CO₂ partial pressures of 0,7MPa and 1,4MPa, respectively.

Chapter 3

Experimental Method

3.1 Material

3.1.1 Material data

Two duplex SS materials and one austenitic SS were tested. The materials with their composition and PREn (for Duplex SS) as given by their material certificates are listed in table 3.1 and 3.2. For simplicity, the Duplex SS materials, UNS S31803 and UNS S32750, will be referred to as "22Cr Duplex" and "25Cr Duplex", respectively. The austenitic SS, UNS N08830, will be referred to as "ATI-830". Material certificates are shown in Appendix C, D and E

Table 3.1: Composition of Duplex SS test materials and PREn.

Material	Composition [wt%]											PREn	
	C	Si	Mn	Cr	Mo	Cu	Ni	W	P	S	N		Fe
UNS S31803 (22Cr Duplex)	0.021	0.41	1.50	22.24	3.12	0.38	5.72	0.051	0.030	0.003	0.168	fill	35.3
UNS S32750 (25Cr Duplex)	0.024	0.25	0.80	25.53	3.79	0.19	6.90	-	0.024	0.0006	0.2750	fill	42.257

Table 3.2: Composition of ATI-830 test material.

Composition [wt%]										
Al	Co	Ct	Cu	Mn	Mo	Nb	Ni	P	Si	Ti
0.020	2.648	21.608	1.181	4.383	5.106	<0.01	29.993	0.0157	0.238	<0.01
V	W	Fe	Al+Ti	Ni+Co	Al+Ti+W	C	S	N	B	
0.036	34.0658	34.0658	0.020	32.642	0.718	0.004	<0.0003	0.393	0.0021	

3.1.2 Additional material deformation of Duplex SS

The materials were given various degrees of pre-deformation prior to testing. Test materials with deformation grades to be investigated are shown in table 3.4.

3.1.3 Machining

Nace standard tensile test samples were produced,²⁸ according to measurements shown in table 3.3. The Tensile test rod with measurements are shown in figure 3.1

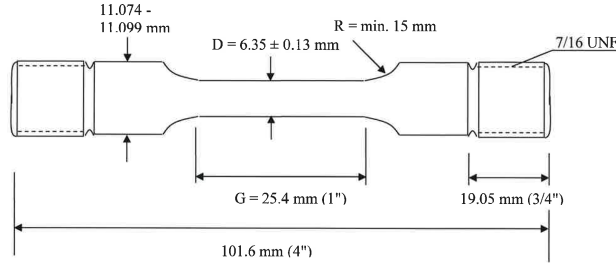


Figure 3.1: NACE standard tensile test rod produced for testing with constant load in H₂S-environment.²⁸

Table 3.3: Dimensions of standard tensile test specimen. D = Diameter, G = Gauge and R = Radius.²⁸

Measurement	Requirement [mm]
D	6.35 ± 0.13
G	25.4
R_{min}	15

Table 3.4: List of materials to be tested with degrees of pre-deformation marked with "X".

Material	Deformation grades		
	0%	4.8%	10%
22Cr Duplex		X	
25Cr Duplex		X	X
ATI-830	X		

3.2 Pre-examination

3.2.1 Tensile test

Prior to the constant load test in H₂S, tensile test data were gathered for all materials shown in table 3.4 at both ambient and actual temperature. Results are shown in section 4.1.1. Due to limited material only one sample was taken for each material/condition.

3.2.2 Hardness Test

Hardness was measured with Rockwell C (HRC) for all deformation grades tested.

3.2.3 Pre examination of Duplex SS with LOM

The Duplex SS materials were given a pre-examination in LOM. Ferrite content was counted and austenite spacing was found for the cross section and the longitudinal direction of the materials. Pictures were taken with magnification of both 500X and 1000X with a Reichert MEF4 A LOM. These results are shown in section 4.1.3. AST-E562⁴⁰ was used as guidance for this process.

3.2.3.1 Material preparation

Materials were embedded in an acrylic resin named Struers ClaroFast, which was done with a Struers LaboPress-3. Resin quantity and embedding settings used are shown in table 3.5.

Table 3.5: Input settings used for embedding Duplex samples in ClaroFast embedding resin

Resin quantity [mL]	Cylinder diameter [mm]	Heating Time [min]	Temperature [C]	Cooling Time [min]	Force [kN]
20	30	3	180	6	25

After embedding, the samples were first prepared with an automatic grinder, Struers Tegrapol-31. Grinding material, suspension and times are shown in table 3.6. Lastly, the samples were etched with 20% NaOH with 3.0V for 3-4s with a Struers LectroPol-5. Safety precautions according to section 3.6.2 were taken whilst handling NaOH.

3.2.3.2 Microstructure analysis

The microstructure were analysed using imageJ, an open source software⁴¹, to find the austenite/ferrite content as well as austenite spacing. Determination of phase fractions were

Table 3.6: List of applied grinding material, suspension and time for material preparation prior to etching.

Grinding Material	Suspension	Time [m:ss]
SiC-Paper #220	Water	5:00
Largo	All/Lar.	6:00
Dac	Dac	4:00
Chem	OP-S	5:00

done by cropping and converting pictures of a clear area with a minimum amount of scratches or contaminations to 8-bit pictures, before being converted to a black/white image. Black (ferrite) and white (austenite) pixels are then counted by the computer. The process is illustrated in figure 3.2.

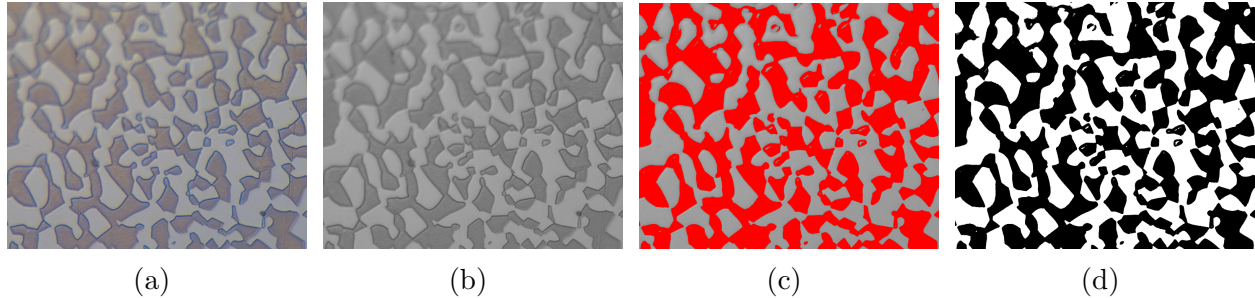


Figure 3.2: The four steps of preparing an image for ferrite counting: crop a clean LOM image (a), convert to 8-bit (b), define ferritic area (c) and convert to black and white for counting of black pixels/ferrite (d).

To find the Austenite-spacing (γ -spacing) a yellow line was drawn parallel to the scale bar, as illustrated in figure 3.3. The scale bar was then measured in the software to determine the pixel per μm ratio. The distance in-between all austenite grains along the yellow line was gathered followed by calculation of average distance and standard deviation. For each material and deformation grade this was done twice; once for the transverse cut and once for the longitudinal. Results are shown in table 4.4.

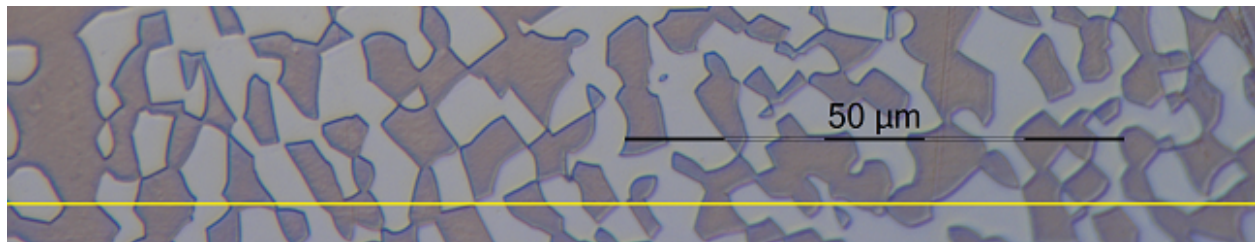


Figure 3.3: Example of setup of yellow line on LOM picture of a Duplex SS to measure and determine the average γ -spacing.

3.3 Constant Load in H_2S

3.3.1 Experimental Setup and General Procedure

All test materials and conditions are listed in table 3.7. The order of the steps taken during setup is listed below. Further explanation and equipment details are given in the following subsections.

1. Prepare test solution
2. Prepare test cell (autoclave).
3. Treat tensile test surface and install in autoclave.
4. Apply load to test sample, and adjust for cold creep (Only for Duplex SS).
5. Prepare and install all other test equipment:
 - (a) N₂ and H₂S sources
 - (b) NaOH-bucket for neutralization of H₂S.
 - (c) Heating equipment.
 - (d) Warning signs at entrance of test area.
6. Fill autoclave with test solution that has been pre-purged with N₂.
7. Purge autoclave with N₂.
8. Purge autoclave with H₂S.
9. Adjust valves:
 - (a) Duplex SS: reduce flow of H₂S to a flow of no more than 1 bubble a second. Bubbles are seen in the NaOH bucket.
 - (b) ATI-830: Close inlet and outlet valves around the test cell
10. Apply test temperature:
 - (a) Duplex SS: Increase temperature slowly and adjust H₂S flow according to step above.
 - (b) Increase temperature slowly and monitor pressure gauge.
11. Monitor at regular intervals until experiment has ended.
12. Disconnect equipment.

Table 3.7: All materials to be tested with test conditions as well as applied and estimated loads at ambient and test temperature, respectively. %AYS is the % of the Actual Yield Strength at the given temperature. (*)Load never decided due to delayed discussions.

Test series	ID's	Material		Temperature [°C]	Gas [MPa]		Load [%AYS]	
		Type	Def.		H2S	CO2	amb. T	test T.
1	A, B	22Cr Duplex	4,8%	90	0.010	fill	100	>100
1	C, D	25Cr Duplex	4.8%	90	0.020	fill	100	>100
2	E, F	22Cr Duplex	4.8%	80	0.010	fill	89.5	100
2	G, H	22Cr Duplex	4.8%	80	0.020	fill	89.5	100
2	I, J	25Cr Duplex	4.8%	80	0.020	fill	88.4	100
3	K, L	22Cr Duplex	4.8%	80	0.020	fill	89.5	100
3	M, N	25Cr Duplex	10%	80	0.020	fill	90.4	100
4	O, P	ATI-830	0%	150	50	200	(*)	100

3.3.2 Test equipment

3.3.2.1 Inlet Control Valves and Manifold

Main gas pressure and flow control valves are shown in figure 3.4. Both the N_2 and the H_2S gas is led into a manifold where output gas for each test cell can be controlled, as well as another flow control valve. In addition, the figure shows how extra gas lines are connected to flush the H_2S lines with N_2 . Figure 3.5 shows the manifold with inlets, outlets, gas selection and gas flow valves.

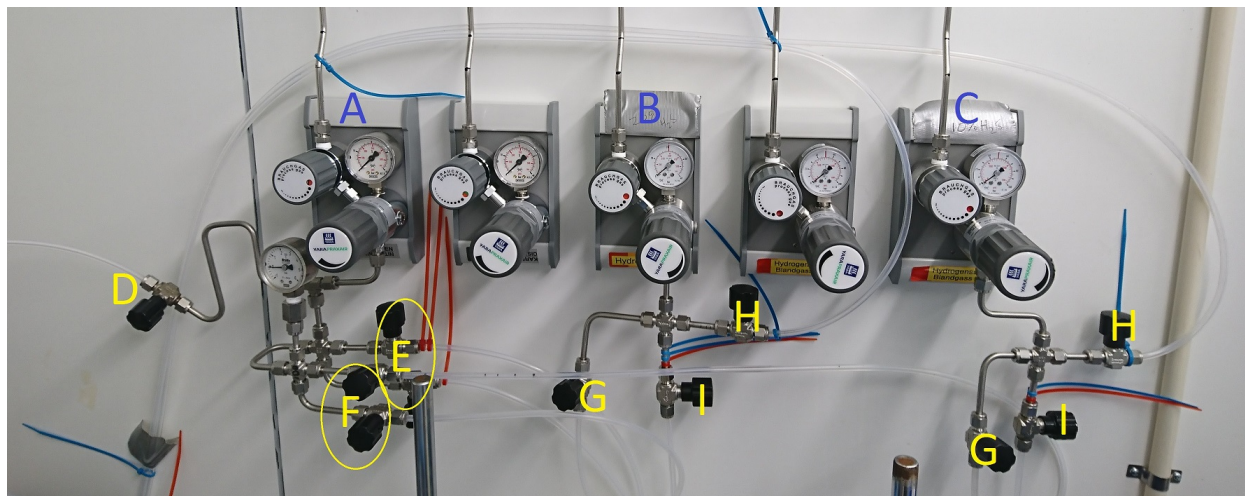


Figure 3.4: Inlet pressure control valves for N_2 and H_2S : N_2 control valves (A), 10/20% H_2S control valves (B/C), N_2 to NACE Solution A container (D), N_2 to Manifold (E), N_2 to flush H_2S systems through valve G (F), inlet valve for flushing H_2S system with N_2 (G), outlet to filter used when flushing (H), H_2S to manifold (I).



Figure 3.5: Control manifold used to adjust flow and input gas to cells. Yellow circles from upper right to lower left show the input connection points for gas, the output lines to different test cells, gas selection valve (N_2 , closed or H_2S) and flow control valve.

3.3.2.2 Test Cells and Autoclaves

Figure 3.6 shows the final assembly of the test cells in the autoclaves with valves and heating equipment connected. The test cells are sealed with O-rings around the tensile test rod to avoid leakage, as seen in figure 3.7.

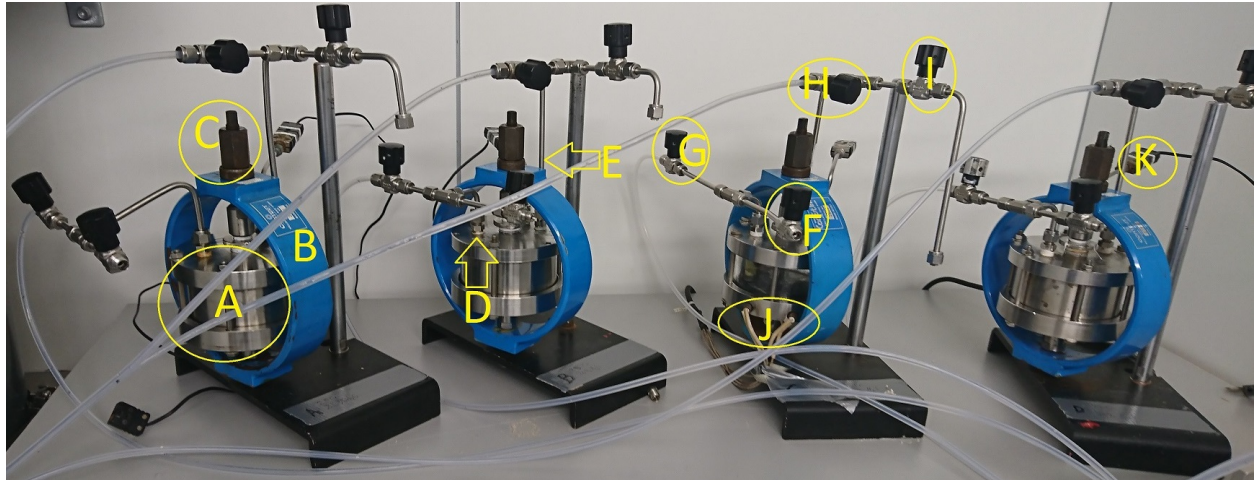


Figure 3.6: Final assembly of test cells in autoclaves: Test cell (A), Autoclave (B), bolt for tensioning of sample (C), gas inlet (D), gas outlet (E), valve for liquid filling from test solution storage container (F), valve for gas from manifold to inlet (G), valve for normal gas outlet to NaOH-bucket (H), "contingency-valve" (I), heating rods (J), thermocouple connection (K).

3.3.2.3 Heating Equipment

The test solution was heated with two test rods that were inserted in the bottom of the test cells. Temperature control was done by measuring the temperature within the cell. The heating rods and connection to thermocouple are shown as item J and K in figure 3.6.

3.3.2.4 NaOH-solution Container

The bucket of NaOH-solution was made of approximately 8L of water and 3kg of solid NaOH. The NaOH bucket, as shown in the bottom left in figure 3.10, was placed close to the ventilation inlet to remove as much as possible H_2S directly if the NaOH-solution would be saturated. Mixing of NaOH was done according to safety precautions as described in section 3.6.2.

The gas hoses from the test cells to the NaOH-solution were split in two just before entering the bucket, so that there would be a backup flow line in case one of the hoses were to be clogged.

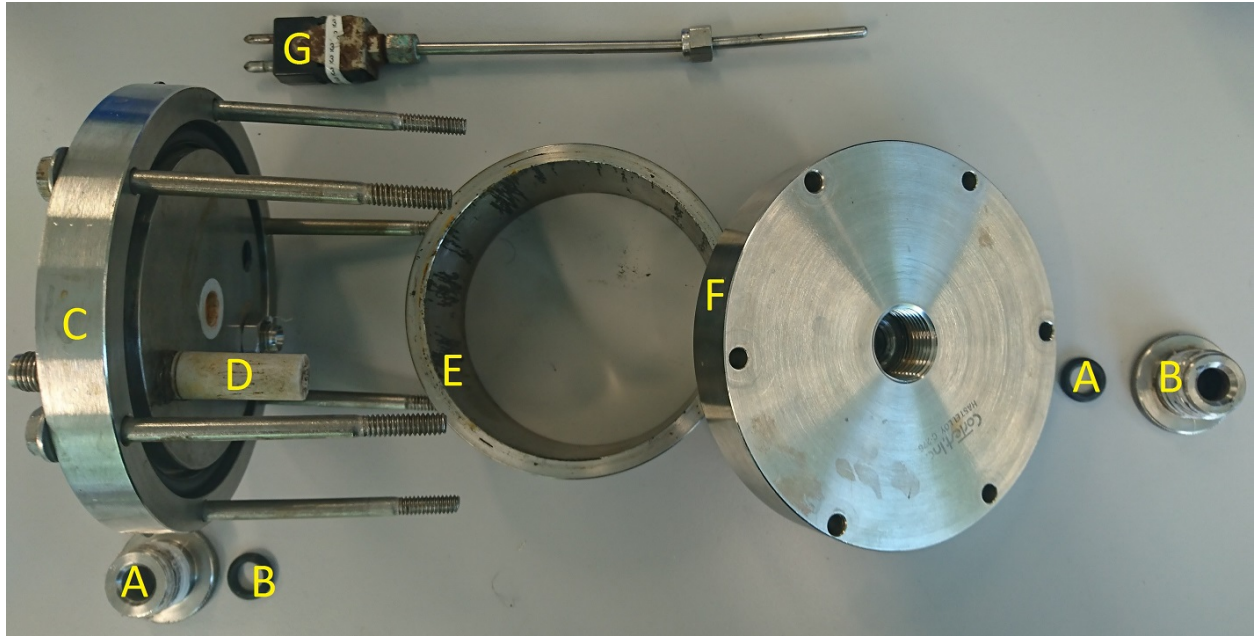


Figure 3.7: Disassembled test cell with showing container lock bolts for tensile test rod (A), O-rings for tensile test rod (B), top lid (C), gas inlet for bubbling in solution (D), container wall (E), bottom lid (F), thermocouple (G).

3.3.2.5 Test Solution Containers

The NACE Solution A container, as shown in figure 3.10, item D, was used for all mixing of NACE Solution A. When in use, the container was sealed and held under a slight overpressure of N_2 to limit oxygen intrusion. A sketch of the container with associated hoses and valves are shown in figure 3.8

No permanent solution container was needed for the ATI-830 samples.

3.3.2.6 pH-equipment

All pH measuring was done using a PHM 92 Lab pH meter, as shown in figure 3.9. Whenever the solution measured contained or could contain H_2S , measurements were done under a ventilated fume hood. All tests were done after calibration with reference solutions of pH 1.679 ± 0.01 and 4.04 ± 0.01 .

3.3.3 Assembled Test Equipment

3.3.3.1 Duplex SS

The final setup is shown in figure 3.10. Details about components and setup procedure are explained in the preceding sections. A simplified sketch of the setup is shown in figure 3.11.

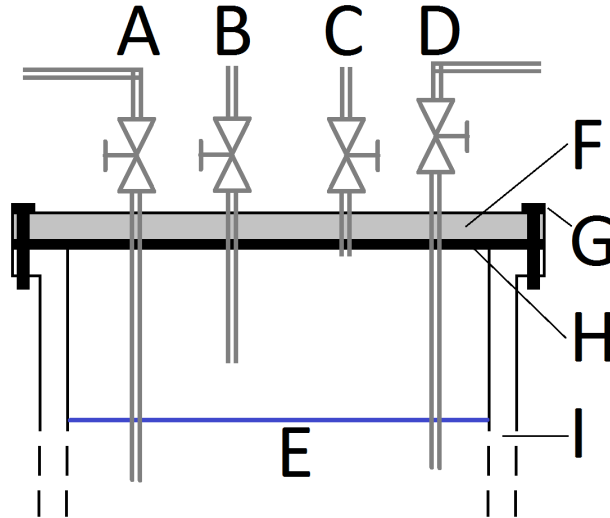


Figure 3.8: Sketch of NACE Solution A container: outlet for NACE Solution A to test container (A), inlet for new NACE Solution A (B), outlet for air during purging (C), inlet for N₂ (D), NACE Solution A (E), Plexiglas Lid (F), bolts (G), O-ring (H) and container (I)

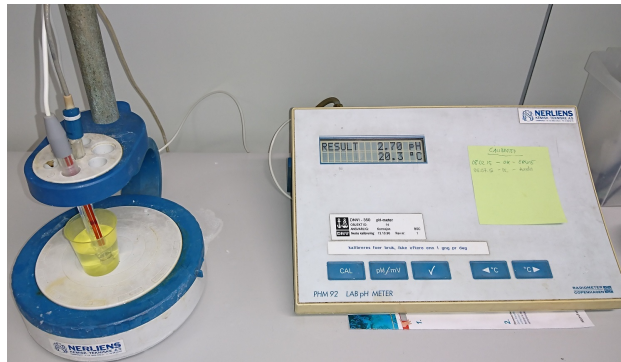


Figure 3.9: Equipment used for pH measurements

Note that the manifold is excluded from this sketch, and instead drawn as a 3-point valve (gas selection) followed by a normal ball valve (flow control).

3.3.3.2 ATI-830

The setup of ATI-830 testing is the same as for Duplex SS with exception of an added safety wall due to the high pressure in the test container. The system will also have a NACE-bucket, but the outlet and inlet will be closed throughout the experiment as this test is performed at an elevated pressure.

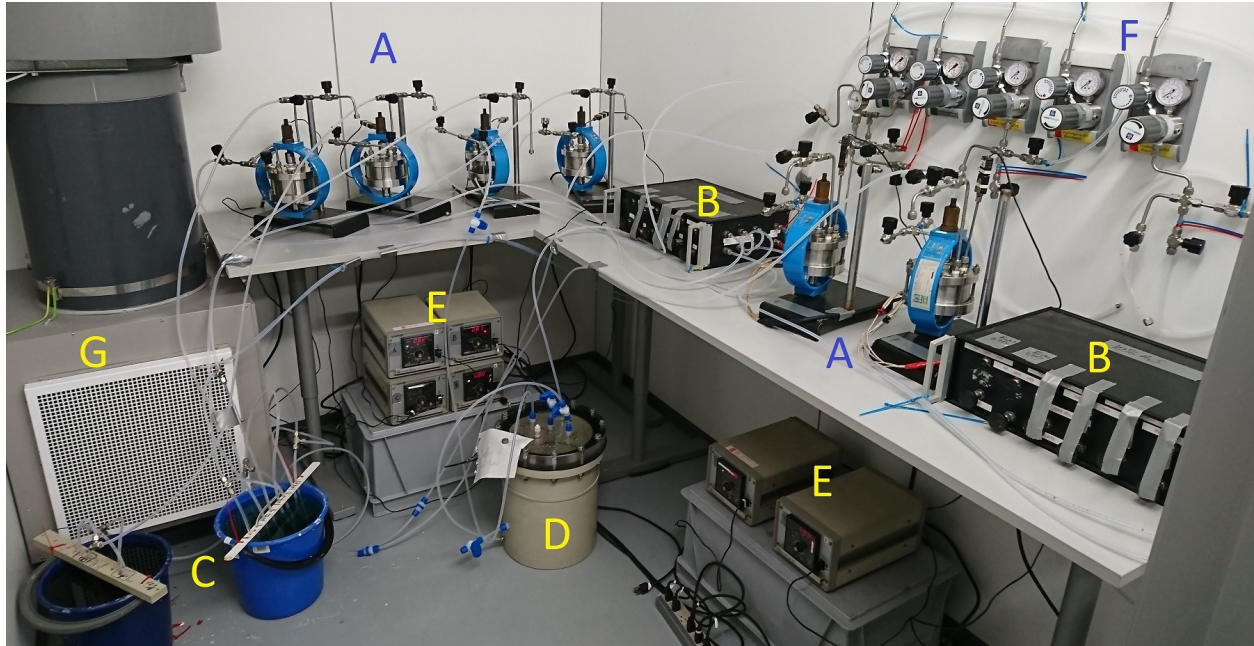


Figure 3.10: Overview of the experiment: Autoclaves with tensile test rods (A), manifold (B), NaOH buckets (C), container for NACE Solution A (D), heating equipment (E), main inlet valves with pressure control valve and gauge (F) and inlet to filter (G).

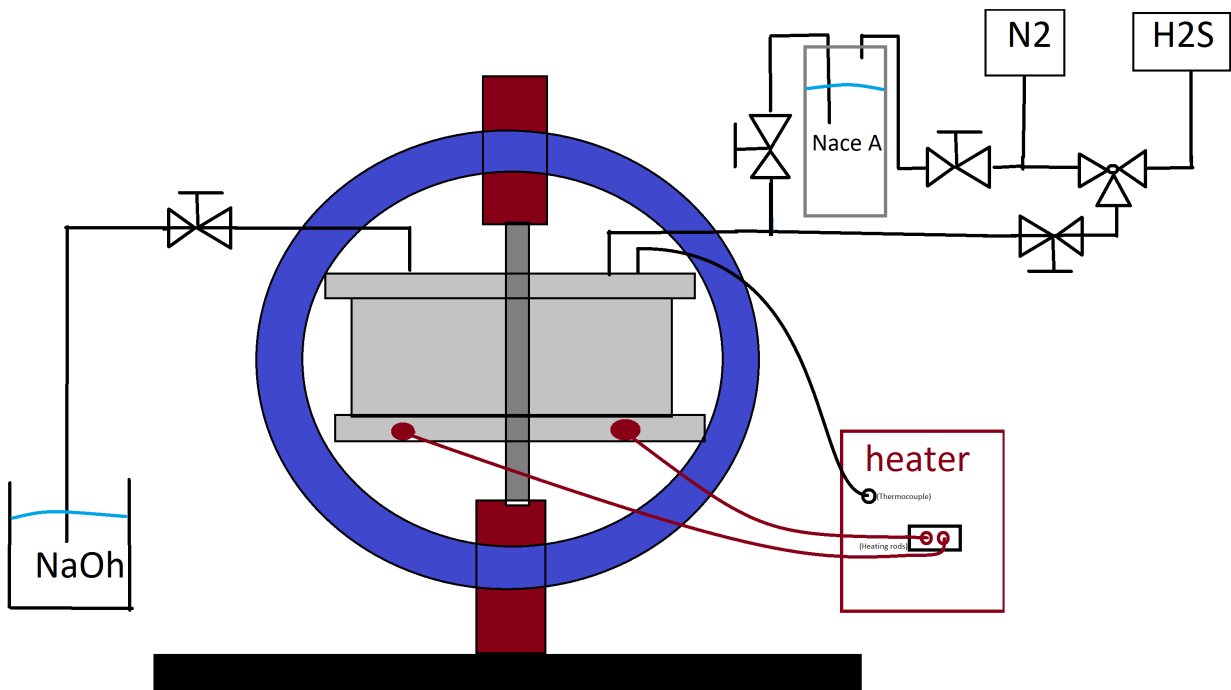


Figure 3.11: Simplified sketch of experiment setup

3.3.4 Step 1: Test Solution

3.3.4.1 Duplex SS: NACE Solution A

Nace Solution A was used in all Duplex SS tests. The solution was made of 5.0% NaCl and 0.5% CH₃COOH (glacial acetic acid) dissolved in deionized water. A quantity of ca 3L were made each time.

To make sure that no oxygen were in the solution prior to filling the cells, the solution was purged over night in N₂ with a flow of 1-2 bubbles per second. After purging the solution was controlled to have a pH of 2.7 ± 0.1 .

3.3.4.2 ATI-830: ISO Level V

For ATI-830 deionized water with >91g/L NaCl shall be used. For this solution there are no pH requirements. pH value after purging as well as after test will nevertheless be recorded.

3.3.5 Step 2-3: Preparation and Installation of Tensile Test Rods

Machined test samples were prepared by manual grinding along the longitudinal axis with grit paper grades 320, 500 and 800. Before changing to a finer grit size the sample was examined using a macroscope to reveal any tracks/notches going around the sample. If the sample did not show only longitudinal tracks further grinding with the same grit size was done. Before installing the test rods in the cells the minimum diameter was determined using a calibrated digital calliper with a resolution of 0.01mm. Measurements are shown in section 4.2.

3.3.6 Step 4: Tensioning of Test Samples

Loading of test samples were done by measuring the calculated expected downwards deflection of the ring whilst tensioning the test sample. The autoclaves are calibrated every 2nd year. The deflection was calculated using the minimum diameter, and was measured using calibrated dial gauges with a resolution of 0.001 inches.

Due to the cold creep effect of Duplex SS, loading of these samples required additional adjustments (re-application of load) when the tension fell. Each adjustment made was subsequently followed by at least 1 hour of waiting before applying additional load or concluding that the target load was met. Due to limited available equipment, no dial gauges was available to monitor the deflection of the autoclave during the actual test.

While setting up the first round (sample A through D as listed in table 3.7) the load was wrongfully set to a higher load than intended, as no consideration of change of YS as a function of temperature were given. A list of applied and estimated loads at ambient and test temperatures, respectively, are also shown in table 3.7. For the other tests, load was applied (at ambient temperature) as a function of the AYS at the test temperature, i.e. as a load of 100% AYS at test temperature was wanted, the samples were loaded to the YS values found at the elevated temperature tensile tests, as described in section 4.1.1.

3.3.7 Step 5: Assemble Equipment

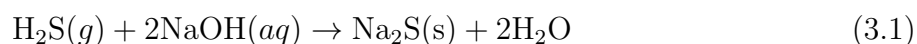
Before any test solution can be filled in the test containers, all other equipment was connected/set up; NaOH-container, Heating equipment, warning sign at entrance to test room, and all gas-equipment including hoses, valves and manifold.

After installation of test equipment all components (including H₂S-components) were flushed with pure N₂. The H₂S-hoses and pipes were flushed by connecting a N₂-hose to the outlet from the main H₂S pressure control valve, reducing the risk of O₂-contamination as much as possible.

3.3.8 Step 6-8:Filling with Test Solution and Purging

10% or 20% H₂S gas mixtures with CO₂ as fill gas was used in all tests. The Duplex SS materials were tested under ambient pressure, and had therefore a very low flow of H₂S bubbling through the test cell throughout the experiment to avoid any O₂-contamination.

All gas outlets were led to a bucket of NaOH solution, so that the H₂S was "eliminated" by production of Sodium Sulfide and water (equation 3.1).



Test cells were purged with N₂ for at least 1 hour, followed by H₂S-purging for 1 hour. Flow during purging was set to approximately 3-5 bubbles per second.

3.3.9 Step 9-10: Gas and Temperature Adjustments

3.3.9.1 Duplex SS

As purging was complete the flow of H₂S-gas was reduced so that no more than 1 bubble per second could be observed in the NaOH-container. Temperature was then gradually increased for each cell, and gas flow was monitored continuously until temperature was stable. Flow was then further reduced to roughly 0.2 to 0.5 bubbles per second when the final temperature was reached.

3.3.9.2 ATI-830

Upon completion of purging all outlet valves are to be closed and pressure and gradually increased. After each increment of gas pressure, the inlet valve is to be closed, and pressure read from manometer to make sure no leaks are present. As the total pressure of the cell has reached 250MPa, the inlet gas shall be closed.

Temperature shall gradually be increased towards 150°C whilst pressure gage is monitored. When target temperature is reached, total pressure shall be noted and checked to be in compliance with expected added partial pressure from the water vapour phase.

3.3.10 Step 11: Monitoring

3.3.10.1 Duplex SS

During the experiment temperature and gas flow was monitored on a near-daily basis. Hoses in the NaOH solution were checked to make sure that no deposits had clogged the hose, making sure the H₂S-gas could flow freely. To make sure sufficient NaOH was available in the solution the buckets were refilled with a fresh NaOH-solution after approximately 2 weeks. Furthermore, as water vapour escaped the bucket, more water was put in 1 week after the refill, to make sure all hoses were submerged at all times.

3.3.10.2 ATI-830

Due to the high pressure and temperature of this test, no unnecessary contact with equipment will be made. The position of the pressure gages on the test cells are however placed in such a way that pressure can be monitored from outside the test room.

3.3.11 Step 12: Disconnection

3.3.11.1 Duplex SS

When the test came to an end the temperature control dials were all set to minimum temperature so that the test cells would cool of to room temperature. At the same time inlet valves for H₂S was shut, and a slight flow of N₂ was introduced to the test cells.

As the test cells reached 30°C or lower, at least 1 hour after cooling and post-purging was initiated, all valves were closed and equipment around the test cell was removed. Unfractured test cells had their load removed to allow for removal of the test cell. Test cells were prior to opening moved to a ventilated fume hood to avoid unnecessary contact with any H₂S-rests. As the tensile test rods were removed, volume of the remaining test solution as well as its pH was recorded.

The test cells were completely disassembled and washed with hot water and soap before being cleaned in deionized water and reassembled for the next test series.

3.3.11.2 ATI-830

Prior to disconnecting any equipment or dumping pressure, heating equipment shall be turned of and equipment left alone until temperature of less than 30°C is measured.

Reduction of pressure will be done by gradually alternately opening the two dump valves a tiny bit and observing if any pressure is released (either by watching the pressure gauge dropping, or by observing gas bubbles in the NaOH-container). When pressure begins to drop, equipment will be left alone until the pressure gauge showed ambient pressure. N₂ shall then used to purge the equipment for at least 1 hour with 3-5 bubbles per second observed in the NaOH-solution.

After purging, equipment is to be disconnected and measurements shall be taken as done in disconnection of Duplex SS, described in section 3.3.11.2

3.4 Duplex SS: Revised Test Procedure

Due to several revisions the test procedure has varied a bit for the different Duplex SS materials. The matrix shown in table 3.8 shows which test procedure that was used for the different Duplex SS samples.

3.4.1 Initial Test-Procedure

Due to the design of the initial setup, water vapour was allowed to escape the test cells through the outlet tubes, as no condenser was available. This was wrongfully assumed to be of a negligible as shown by the high loss of liquid in the result section. This resulted in the need of a revised test procedure.

Table 3.8: Test procedures used for Duplex SS test samples listed in table 3.7.

Procedure	Test Sample ID's						
	A,B	C,D	E,F	G,H	I,J	K,L	M,N
Initial	X	X					
1st Revision			X	X	X		
2nd Revision						X	X

3.4.2 Revised Test-Procedure

3.4.2.1 1st Revision

With exception of the following step, the revised test-procedure followed the same steps as the initial, which were described in sections 3.3.4-3.3.10. Temperature was also reduced from 90°C to 80°C to reduce the water vapour pressure.

No major changes was made to the equipment setup, but a liquid refill procedure was applied: After approximately halfway through the duration of the experiment, the test was completely shut down; temperature reduced to ambient and H₂S gas flow was closed. New pre-purged NACE Solution A was then introduced to the container until liquid could be seen coming out through the outlet. At this point normal purging procedure with N₂ followed by H₂S was done. The test samples were reheated and gas flow was adjusted as per normal procedure.

3.4.2.2 2nd Revision

The temperature reduction done in the first revision appeared to be a sufficient step to reduce the water vapour pressure. Since the refill procedure deemed a risk in terms of NaOH-contamination, this part of the revised procedure was cut out. The lowered test temperature of 80°C was kept.

Remaining liquids after the test was recorded and calculated as a percentage of maximum gauge coverage. Measurements used for the calculation of maximum and minimum coverage were taken with an "open cell" as shown in figure 3.12.

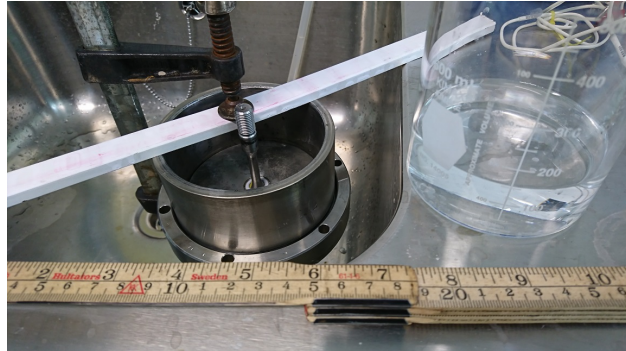


Figure 3.12: Setup to measure max and minimum depths/volumes required 100% and 0% coverage of the gauge area on the tensile test samples.

3.5 Post-examination

3.5.1 LOM

All test rods were initially examined with a macroscope at 10X and 40X magnification to give a general picture of the extent of surface corrosion.

Due to limited available moulding material, only one 22Cr Duplex SS and one 25Cr Duplex SS were investigated further in the LOM. However, for each material, one sample exposed to the assumed worst condition (highest deformation and highest H₂S-concentration) was investigated. This process was used to reveal the typical size of any pits as well as to see if there were any micro-cracking in the pits.

3.5.2 SEM

As none of the samples fractured or showed micro-cracking, no SEM investigation was deemed necessary.

3.6 Safety Precautions

3.6.1 H₂S-gas

H₂S is a poisonous gas that may in worst case lead to loss of consciousness or life. At higher concentration the gas may also be explosive. It was therefore taken strict precautions to avoid any unnecessary contact with the gas both during connection, maintenance and completion of the tests.

Experiments including H₂S were performed within a closed Ex-secured area with a security system that monitored H₂S levels at the floor (H₂S is heavier than air), oxygen level as well as % LEL (Lower Explosion Limit). If any limits were breached, pneumatically controlled normally closed valves would shut down all H₂S supply, as well pumping air out of the test chambers through a filter. This shutdown could also be activated by a emergency switch by the exit of the test area.

Any change to the main pressure control valve, or opening of the main inlet valve on the H₂S-system was always done with 2 persons present. And at all times a hand held gas detector was used, shown in figure 3.13b.

As described in the test equipment section, handling of equipment that has had H₂S inside was purged with N₂, and then opened under a ventilated fume hood, as shown in figure 3.13c.



(a) Closed of test room with warning sign.



(b) Gas detector



(c) Disassembly of test cell under ventilated fume hood.

Figure 3.13: Equipment used as different safety tools

3.6.2 Concentrated NaOH

The NaOH solution used was treated carefully as it was very basic. Any mixing was done under a ventilated fume hood, with thick rubber gloves, eye goggles, face screen and protective clothing. During etching the same safety equipment was used.

Deposition of NaOH solution was done in the sink under the fume hood, heavily diluted in tap water.

3.6.3 Handling of Nace solution A

Mixing of Nace solution A involves handling of CH_3COOH , glacial acetic acid, and was therefore handled with the same care as mixing of NaOH . Deposition of Nace solution A was done in the sink under the fume hood, heavily diluted in tap water.

3.6.4 High-pressure/temperature testing

Due to the dangers related to high pressure and high temperature water with H_2S , a safety wall with a thick Plexiglas was put between the user and the test cells. Valves for dumping pressure are put just behind the wall so that they can be reached from the safe side of the safety wall. A warning sign was also put on the entrance of the test room warning anyone against entering.

Chapter 4

Results

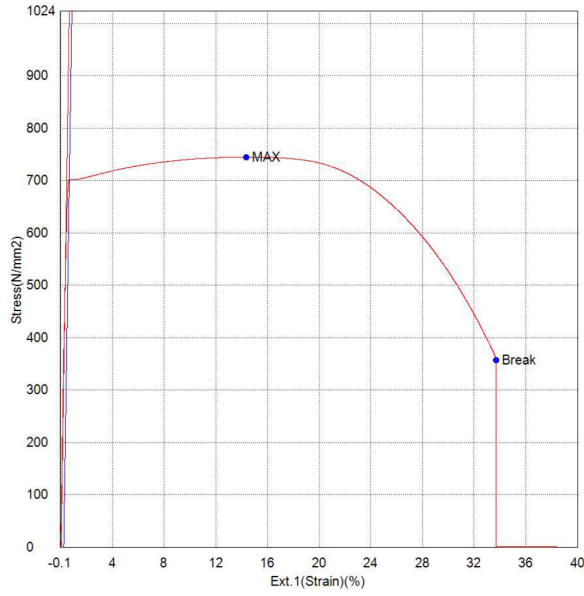
4.1 Pre-exposure tests

4.1.1 Tensile Test

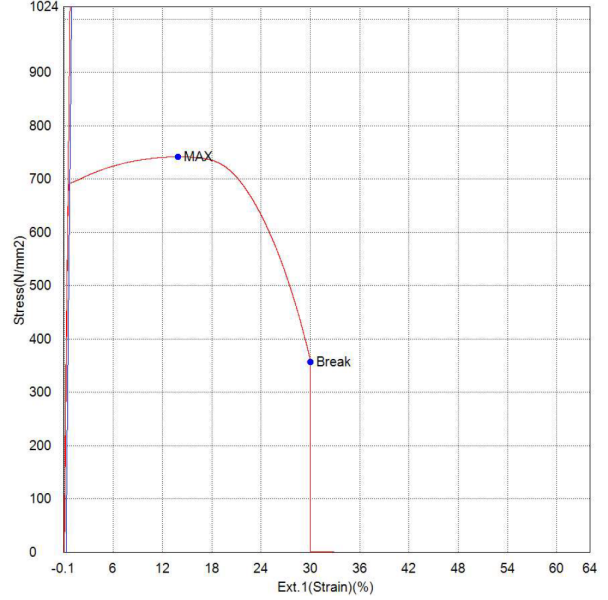
Results from tensile tests with various degrees of pre-deformation and temperature are shown in table 4.1. The table shows the YS, Ultimate Tensile Strength (UTS) and fracture elongation in percent. Stress-strain diagram of the five tensile tests performed at elevated temperature are shown in figures 4.1-4.3

Table 4.1: Results from tensile testing of materials of interest prior to H₂S-testing. Values were taken for various degrees of deformation as well as for ambient and test temperature. Values marked ⁽¹⁾ are test data received from manufacturer.

Material	Temperature [°C]	Deformation [%]	YS [MPa]	UTS [MPa]	Fracture elongation [%]
22Cr Duplex	ambient	4.8	774	818	32.4
22Cr Duplex	80	4.8	699	744	34.0
22Cr Duplex	90	4.8	690	741	30.0
25Cr Duplex	ambient	4.8	832	927	37.6
25Cr Duplex	90	4.8	735	841	34.8
25Cr Duplex	80	10	847	887	27.0
ATI-830	ambient	0	1151 ⁽¹⁾	1255 ⁽¹⁾	21.8 ⁽¹⁾
ATI-830	150	0	1040	1080	19.0

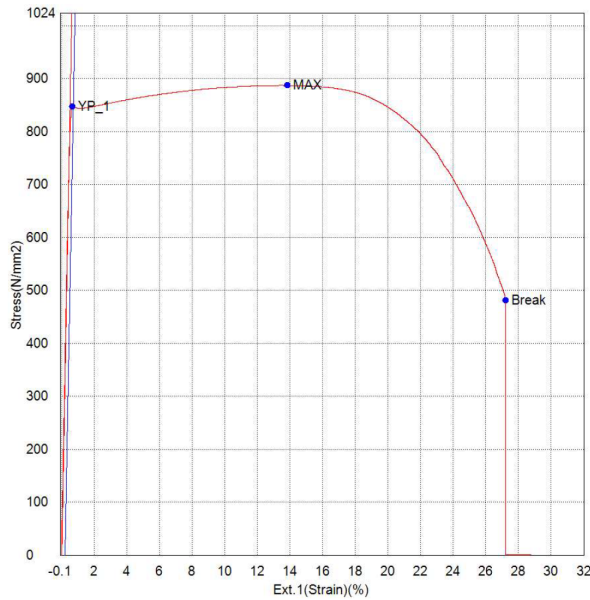


(a) 80°C

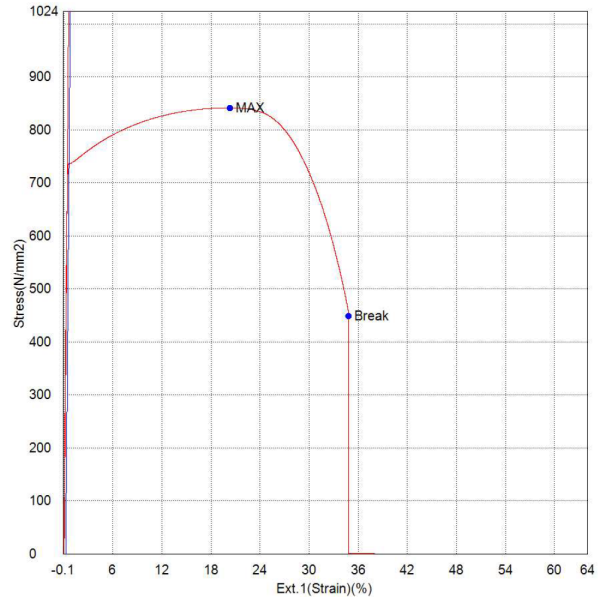


(b) 90°C

Figure 4.1: Stress-strain diagrams of tensile tests of 22Cr Duplex SS with 4.8% pre-deformation at elevated temperatures.



(a) 80°C and 10% pre-deformation



(b) 90°C and 4.8% pre-deformation

Figure 4.2: Stress-strain diagrams of tensile tests of 25Cr Duplex SS at elevated temperatures.

4.1.2 Hardness Test

Results of HRC test are shown in table 4.2. The table shows 3 measured values (Sample 1 through 3), the average HRC value and the standard deviation.

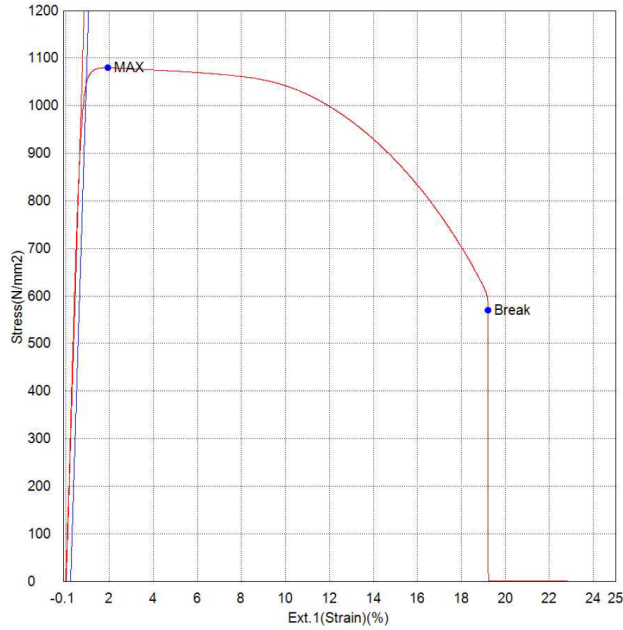


Figure 4.3: Stress-strain diagram of tensile test of ATI-830 at 150°C with 0% pre-deformation.

Table 4.2: HRC Samples taken for both 22Cr and 25Cr Duplex materials with various degree of pre-deformation.

Material	Deformation	Sample 1	Sample 2	Sample 3	Average	Std.Dev
22Cr Duplex	0%	19.50	21.41	22.75	21.22	1.63
22Cr Duplex	4.8%	21.38	22.36	22.08	21.94	0.50
25Cr Duplex	0%	22.77	25.91	24.86	24.51	1.60
25Cr Duplex	4.8%	27.61	27.95	27.82	27.79	0.17
25Cr Duplex	10%	32.53	31.86	28.98	31.12	1.89

4.1.3 Duplex SS characterization in LOM

4.1.3.1 Calculation of ferritic content

Table 4.3 shows the ferrite content in the tested Duplex SS samples.

Photos of areas that has been used to calculate the content are shown in figure 4.4-4.5 and figure 4.6-4.7 for the 22Cr Duplex and 25Cr Duplex, respectively.

4.1.3.2 Calculation of austenite spacing

Calculated average austenite spacing, with standard deviation and resolution of measurements are shown in table 4.4. Calculation of austenite spacing is shown for both longitudinal and transversal direction of all degrees of deformation used for the different Duplex SS alloys.

Table 4.3: Result of counting ferritic phase using imageJ. (*)Pixel count lower due to other software settings.

Material	Deformation	Ferrite count [%]	Pixel count.
22Cr Duplex	0%	53.698	2304080
22Cr Duplex	4.8%	55.056	3109184
25Cr Duplex	0%	53.274	2919280
25Cr Duplex	4.8%	52.245	1455543
25Cr Duplex	10%	53.151	609(*)

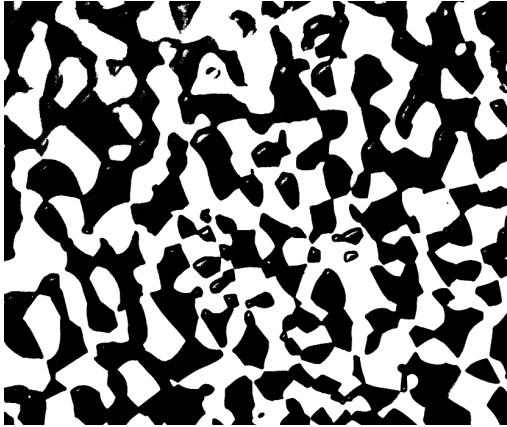


Figure 4.4: 22Cr Duplex with 0% pre-deformation

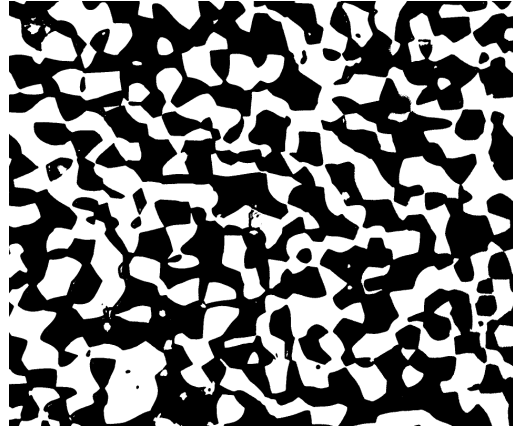


Figure 4.5: 22Cr Duplex with 4.8% pre-deformation

Table 4.4: Austenite spacing for different samples of Duplex SS with various degrees of deformation. Directions are either cross section or longitudinal.

Material	Deformation	Direction	Counts	γ -spacing [μm]	St.Dev [μm]	Resolution [Pixels/ μm]
22Cr Duplex	0%	Long	13	5.30	2.97	20.66
22Cr Duplex	0%	Cross	16	4.21	1.95	20.68
22Cr Duplex	4.8%	Long	12	5.49	3.41	20.62
22Cr Duplex	4.8%	Cross	14	4.74	3.89	20.61
25Cr Duplex	0%	Long	12	4.98	2.86	20.66
25Cr Duplex	0%	Cross	13	4.61	2.09	20.62
25Cr Duplex	4.8%	Long	18	3.50	2.72	20.62
25Cr Duplex	4.8%	Cross	15	3.62	2.95	20.64
25Cr Duplex	10%	Long	13	6.47	4.57	20.63
25Cr Duplex	10%	Cross	17	9.18	5.80	20.60

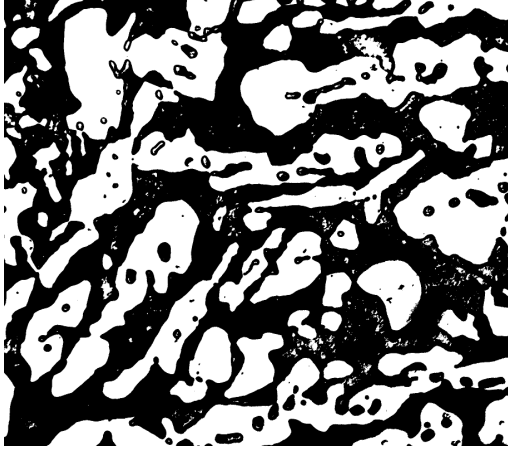


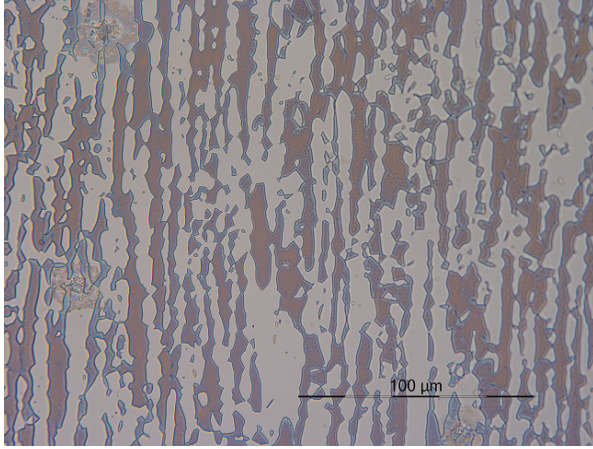
Figure 4.6: 25Cr Duplex with 0% pre-deformation



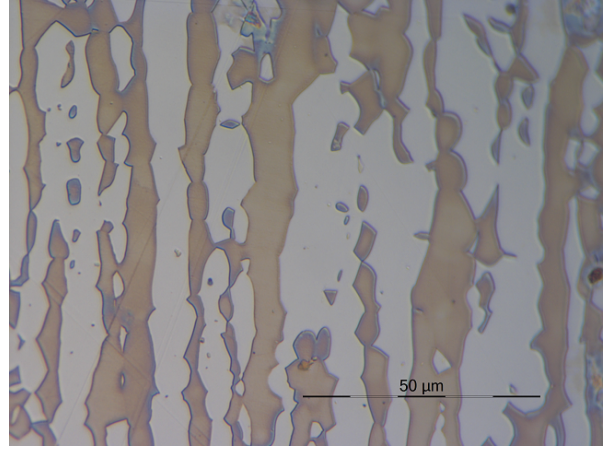
Figure 4.7: 25Cr Duplex with 4.8% pre-deformation

4.1.3.3 LOM Pictures

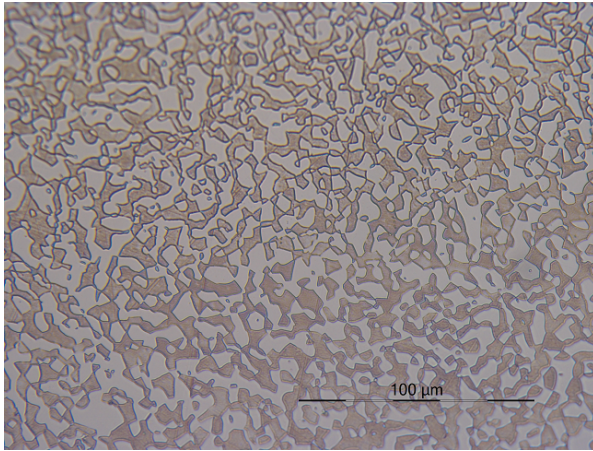
LOM pictures at 500X and 1000X magnification of both Duplex SS materials with the various deformation grades are shown in figures 4.8-4.12.



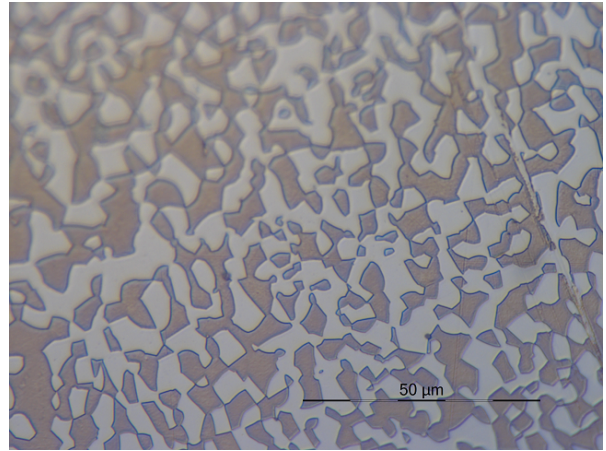
(a) Longitudinal section magnified 500X



(b) Longitudinal section magnified 1000X

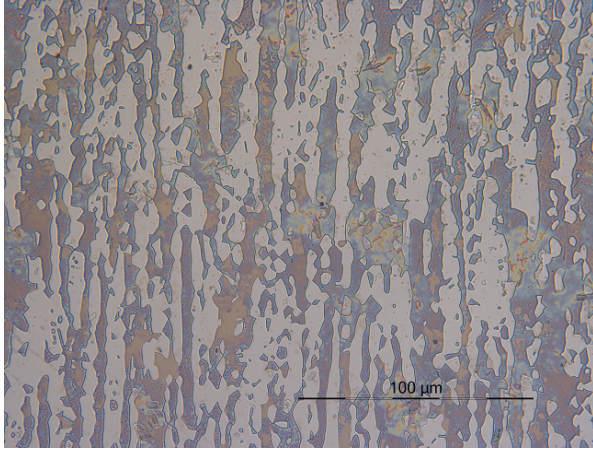


(c) Cross section magnified 500X

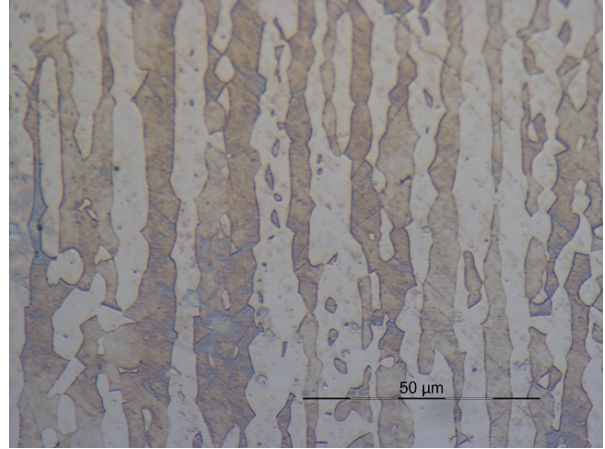


(d) Cross section magnified 1000X

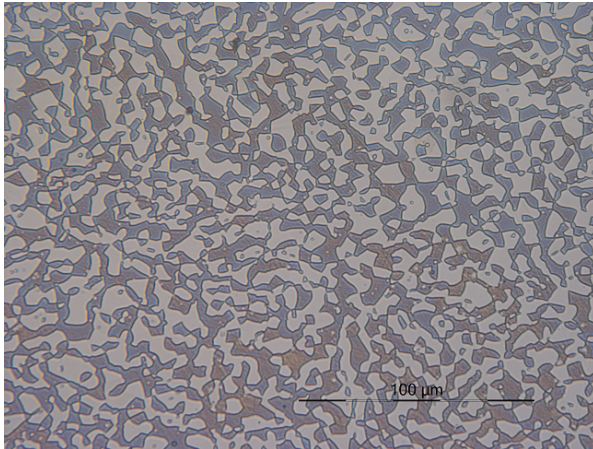
Figure 4.8: LOM pictures of 22Cr Duplex with 0% pre-deformation



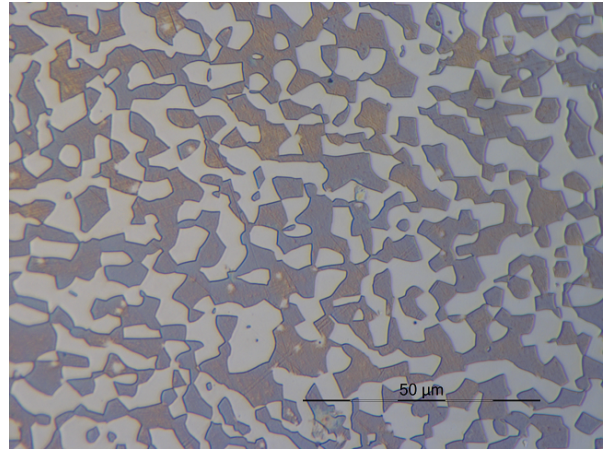
(a) Longitudinal section magnified 500X



(b) Longitudinal section magnified 1000X

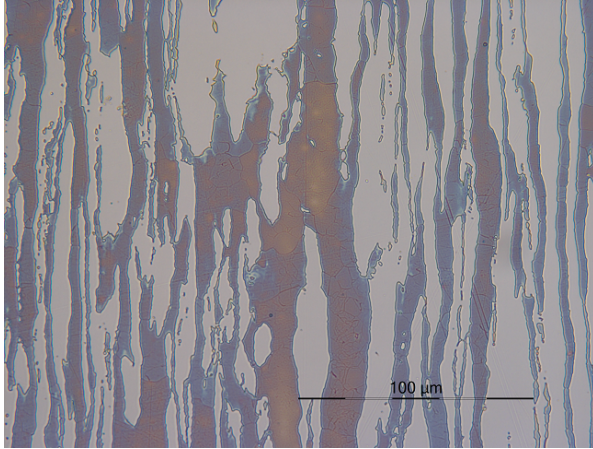


(c) Cross section magnified 500X

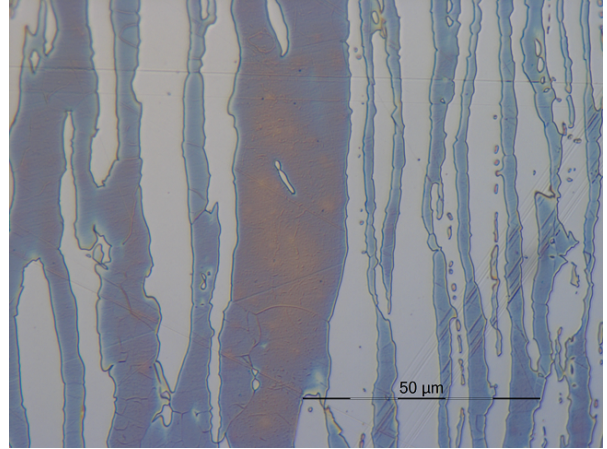


(d) Cross section magnified 1000X

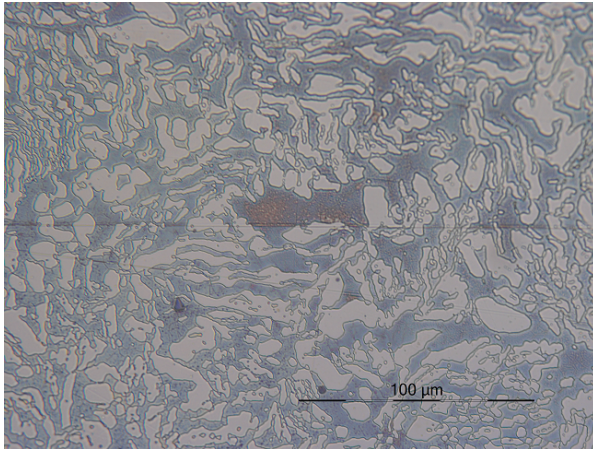
Figure 4.9: LOM pictures of 22Cr Duplex with 4.8% pre-deformation



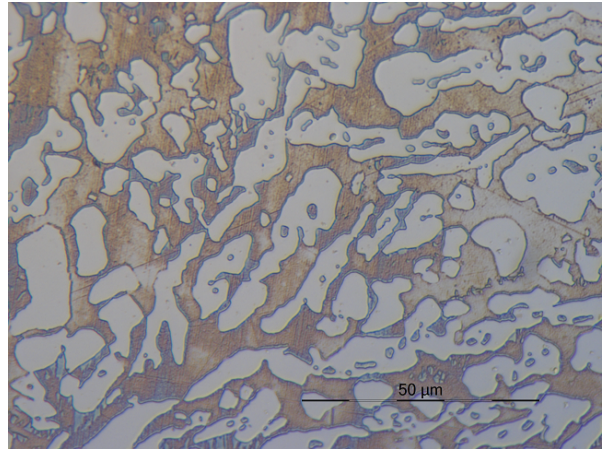
(a) Longitudinal section magnified 500X



(b) Longitudinal section magnified 1000X

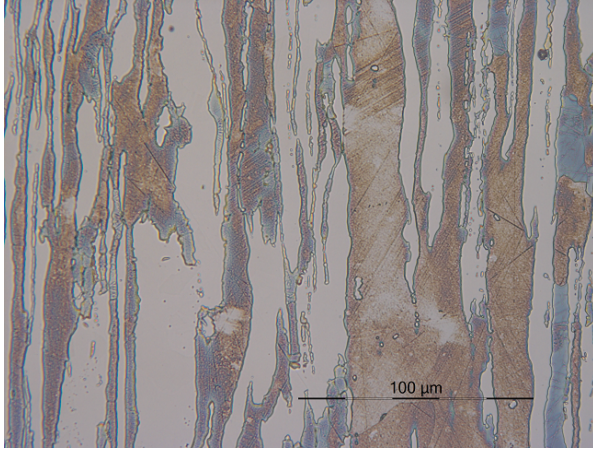


(c) Cross section magnified 500X

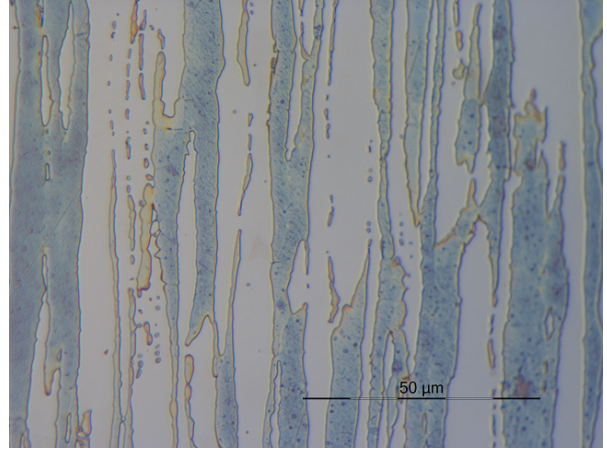


(d) Cross section magnified 1000X

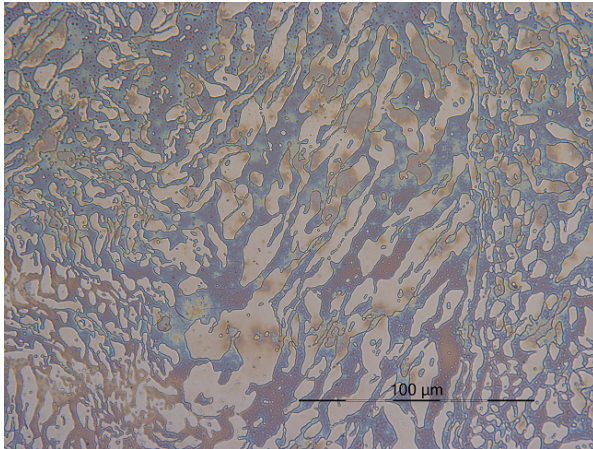
Figure 4.10: LOM pictures of 25Cr Duplex with 0% pre-deformation



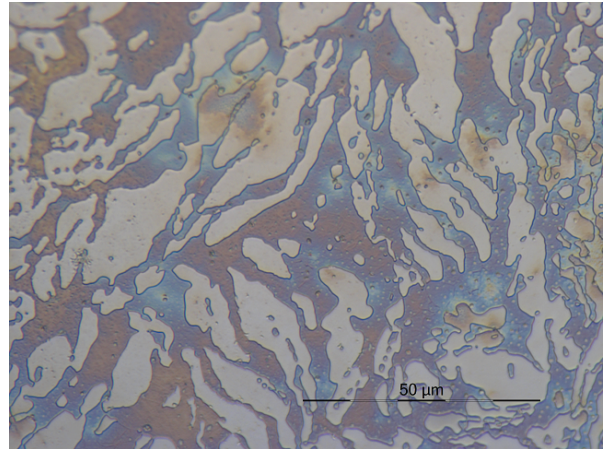
(a) Longitudinal section magnified 500X



(b) Longitudinal section magnified 1000X

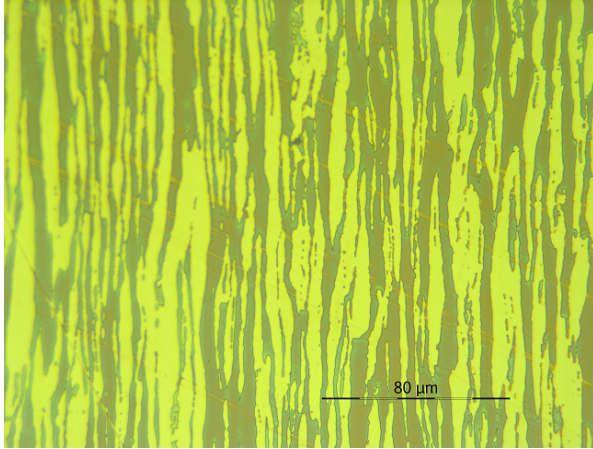


(c) Cross section magnified 500X

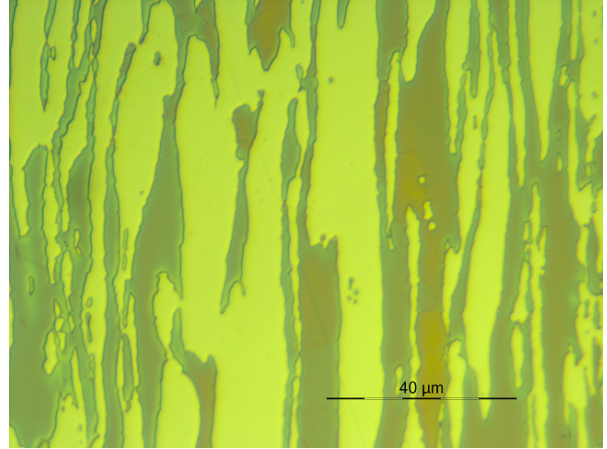


(d) Cross section magnified 1000X

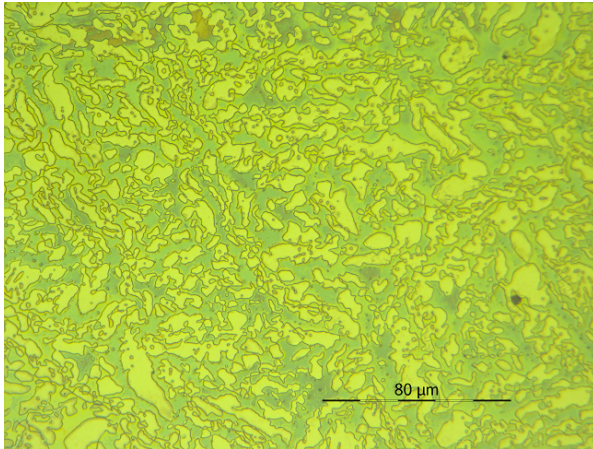
Figure 4.11: LOM pictures of 25Cr Duplex with 4.8% pre-deformation



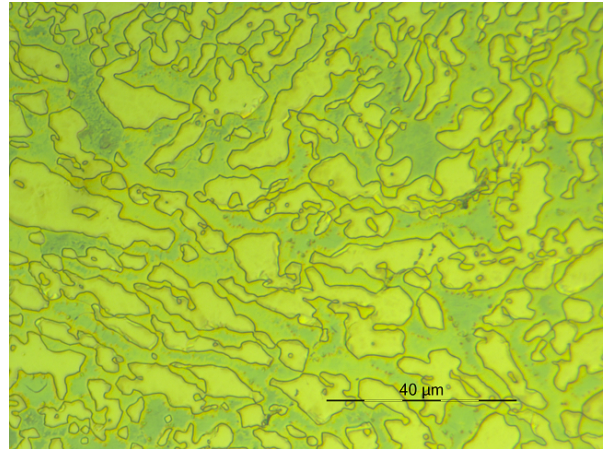
(a) Longitudinal section magnified 500X



(b) Longitudinal section magnified 1000X



(c) Cross section magnified 500X



(d) Cross section magnified 1000X

Figure 4.12: LOM pictures of 25Cr Duplex with 10% pre-deformation

4.2 Constant Load in H₂S

Results of constant load test in H₂S are for 22Cr Duplex and 25Cr Duplex showed in table 4.5, 4.6-4.7 and 4.8, respectively. The tables show the applied load a test temperature as % of AYS, test temperature, partial H₂S-pressure as a percentage of total pressure, test duration in days, whether or not the sample failed (fractured), initial and final pH, initial and final minimum diameter, Final volume in litres, days since last refill and percentage of the gauge area that was covered at the lowest liquid level.

Due to delayed discussions with provider of ATI-830 there was not sufficient time to finish constant load testing of ATI-830 before the deadline of the thesis. As a result of this no results from ATI-830 are shown in this section or the post-examination section.

Table 4.5: Test results of Constant load test with H₂S for 22Cr Duplex with 4.8% pre-deformation. (*)Sample G lost all liquid within 7 days and was disqualified.

ID	Load [%AYS]	T [°C]	$P_{P_{H_2S}}$ [% P_T]	Dur. [days]	Fail?	pH		D_i [mm]	Final Volume		
						Initial	Final		[L]	[days]	[%]
A	>100	90	10	31	no	2.70	3.96	6.24	0.15	31	59
B	>100	90	10	31	no	2.70	3.58	6.26	0.24	31	95
E	100	80	10	30	no	2.70	8.43	6.42	0.30	18	100
F	100	80	10	30	no	2.70	9.20	6.42	0.30	18	100
G	100	80	20	(*)	(*)	2.70	-	6.35	0	<7	0
H	100	80	20	30	no	2.70	4.10	6.34	0.30	18	100
K	100	80	20	31	no	2.70	4.03	6.22	0.28	31	100
L	100	80	20	31	no	2.70	4.04	6.23	0.30	31	100

Table 4.6: Test results of Constant load test with H₂S for 25Cr Duplex with 4.8% pre-deformation.

ID	Load [%AYS]	T [°C]	$P_{P_{H_2S}}$ [% P_T]	Dur. [days]	Fail?	pH		D_i [mm]	Final Volume		
						Initial	Final		[L]	[days]	[%]
C	>100	90	20	31	no	2.70	3.88	6.29	0.20	31	79
D	>100	90	20	31	no	2.70	3.79	6.23	0.21	31	83
I	100	80	20	30	no	2.70	8.67	6.36	0.325	18	100
J	100	80	20	30	no	2.70	8.85	6.36	0.30	18	100

Table 4.7: Test results of Constant load test with H₂S for 25Cr Duplex with 10% pre-deformation. (*)Sample M lost all liquid at an unknown time and was disqualified.

ID	Load [%AYS]	T [°C]	P_{H_2S} [% P_T]	Dur. [days]	Fail?	pH		D_i [mm]	Final Volume		
						Initial	Final		[L]	[days]	[%]
M	100	80	20	(*)	(*)	2.70	-	6.23	0	-	0
N	100	80	20	31	no	2.70	4.04	6.22	0.25	31	99

Table 4.8: Test results of constant load test with H₂S for ATI-830 in modified ISO lvl 5 environment. No data available as testing was not completed prior to deadline of thesis.

ID	Load %AYS	T [°C]	P_{H_2S} [Mpa]	P_{CO_2} [Mpa]	Days	Failure	pH		D_i [mm]	D_f [mm]
							Initial	Final		
O	100	150	50	200	-	-	-	-	-	-
P	100	150	50	200	-	-	-	-	-	-

4.3 Post-examination

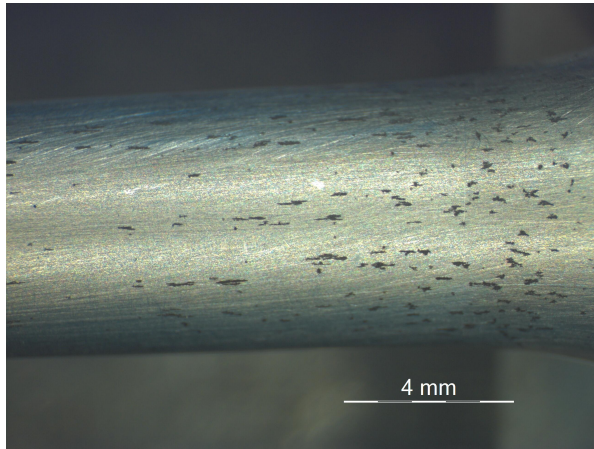
The surface of the test samples were investigated in a macroscope at up to 40X magnification. Pictures of each tensile sample are shown in figures 4.13-4.20 for 22Cr Duplex. 25Cr Duplex are shown in 4.21-4.24 and 4.25 for 4.8% and 10% pre-deformation, respectively. Only a few samples were cleaned properly prior to macroscope investigation. This is specified in each picture.

The following samples had further investigation of the cross section in LOM to measure pitting depth and look for micro-cracking in the pit. Results are shown in section 4.3.2.

- Sample K: 22Cr, 4.8% Pre-deformation, 20% H₂S
- Sample N: 25Cr, 10% Pre-deformation, 20% H₂S

4.3.1 Macroscope

4.3.1.1 22Cr Duplex

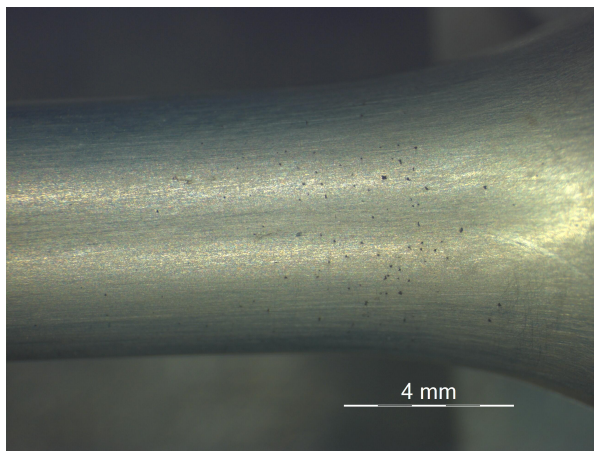


(a) 10X magnification

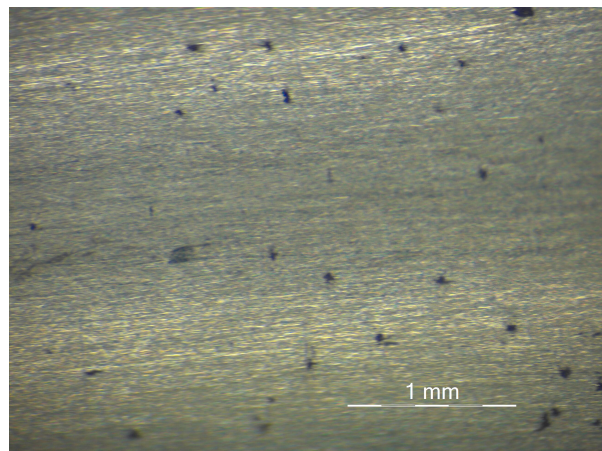


(b) 40X magnification

Figure 4.13: Sample A: 22Cr with 4.8% deformation tested in 10%H₂S and 90°C . Samples not cleaned prior to investigation.

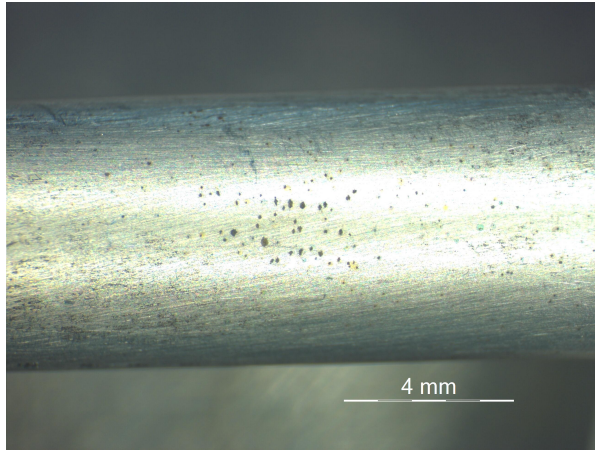


(a) 10X magnification

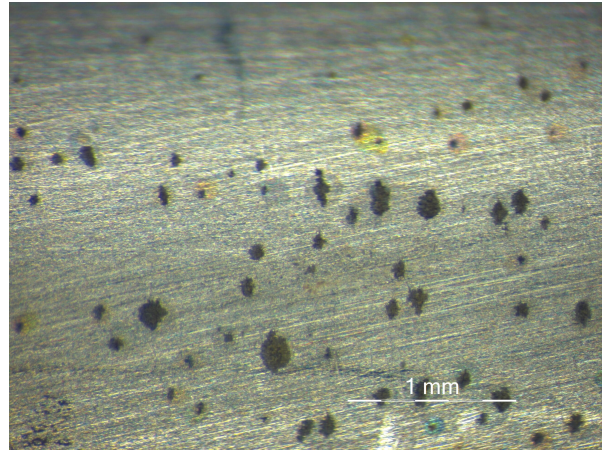


(b) 40X magnification

Figure 4.14: Sample B: 22Cr with 4.8% deformation tested in 10%H₂S and 90°C . Samples not cleaned prior to investigation.

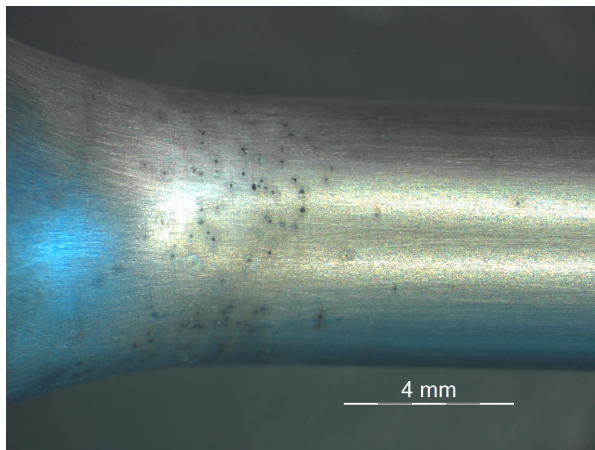


(a) 10X magnification

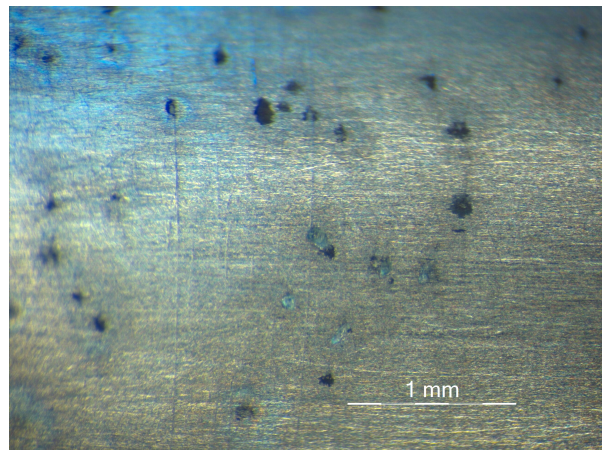


(b) 40X magnification

Figure 4.15: Sample E: 22Cr with 4.8% deformation tested in 10%H₂S and 80°C . Samples not cleaned prior to investigation.

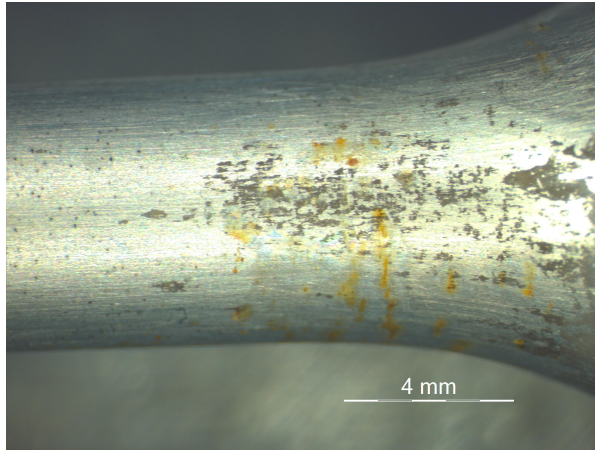


(a) 10X magnification

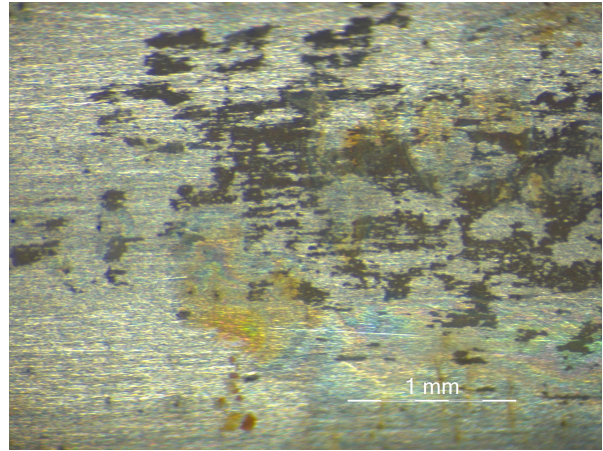


(b) 40X magnification

Figure 4.16: Sample F: 22Cr with 4.8% deformation tested in 10%H₂S and 80°C . Samples not cleaned prior to investigation.

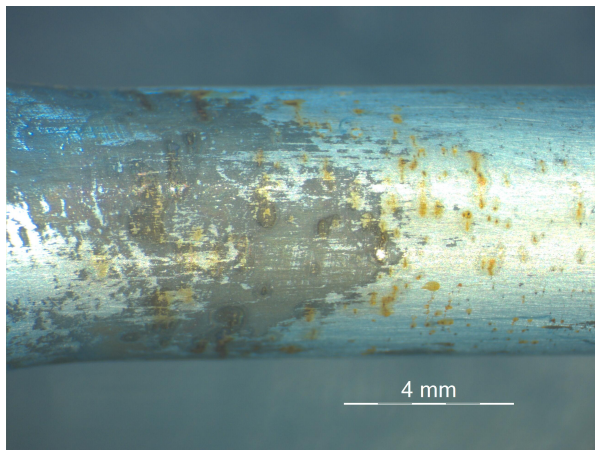


(a) 10X magnification

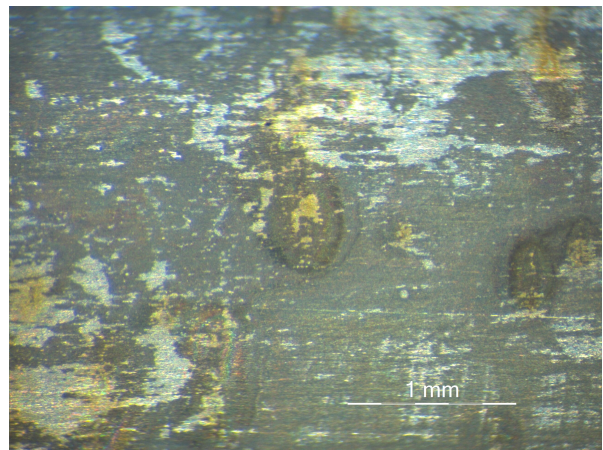


(b) 40X magnification

Figure 4.17: Sample H: 22Cr with 4.8% deformation tested in 20%H₂S and 80°C . First of two locations photographed. Samples not cleaned prior to investigation.

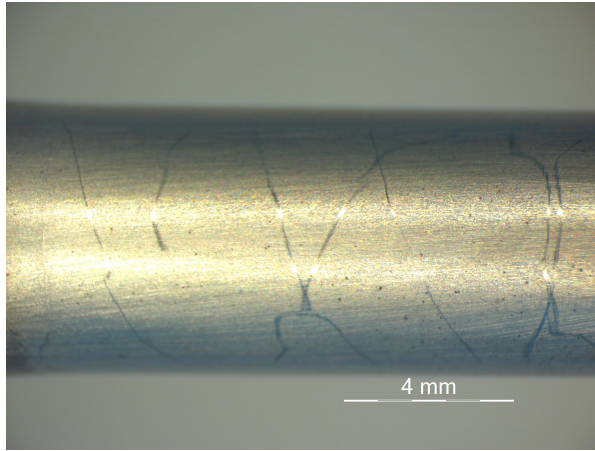


(a) 10X magnification

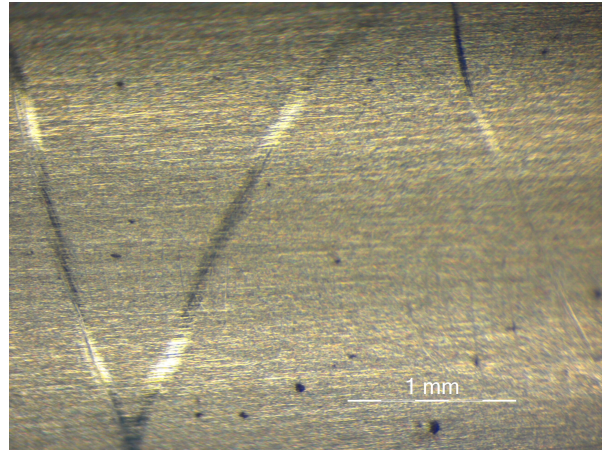


(b) 40X magnification

Figure 4.18: Sample H: 22Cr with 4.8% deformation tested in 20%H₂S and 80°C . Second of two locations photographed. Samples not cleaned prior to investigation.

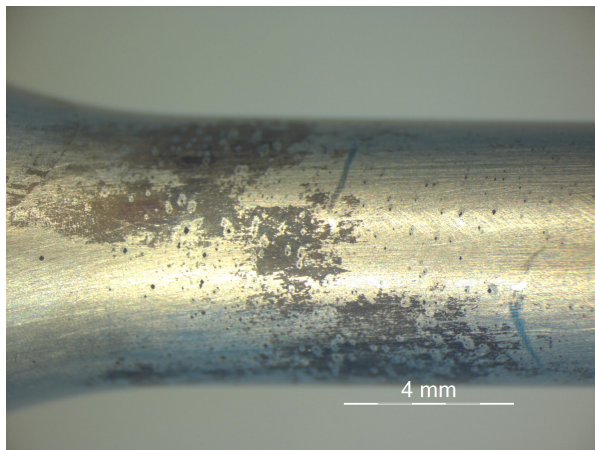


(a) 10 magnification

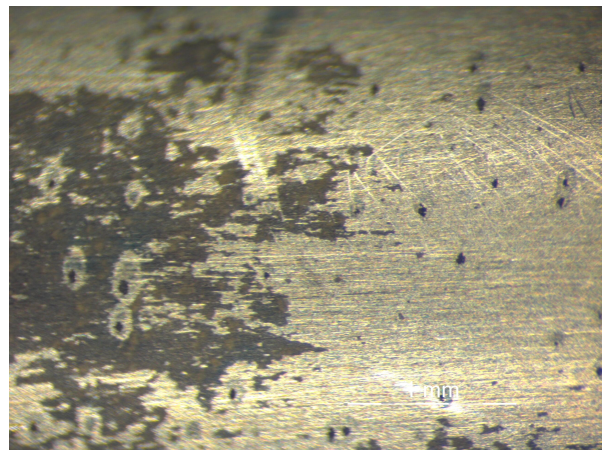


(b) 40 magnification

Figure 4.19: Sample K: 22Cr with 4.8% deformation tested in 20%H₂S and 80°C . Samples cleaned with soap and hot water.



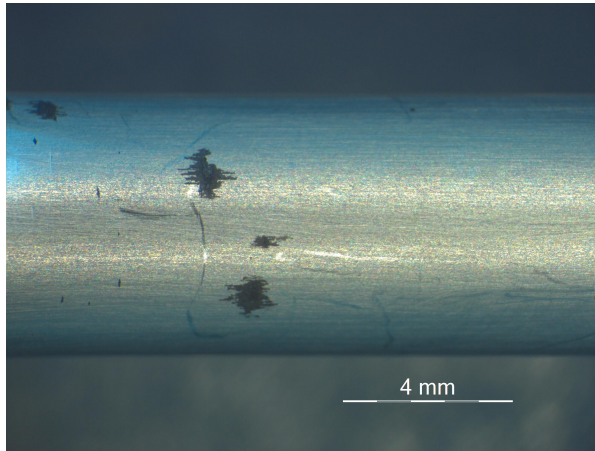
(a) 10X magnification



(b) 40X magnification

Figure 4.20: Sample L: 22Cr with 4.8% deformation tested in 20%H₂S and 80°C . Samples cleaned with soap and hot water.

4.3.1.2 25Cr Duplex

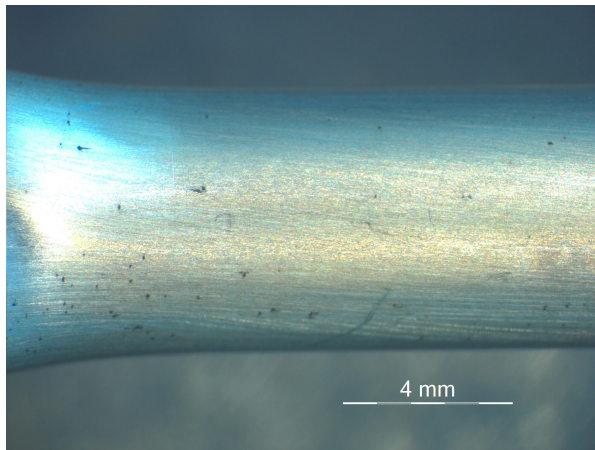


(a) 10X magnification

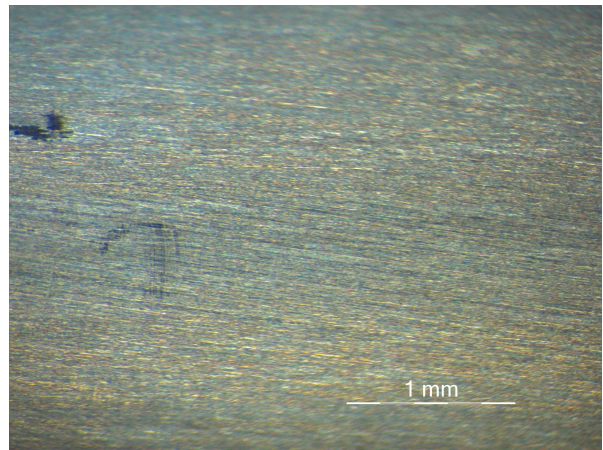


(b) 40X magnification

Figure 4.21: Sample C: 25Cr with 4.8% deformation tested in 20%H₂S and 90°C . Samples not cleaned prior to investigation.

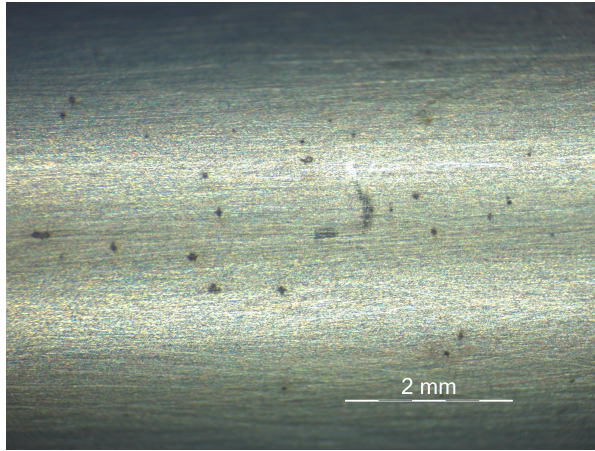


(a) 10X magnification

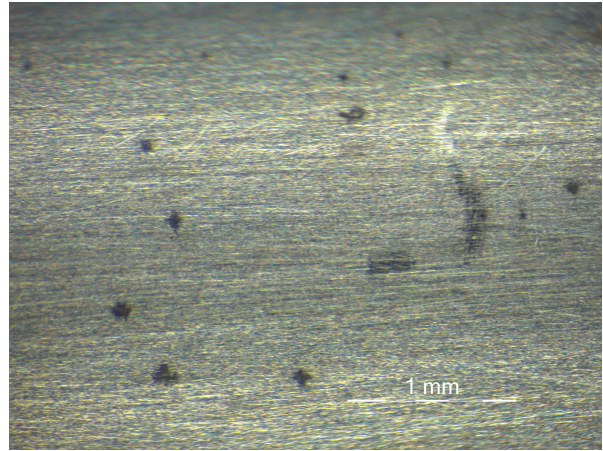


(b) 40X magnification

Figure 4.22: Sample D: 25Cr with 4.8% deformation tested in 20%H₂S and 90°C . Samples not cleaned prior to investigation.

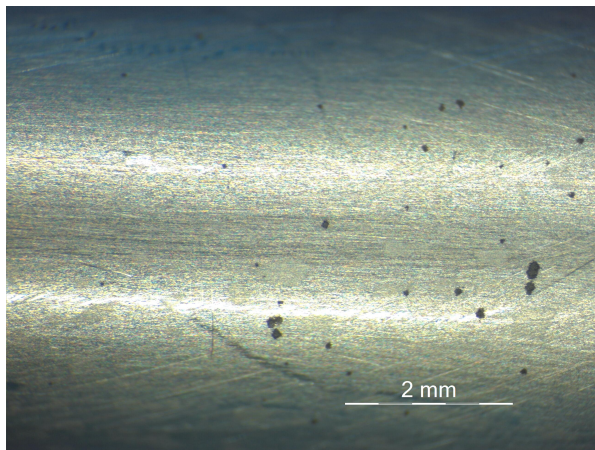


(a) 20X magnification

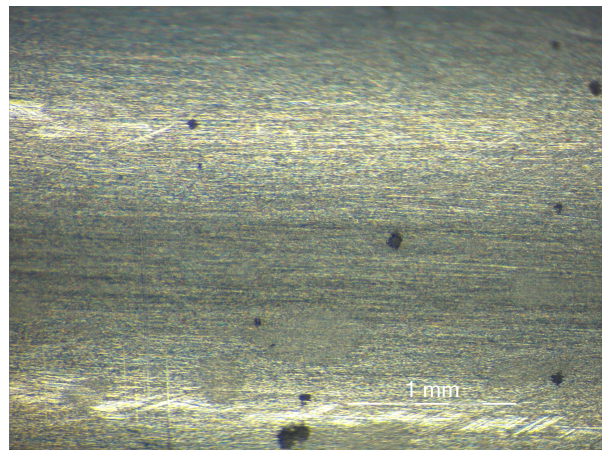


(b) 40X magnification

Figure 4.23: Sample I: 25Cr with 4.8% deformation tested in 20%H₂S and 80°C . Samples not cleaned prior to investigation.

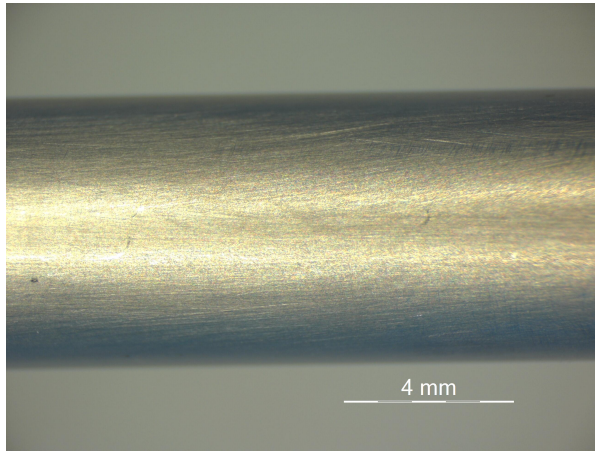


(a) 20X magnification

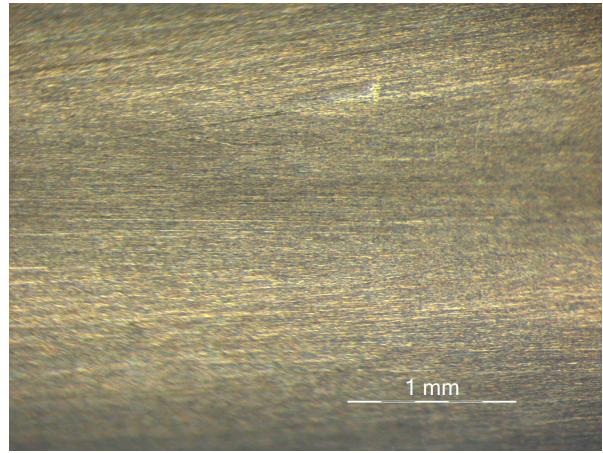


(b) 40X magnification

Figure 4.24: Sample J: 25Cr with 4.8% deformation tested in 20%H₂S and 80°C . Samples not cleaned prior to investigation.



(a) 10 magnification



(b) 40X magnification

Figure 4.25: Sample N: 25Cr with 10% deformation tested in 20% H₂S and 80°C . Samples cleaned with soap and hot water.

4.3.2 LOM of cross sections

A few pits were found on the cross sections of both samples. For sample K typical pits were ≈ 30 , and for sample N ≈ 50 . Figures in sections 4.3.3-4.3.4 show the most detrimental pits found on the samples, as well as a less magnified photo giving an overview of the surface. No signs of micro cracking were found.

Due to a limited amount of available moulding powder, only one sample of 22Cr Duplex SS and 25Cr Duplex SS. The samples investigated were chosen as they were assumed to be exposed to the worst condition in terms of deformation and H_2S -concentration.

4.3.3 Sample K: 22Cr Duplex SS, 4.8% Deformation, 20% H_2S

Two typical pits photographed are shown in figure 4.26. The pits have a typical depth of $< 30\mu m$ and showed no signs of microcracking in the bottom of the pits. The same pits can be seen in the overview picture shown in figure 4.27.

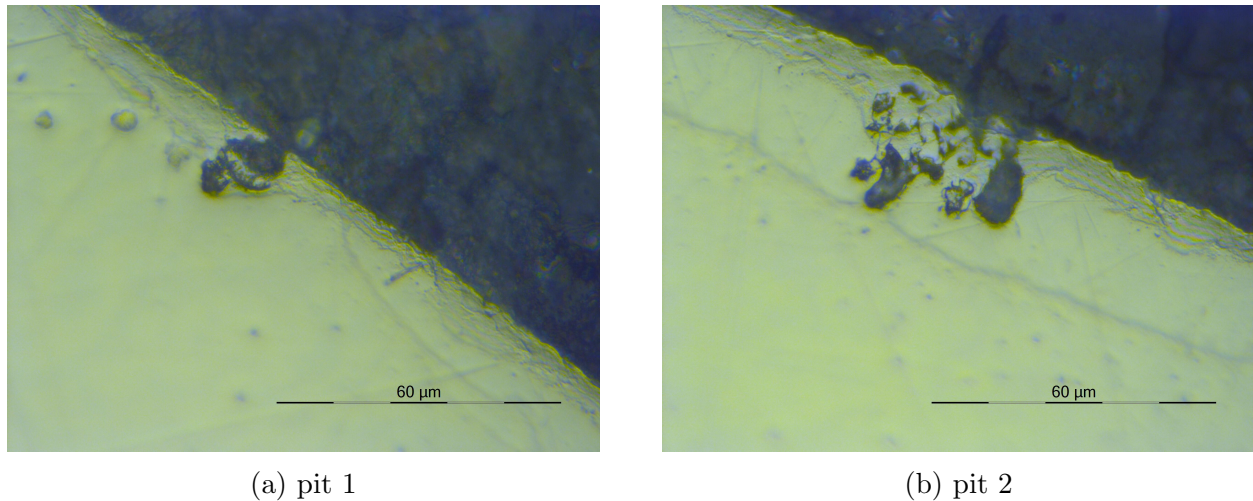


Figure 4.26: Two typical pits found on a cross section of sample K at 1000X magnification

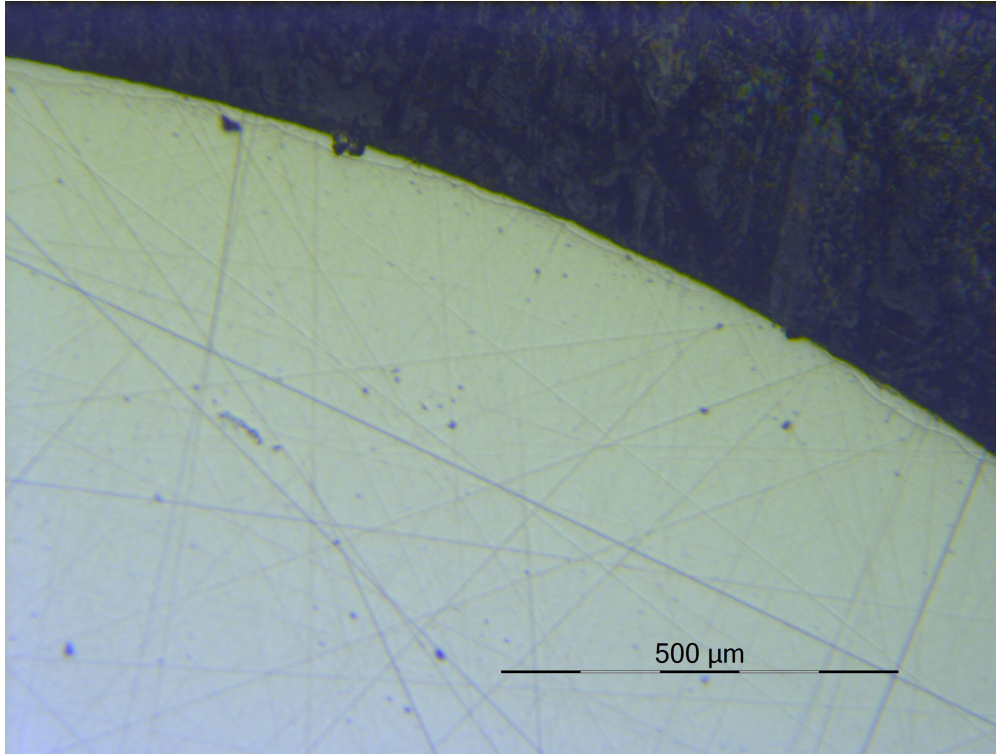


Figure 4.27: An overview of sample K at 100X magnification.

4.3.4 Sample N: 25Cr Duplex SS, 10% Deformation, 20% H_2S

A typical pit photographed is shown in figure 4.28. The pits had a typical depth of $<50\mu m$ and showed no signs of microcracking in the pottom of the pits. The same pit can be seen in the overview picture shown in figure 4.29

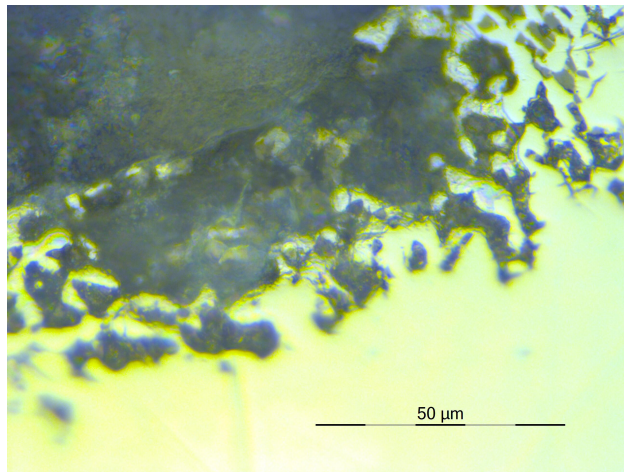


Figure 4.28: A typical pit found on a cross section of sample N at 1000X magnification.

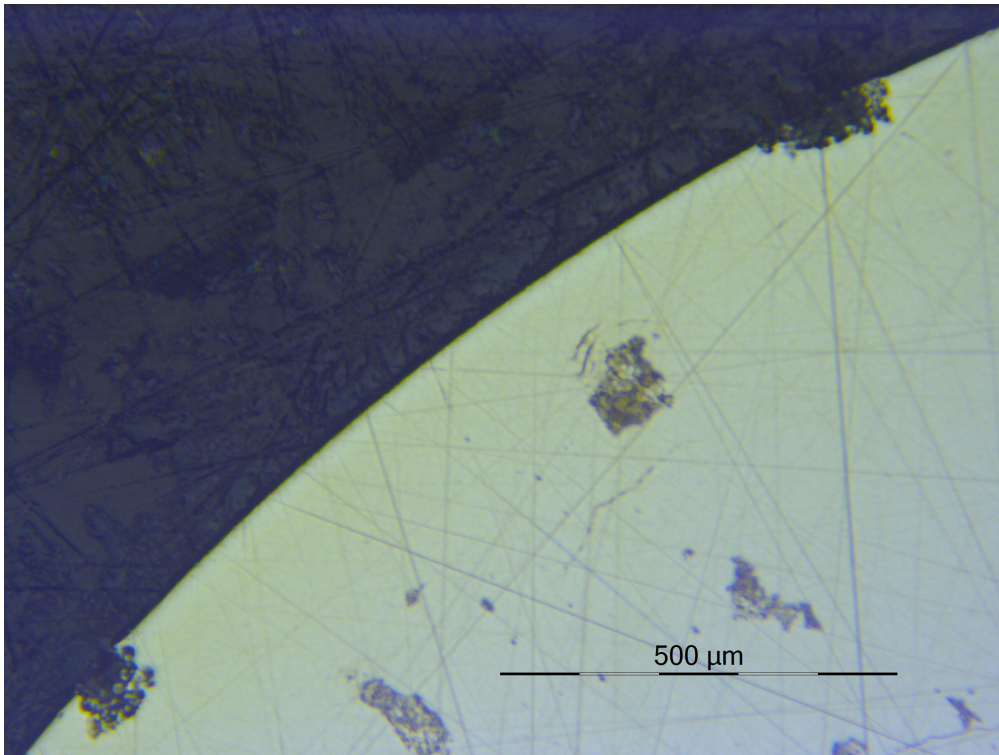


Figure 4.29: An overview of sample N at 100X magnification.

Chapter 5

Discussion

5.1 Comparison with other test results

Little information of earlier testing on these materials in H₂S have been found, and no information of testing on the used Duplex SS materials with deformation in H₂S has been found. However an annealed UNS S31803 sample, the same material as the 22Cr Duplex SS investigated in this work, was tested with various levels of Cl⁻, pH and H₂S partial pressures³³ (see table 2.5). No cracking occurred for gas concentrations of up to 34kPa H₂S, but fractures occurred for samples tested with 69kPa H₂S after roughly 45 days of exposure.

5.2 Experimental Parameters

5.2.1 Test Temperature

As discussed in section 2.6.2, ISO 15156-3 specifies 80-90°C as the worst temperature range,² and other literature supports this as well as that a range as wide as 80-120°C may show the most detrimental effects.^{18,29,30} Temperature was chosen arbitrarily within this range, initially at 90°C, and later 80°C due to difficulties with loss of test liquid. No information about which temperature that will give the most severe environment was found during the literature study, but it seems reasonable that a higher temperature (e.g. 120°C) could increase the pitting growth rate on the samples, thus increasing the risk of micro cracking at the bottom of the pit.

5.2.2 Deformation and Microstructure

ISO 15156-3 does not give any guidance for how much additional deformation the Duplex SS materials can take when exposed to an H₂S-environment.² No signs of cracking was found for sample K and N (22Cr and 25Cr, respectively), which were the samples with highest deformation and H₂S-concentration for each of the materials. This may indicate that some deformation (up to 4.8% for 22Cr Duplex SS and 10% for 25Cr Duplex SS) has little effect

on the materials susceptibility to SSC, but more testing, perhaps at longer intervals, should be done before this can be concluded.

Unpublished resources has shown that for a plain carbon steel deformation under exposure to sour service has a much higher risk of causing fracture than deformation occurring prior to sour service. That is, deformation caused by for instance on and of-reeling of a pipe should be less detrimental than deformation caused during operation. As the constant load test only gives information about the material's susceptibility to H₂S-related failures with pre-deformation, it would be very useful to see whether or not the material's would show the same resistance using SSRT. As described in section 2.9.1.2, this method applies and increases load during testing. This test would possibly give a more precise idea of the area where the material will fail as a constant load test that does not lead to fracture says nothing about the upper limits of the material.

As discussed in see section 2.7.1-2.7.2, the pre-examination of the materials showed a very fine-grained microstructure, which is beneficial against risk of cracking.²¹ The added material deformation was done along its longitudinal axis, i.e., parallel to the elongated duplex grains. It was therefore expected, with good reason, that cracking resistance along the cross section was largely conserved. However, theory also shows a larger hydrogen ingress with added cold work.²¹ Given the longitudinal structure, a higher risk of crack propagation is to be expected along the longitudinal direction with higher cold deformation, as this increases the distance between the -islands, which act as crack barriers.

5.2.3 H₂S-concentration

A maximum of 10% H₂S is recommended for the 22Cr Duplex SS according to ISO 15156-3,² however none of the 22Cr Duplex SS samples that were tested with 20% failed or showed signs of cracking (sample K and L). Some pitting did however occur, and it can therefor not be concluded that the material will be safe within this environment before further testing is done. As with deformation, testing for a longer interval could be of interest, to see if the pits grow further, followed by crack initiation.

5.3 Experimental challenges

5.3.1 Loading of samples

Loading of samples was done at ambient temperature, and adjustments were made to adjust for cold creep. A typical case would be to apply a load of approximately 90% of AYS, which should then result in 100% AYS at test temperature. However, if any cold creep occurred during heating of the samples this would not be possible to adjust. This means that in some cases the applied load could be a bit lower than the intended value of 100% AYS at test temperature. For the first samples (A-F) load a load of 100% AYS at room temperature was applied by mistake, which led to a higher load during test temperature. These results of these samples are therefore more conservative with regards to applied load.

5.3.2 NaOH contamination of test solution

Certain samples in test set 2 were exposed to NaOH solution during the refill procedure. This resulted in pH values in the area of 8 to 9. During the refill procedure, temperature was shut of, which resulted in NaOH-solution creeping up the hoses and in to the test cells. The tests did therefor not contain uncontaminated NACE Test Solution A for longer than 12 days. It is likely that use of a condenser as required NACE TM0177²⁸ this would not have happened as liquid loss should have been limited. Unfortunately, this equipment was not available.

5.4 Validity of results

Due to the loss of water through the vapour phase, some samples were not fully exposed to the test solution throughout the experiment. The worst case (sample G) was measured to have a gauge area coverage of only 59%. Most samples did however have 80-100% Coverage. As loss of water from the test solution leads to a higher salinity, the test solution is assumed to be give more concervative results (for the part that was exposed to liquid throughout the test). For further testing use of a condenser is highly recommended.

Lastly, it is important to emphasize, as discussed in section 5.1, that similar materials did fail in similar experiments with longer test periods. This gives a good reason to question whether or not some of the samples tested in this paper would fracture, or at least show signs of micro-cracking in the pits, if a longer time of exposure was used.

Chapter 6

Conclusion

22% Cr duplex SS (wrought) and 25% Cr Duplex SS (wrought) were tested with constant load under exposure to H₂S-partial pressure of 10 or 20kPa. The materials were cold deformed to 4.8% or 10% prior to testing. The first samples were loaded to 100% AYS at room temperature, whereas the rest were loaded to a lower value that was estimated to be 100% AYS at actual test temperature. Materials and parameters are summarized in table 6.1. No samples failed, but some pitting was found during LOM investigation of samples subjected to the most detrimental parameters. No signs of micro-cracking were found in the pits.

This may indicate that limits given for sour service of Duplex SS in ISO 15156-3 are too strict, but due to uncertainties in the experiments further testing is required to be certain.

The preliminary theoretical study gave reason to expect a higher susceptibility to cracking with higher deformation or H₂S-partial pressure. This was neither confirmed nor rejected due to the limited experimental scope.

Table 6.1: Summary of materials tested with key parameters.

Material	Deformation [%]	Load [%AYS]	Temperature [°C]	$P_{\text{H}_2\text{S}}$ [kPA]
22Cr Duplex SS	4.8	>100	90	10
22Cr Duplex SS	4.8	100	80	10
22Cr Duplex SS	4.8	100	80	20
25Cr Duplex SS	4.8	>100	90	20
25Cr Duplex SS	4.8	100	80	20
25Cr Duplex SS	10	100	80	20

Bibliography

- ¹ ISO 15156-1:2015(E) Petroleum and natural gas industries - Materials for use in H₂S-containing environment in oil and gas production - Part1: General principles for selection of cracking-resistant materials. Standard, International Organization for Standardization, Geneva, CH, September 2015.
- ² ISO 15156-3:2015(E) Petroleum and natural gas industries - Materials for use in H₂S-containing environment in oil and gas production - Part3: Cracking-resistant CRAs (corrosion-resistant alloys) and other alloys. Standard, International Organization for Standardization, Geneva, CH, September 2015.
- ³ Jakob Enerhaug. *A study of localized corrosion in super martensitic stainless steel weldments*. Phd thesis, Norges teknisk-naturvitenskapelige universitet, Instituttfor maskinkonstruksjon og materialteknikk, 2002.
- ⁴ Christophe Mendibide and Thomas Sourmail. Composition optimization of high-strength steels for sulfide stress cracking resistance improvement. *Corrosion Science*, 51(12):2878–2884, 2009.
- ⁵ P. R. Rhodes. Environment-assisted cracking of corrosion-resistant alloys in oil and gas production environments: A review. *Corrosion*, 57(11):923–966, 2001.
- ⁶ Johnson W. H. On some remarkable changes produced in iron and steel by the action of hydrogen and acids. *Proceedings of the Royal Society of London*, 23:168–179, 1874.
- ⁷ J Ćwiek. Prevention methods against hydrogen degradation of steel. *Manufacturing Engineering*, 43(1):214–221, 2010.
- ⁸ N. Nanninga, J. Grochowski, L. Heldt, and K. Rundman. Role of microstructure, composition and hardness in resisting hydrogen embrittlement of fastener grade steels. *Corrosion Science*, 52(4):1237–1246, 2010.
- ⁹ A. Taha and P. Sofronis. A micromechanics approach to the study of hydrogen transport and embrittlement. *Engineering Fracture Mechanics*, 68(6):803–837, 2001.
- ¹⁰ P. Sofronis, Y. Liang, and N. Aravas. Hydrogen induced shear localization of the plastic flow in metals and alloys. *European Journal of Mechanics / A Solids*, 20(6):857–872, 2001.

- ¹¹ Peter F. Timmins. *Solutions to hydrogen attack in steels*. 1997.
- ¹² N. Eliaz, A. Shachar, B. Tal, and D. Eliezer. Characteristics of hydrogen embrittlement, stress corrosion cracking and tempered martensite embrittlement in high-strength steels. *Engineering Failure Analysis*, 9(2):167–184, 2002.
- ¹³ P. Roffey and E. H. Davies. The generation of corrosion under insulation and stress corrosion cracking due to sulphide stress cracking in an austenitic stainless steel hydrocarbon gas pipeline. *Engineering Failure Analysis*, 44:148–157, 2014.
- ¹⁴ B. Y. Fang, A. Atrens, J. Q. Wang, E. H. Han, Z. Y. Zhu, and W. Ke. Review of stress corrosion cracking of pipeline steels in “low” and “high” pH solutions. *Journal of Materials Science*, 38(1):127–132, 2003.
- ¹⁵ Sridhar Ramamurthy and Andrej Atrens. Stress corrosion cracking of high-strength steels. *Corrosion Reviews*, 31(1):1–31, 2013.
- ¹⁶ Ming-Chun Zhao, Bei Tang, Yi-Yin Shan, and Ke Yang. Role of microstructure on sulfide stress cracking of oil and gas pipeline steels. *Metallurgical and Materials Transactions A*, 34(5):1089–1096, 2003.
- ¹⁷ P. R. Rhodes, L. A. Skogsberg, and R. N. Tuttle. Pushing the limits of metals in corrosive oil and gas well environments. *Corrosion*, 63(1):63–100, 2007.
- ¹⁸ R. D. Kane. Roles of H₂S in behaviour of engineering alloys. *International Metals Reviews*, 30(1):291–301, 1998.
- ¹⁹ The European Federation of Corrosion. Guidelines on materials requirements for carbon and low alloy steels for H₂S-containing environments in oil and gas production. *Publication Number 16*, 1995.
- ²⁰ H. K. D. H. Bhadeshia and Sir Robert Honeycombe. *Steels: Microstructures and Properties (Third Edition)*, 5 - Formation of Martensite, pages 95–128. Butterworth-Heinemann, Oxford, 2006.
- ²¹ Thierry Cassagne and Freddy Embrittlement. A review on hydrogen embrittlement of duplex stainless steels. *Corrosion*, Paper No. 5098, 2005.
- ²² H. K. D. H. Bhadeshia and Sir Robert Honeycombe. *Steels: Microstructures and Properties (Third Edition)*, 12 - Stainless Steel, pages 259–286. Butterworth-Heinemann, Oxford, 2006.
- ²³ Jan Kjetil Solberg. Teknologiske metaller og legeringer. 2014.
- ²⁴ William D. Callister and David G. Rethwisch. *Materials science and engineering : an introduction*. Wiley, New York, 7th ed. edition, 2007.

- ²⁵ George E. Dieter and David Bacon. *Mechanical metallurgy*. McGraw-Hill series in materials science and engineering. McGraw-Hill, London, si metric ed. edition, 1988.
- ²⁶ P. Marcus. *Corrosion Mechanisms in Theory and Practice: Second Edition, Revised and Expanded, Sulfur-Assisted Corrosion Mechanisms and the Role of Alloyed Elements*, pages 287–310. 202.
- ²⁷ O. I. Radkevych and V. I. Pokhmurs'kyi. Influence of hydrogen sulfide on serviceability of materials of gas field equipment. *Materials Science*, 37(2):319–332, 2001.
- ²⁸ Nace standard tm0177-2005, "laboratory testing of metals for resistance to sulfide stress cracking and stress corrosion cracking in H₂S environments. Standard, International Organization for Standardization, Geneva, CH, September 2015.
- ²⁹ The European Federation of Corrosion. Corrosion resistant alloys for oil and gas production: guidance on general requirements for test methods for H₂S service. *Publication Number 17*, 1996.
- ³⁰ Fiona Ruel, Saghi Saedlou, Sandra Le Manchet, Christian Lojewski, and Krzysztof Wolski. The influence of temperature and ph on the eac behavior of the uns(1) s32304 lean duplex stainless steel. 2014.
- ³¹ A. M. Brass and J. Chene. Influence of deformation on the hydrogen behavior in iron and nickel base alloys: a review of experimental data. *Materials Science & Engineering A*, 242(1):210–221, 1998.
- ³² V. Olden, C. Thaulow, and R. Johnsen. Modelling of hydrogen diffusion and hydrogen induced cracking in supermartensitic and duplex stainless steels. *Materials & Design*, 29(10):1934–1948, 2008.
- ³³ Julio G. Maldonado and James W. Skogsberg. Cracking susceptibility of duplex stainless steel at an intermediate temperature in the presence of h₂s containing environments. *Corrosion*, Paper No. 4134, 2004.
- ³⁴ Gerit Siegmund, Guenter Schmitt, and Lars Kuhl. Unexpected sour cracking resistance of duplex and superduplex steels. *Corrosion*, Paper No. 7631, 2016.
- ³⁵ K. Saarinen, E. Hamalainen, and H. Hanninen. Slow strain rate testing of corrosion resistant alloys in high temperature h₂s environments. *NACE International*, 1997.
- ³⁶ Shuji Hashizume and Yasuto Inohara. Effects of ph and ph₂s on ssc resistance of martensitic stainless steels. *NACE International*, 2000.
- ³⁷ J. A. Beavers and G. H. Koch. Limitations of the slow strain rate test for stress corrosion cracking testing. *NACE International*, 1992.

- ³⁸ A. J. Griffiths, G. Hinds, and A. Turnbull. Monotonic and cyclic slow strain rate testing of super 13% chromium steel welds under cathodic protection, february 2005. *Corrosion*, 62(2):111–118, 2005.
- ³⁹ Kenji Kobayashi, Masakatsu Ueda, Keiichi Nakamura, and Tomohiko T. Omura. Effect of testing temperature on ssc properties of low alloy steel. *Corrosion*, Paper No. 6127, 2006.
- ⁴⁰ Astm e562 - 02 standard test method for determining volume fraction by systematic manual point count. Standard.
- ⁴¹ <https://imagej.nih.gov/ij/index.html>. 29/05/2017.

Appendix

A Risk analysis

	Kartlegging av risikofylt aktivitet	Uarbeidet av	Nummer	Dato	
		HMS-avd	HMSRV2601	22.03.2011	
		Godkjent av		Eretatter	
		Rektor		01.12.2006	

Enhet: IPM

Dato: 03/02/2017

Linjeleder: Roy Johnsen

Deltakere ved kartleggingen (m/ funksjon): Roy Johnsen (hovedveileder), Svein Olestad (student), Erik K. Sverre (Technical Manager Laboratory Facilities)
 (Ansv. veileder, student, evt. medveileder, evt. andre m. kompetanse)



Kort beskrivelse av hovedaktivitet/hovedprosess: Hydrogen Embrittlement of 25Cr duplex stainless steel exposed to well fluid with H₂S - effect of cold working and product form

Er oppgaven rent teoretisk? (JA/NEI): NEI «JA» betyr at veileder innstår for at oppgaven ikke inneholder noen aktiviteter som krever risikovurdering. Dersom «JA»: Beskriv kort aktivitetene i kartleggingskjemaet under. Risikovurdering trenger ikke å fylles ut.

Signaturer: Ansvartlig veileder: 

Student: 

ID nr.	Aktivitet/prosess	Ansvartlig	Eksisterende dokumentasjon	Eksisterende sikringstiltak	Lov, forskrift o.l.	Kommentar
1	SEM work: investigation of material prior to H ₂ S-testing	- Svein Olestad (user) - DNV-GL (equipment prov)	Internal general HSE docs at DNV-GL Bergen	Training on site by experienced personnel		
2	Constant load test of material in H ₂ S-environment	- Svein Olestad (user) - DNV-GL (equipment prov)	(1) "Handling and use of H ₂ S gas" (DNV-GL) (2) "Risk and safety brief for non-employed personnel" (DNV-GL) (3) "HSE and security lab Marineholmen" (DNV-GL) (4) "Fire escape hood instruction manual" (5) "Gas alert micro clip XT use and maintenance manual"	- Training on site by experienced personnel - Safety documents prior to work - use of local gas detector on body in addition to detection system in each room - familiarization given in lab (escape route, alarm levels, shut down system muster station)		

 NTNU HMS	Risikovurdering			Utbildet av	Nummer	Dato	
	HMS-avd	HMSRV2601	22 03 2011				
	Godkjent av		Erstatter				
	Rektor		01.12.2006				

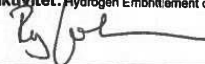
Enhet: IPM

Dato: 03/02/2017

Linjeleder: Roy Johnsen



Deltakere ved kartleggingen (m/ funksjon): Roy Johnsen (hovedveileder), Svein Ollestad (student), Erik K Sverre (Technical Manager Laboratory Facilities)
 (Ansv. Veileder, student, evt. medveileder, evt. andre m kompetanse)

Risikovurderingen gjelder hovedaktivitet: Hydrogen Embrittlement of 26Cr duplex stainless steel exposed to well fluid with H2S - effect of cold working and product form

Signaturer: Ansvarlig veileder: 

Student: 

ID nr	Aktivitet fra kartleggings-skjemaet	Mulig usøsket hendelse/belastning	Vurdering av sannsynlighet (1-5)	Vurdering av konsekvens:				Risiko-Verdi (menn-øske)	Kommentarer/status Forslag til tiltak
				Menneske (A-E)	Ytre miljø (A-E)	ØK/materiell (A-E)	Om-demme (A-E)		
1	Use of SEM	Damage to equipment	3	A	A	A	A	Follow instructions as given Take care when removing sample from chamber	
2	Connection of equipment	Damage to equipment (o-rings) (or other sealing component)	3	A	A	A	A	Perform pressure test with leak detection to avoid that non-sealing equipment is used with H2S	
2	Application of H2S atm	Leakage of H2S gas. H2S is highly toxic and may lead to unconsciousness if sufficient H2S is in the atmosphere	1	E	B	B	D	<ul style="list-style-type: none"> - No personnel is given access to lab without sufficient training prior to work - use of gas alarm in room and on personnel issues warning before concentration is too high - ventilation and H2S scrubber to evacuate H2S atmosphere and "jet" that sends H2S alarm system with SMS warning to relevant personnel - personnel protective gear including "escape gas mask", gloves, eyewear, coat 	
2	Disconnection of H2S connection and removal of H2S gas	Leakage of H2S gas unconsciousness of personnel	1	E	B	B	D	<ul style="list-style-type: none"> - Same as for "application of H2S" - flushing of test chamber with Nitrogen for at least 24 hours before opening 	

NTNU	Risikovurdering			Utarbeidet av	Nummer	Dato
 HMS				HMS-avd.	HMSRV/2601	22.03.2011
		Godkjent av		Erstatter		
		Rektor			01.12.2006	

Sannsynlighet vurderes etter følgende kriterier:

Svært liten 1	Liten 2	Middels 3	Stor 4	Svært stor 5
1 gang pr 50 år eller sjeldnere	1 gang pr 10 år eller sjeldnere	1 gang pr år eller sjeldnere	1 gang pr måned eller sjeldnere	Skjer ukentlig

Konsekvens vurderes etter følgende kriterier:

Gradering	Menneske	Ytre miljø Vann, jord og luft	Øk/materiell	Omdømme
E Svært Alvorlig	Død	Svært langvarig og ikke reversibel skade	Drifts- eller aktivitetssjans > 1 år.	Troverdighet og respekt betydelig og varig svekket
D Alvorlig	Alvorlig personskade. Mulig uførhet.	Langvarig skade. Lang restitusjonstid	Drifts- eller aktivitetssjans i opp til 1 år	Troverdighet og respekt betydelig svekket
C Moderat	Alvorlig personskade.	Mindre skade og lang restitusjonstid	Drifts- eller aktivitetssjans < 1 mnd	Troverdighet og respekt svekket
B Liten	Skade som krever medisinsk behandling	Mindre skade og kort restitusjonstid	Drifts- eller aktivitetssjans < 1 uke	Negativ påvirkning på troverdighet og respekt
A Svært liten	Skade som krever førstehjelp	Ubetydelig skade og kort restitusjonstid	Drifts- eller aktivitetssjans < 1 dag	Liten påvirkning på troverdighet og respekt

Risikoverdi = Sannsynlighet x Konsekvens

Beregn risikoverdi for Menneske. Enheten vurderer selv om de i tillegg vil beregne risikoverdi for Ytre miljø, Økonomi/materiell og Omdømme. I så fall beregnes disse hver for seg.

Til kolonnen "Kommentarer/status, forslag til forebyggende og korrigerende tiltak":

Tiltak kan påvirke både sannsynlighet og konsekvens. Prioriter tiltak som kan forhindre at hendelsen inntreffer, dvs. sannsynlighetsreduserende tiltak foran skjerpet beredskap, dvs. konsekvensreduserende tiltak.

NTNU		Risikomatrise		Dato	
HMS/KKS				08.03.2010	
		utarbeidet av		Nummer	
		HMS-avd.		HMSRV2604	
		godkjent av		Erstatter	
		Rektor		09.02.2010	



MATRISSE FOR RISIKOVURDERINGER ved NTNU

KONSEKVENNS		E1	E2	E3	E4	E5
Svært alvorlig						
Alvorlig		D1	D2	D3	D4	D5
Moderat		C1	C2	C3	C4	C5
Liten		B1	B2	B3	B4	B5
Svært liten		A1	A2	A3	A4	A5
		Svært liten	Liten	Middels	Stor	Svært stor
SANNSYNLIGHET						

Prinsipp over akseptkriterium. Forklaring av fargene som er brukt i risikomatrisen.

Farge	Beskrivelse
Rød	Uakseptabel risiko. Tiltak skal gjennomføres for å redusere risikoen.
Gul	Vurderingsområde. Tiltak skal vurderes.
Grønn	Akseptabel risiko. Tiltak kan vurderes ut fra andre hensyn.

B Poster

Masteroppgave ved

IPM

Våren 2017

Hydrogen Embrittlement of
25Cr duplex stainless steel
exposed to well fluid with
 H_2S – effect of cold working
and product form

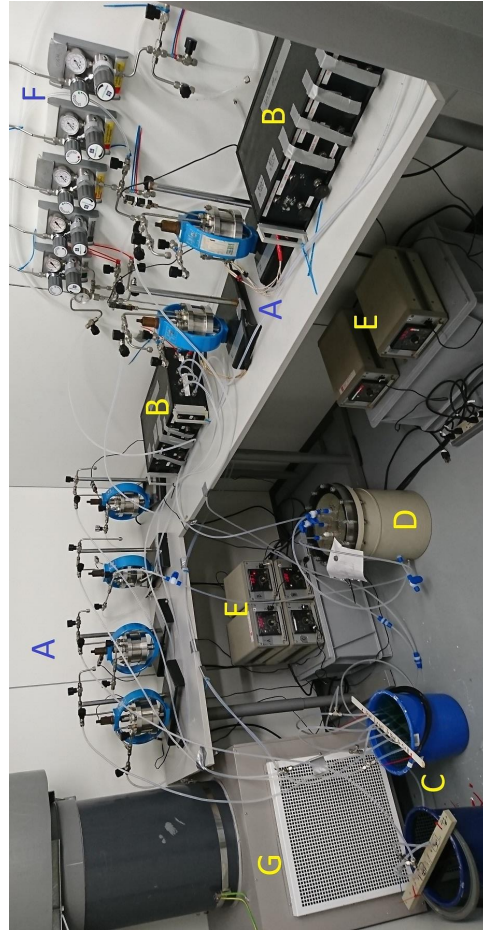
-
Svein Ollestad



Faglærer: Roy Johnsen

It is known that cold deformation may have detrimental effects on resistance against Sulphide Stress Cracking/Stress Corrosion Cracking and Hydrogen Induced Stress Cracking. Though it is clear that cold deformation should be restricted, it is sometimes necessary due to e.g. reeling installation or cold sizing. However, the most common standards relevant for pipe production and fabrication are not specific in how much cold deformation that can be allowed. NACE0175/ISO 15156 and ASME B31.3 allows maximum 5% cold deformation for carbon steel without subsequent heat treatment, but no limits are given for stainless steels (SS). Norsok M-101 allows up to 10% for austenitic SS and 5% for duplex SS and Ni alloys, but as this is a standard for structural steel fabrication, this limit does not consider H_2S service.

Testing was carried out on duplex stainless steel to get a better understanding of limitations on the amount of cold deformation these materials can have in a sour environment. 25% Cr duplex SS (wrought) and 22% Cr duplex SS (wrought) was tested by constant load in NACE Solution A at various temperatures, H_2S -partial pressure and deformation grades.



C Material Certificate - 22Cr

Acciaierie Valbruna S.p.A.



**CERTIFICATO DI COLLAUDO
ABNAHMEPRUEFZEUGNIS
INSPECTION CERTIFICATE
CERTIFICAT DE RECEPTION
EN 10204 (2004) , 3.1**

QUALITY MANAGEMENT SYSTEM CERTIFIED BY LLOYD'S REGISTER

36100 VICENZA (Italia) - Viale della scienza, 25 z.i.
Telefono 0444.968211 - Fax 0444.963836
Stab.: 39100 BOLZANO (Italia) - Via A. Volta, 4/37
Telefono 0471.924111 - Fax 0471.924497

Cliente / Besteller/Purchaser/Client
VALBRUNA NORDIC AB
LOVARTSGATAN 7
65221 - KARLSTAD - SWEDEN - SE

Produttore : **ACCIAIERIE VALBRUNA S.P.A.**
Hersteller/Item/Usine produttrice

Stato di fornitura : Hot rolled Descaled Annealed Hot
Lieferzustand / Delivery state rolled
Etat de livraison

Avviso di Spedizione: D-VI15027802
Lieferanzeige/Packing list/B.L.

Ordine nr: R31641 R31641
Bestell Your order Commande

Tipo di Elaborazione: E+AOD
Erschmelzungsart/Melting process/Mode d'elaboration

Certificato nr: MEST768512/2015/
Prüfung/Test/Essai

Conferma ordine nr: EI15000377
Werks/Our Order/Ref nr.

Marchio di Fabbrica:

Zeichen des Lieferwerkes
Trade mark
Sigle de fusine produtrice

Punzone del Collaudatore:
Stempel des Werksachverständigen
Inspector's stamp/Poinçon de l'essayeur



MR

Specifiche:
Anforderungen / Requirements / Exigences

MS-RB-4462 9 1.4462/F51/60 A
ASTM A182 2014A S32205 A (2)
ASTM A479 2014 S31803 A
ASTM G48 2011 METHOD A
NACE MR0103 2010 S31803 A

(0)Norsok-standard M-630 Edition 6, October 2013
(0)QTR N°10 for forged bars and N°38 for hot rolled bars.
(1)to ASTM A479.
(2)to ASTM A479.
(3)Technical circular 1:2011 Published 2011-06-14

Qualità: S31803

Werkstoff/Grade/Nuance

MDS D47 5 S31803 A (0)
ASTM A276 2013A S31803 A
ASTM A479 2014 S32205 A
EN 10088-3 2005 1.4462 A
NACE MR0175 2009 S31803 A (3)

(0)Approval Norsok-standard M-650 Edition 4, September 2011
(1)For products machined directly from bar refer also
(2)For products machined directly from bar refer also
(3)ANSI/NACE MR0175/ISO 15156-3, second edition 2009-10-15

ASTM A182 2014A S31803 A (1)
ASTM A276 2013A S32205 A
ASTM E562 2005 .
EN 10272 2007 1.4462 A

Marca:

Markenbezeichnung Brand/Nuance **V225MN**

Tolleranza: Tol. as requested
Tolleranza/Allowance/Tolerance

Punzonatura: S31803
Kennzeichnung/Marking/Marquage

Pos. nr. Pos. nr. Item nr. Nr. de poste	Oggetto Gegenstand Product description Descrip. du produit	Dimensioni - mm Abmessungen Dimension Dimension	Lunghezza - mm Länge Length Longueur	Colata Schmelze Heat Coulée	Pezzi Stückzahl Pieces	Peso - KG Gewicht Weight Poids	Lotto nr. Losr. Lot nr. Lot nr.
0070	Round	16,000	3300/ 3300	427440		877,0	501604210

TEST ALLO STATO DI FORNITURA Test on delivery condition Prüfung auf lieferbarem produkt test a l'etat de fourniture Prueba sobre el material así como entregado													
TEST	Provetta/Probestab Specimen/Eprovette Larg diam Spess. Brosle Diam. Dicke Width diam. Thickness Larg. diam. epais mm	°C Posiz. Saggio Probenlage Location Emploiment 1)	Snervamento Streckgrenze Yield Stress Limite elastique Rp 0,2% N/mm2	Snervamento Streckgrenze Yield Stress Limite elastique	Resistenza Zugfestigkeit Tensile strength Resistance à traction Rm N/mm2	Allungamento Bruchdehnung Elongation Allongement A5 %	Strizione Einschnürung Reduction of area Striction Z %	Resilienza Kerbschlagarbeit Impact Value Resilience KV J	Durezza Härte Hardness Dureté HB	Valori richiesti Anforderungen/Required values Valeurs demandées			
										min	max		
A	10	20	L	628	768	38	81			264	269	265	258

Test On Delivering Condition Test on delivery condition / Prüfung auf lieferbarem produkt / Test a l'etat de fourniture / Prueba sobre el material así como entregado			
TEST		min	max
A	HRc		28,0
			23,6

TEST ALLO STATO DI FORNITURA Test on delivery condition / Prüfung auf lieferbarem produkt / Test a l'etat de fourniture / Prueba sobre el material así como entregado			
TEST		min	max
A	Delta Ferrite	35,0	55,0
			48,0 %

Vicenza, 28/10/15 VCQ008 (Mod. MCE2) WSPR06EFPFD10447081001AAA3E34045	Il collaudatore di stabilimento / der Werksachverständige / Works inspector / L'agent d'usine M. Rizzotto	Pagina - 1 di 4
---	---	-----------------

Acciaierie Valbruna S.p.A.



CERTIFICATO DI COLLAUDO
ABNAHMEPRUEFZEUGNIS
INSPECTION CERTIFICATE
CERTIFICAT DE RECEPTION
EN 10204 (2004) , 3.1

36100 VICENZA (Italia) - Viale della scienza, 25 z.i.
 Telefono 0444.968211 - Fax 0444.963836
 Stab.: 39100 BOLZANO (Italia) - Via A. Volta, 4/37
 Telefono 0471.924111 - Fax 0471.924497

Cliente / Besteller/Purchaser/Client

VALBRUNA NORDIC AB
 LOVARTSGATAN 7
 65221 - KARLSTAD - SWEDEN - SE

Produttore : **ACCIAIERIE VALBRUNA S.P.A.**
 Hersteller/Item/Usine productrice

Stato di fornitura : Hot rolled Descaled Annealed Hot
 Lieferzustand / Delivery state : rolled
 Etat de livraison : rolled

QUALITY MANAGEMENT SYSTEM CERTIFIED BY LLOYD'S REGISTER

Avviso di Spedizione:
 Lieferanzeige/Packing list/B.L. D-VI15027802

Ordine nr: R31641 R31641
 Bestell Your order
 Commande

Tipo di Elaborazione: E+AOD
 Erschmelzungsart/Melting process/Mode d'elaboration

Certificato nr: MEST768512/2015/
 Prüfung/Test/Essai

Conferma ordine nr: EI15000377

Werks/Our Order/Ref nr.

Marchio di Fabbrica:
 Zeichen des Lieferwerkes
 Trade mark
 Sigle de l'usine productrice



Punzone del Collaudatore:
 Stempel des Werkassachverständigen
 Inspector's stamp/Pointon de l'essayeur

MR

1) L=longitudinale/längs, T=trasversale/quer, Q=Tangenziale/tangential										
TEST	Provetta/Probestab Specimen/Eprouvette Larg diam Specs. Breite Diam, Dicke Width Diam, Thickness Larg. diam. epais mm	°C	Posiz. Saggio Probestage Location Emplacement 1)	Resilienza Kerbschlagarbeit Impact Value Resilience KV J			Espansione laterale Lateral Expansion			Shear Shear
Valori richiesti Anforderungen/Required values Valeurs demandées		min max		45	45	45	-	-	-	-
B	10X10	-46	L	235	238	262				

Test on delivery condition										
1) L=longitudinale/längs, T=trasversale/quer, Q=Tangenziale/tangential										
TEST	Provetta/Probestab Specimen/Eprouvette Larg diam Specs. Breite Diam, Dicke Width Diam, Thickness Larg. diam. epais mm	°C	Posiz. Saggio Probestage Location Emplacement 1)	Snervamento Streckgrenze Yield Stress Limite élastique Rp 0,2% N/mm2	Snervamento Streckgrenze Yield Stress Limite élastique	Resistenza Zugfestigkeit Tensile strength Resistance à traction Rm N/mm2	Allungamento Bruchdehnung Elongation Allongement E 4d %	Strizione Einschnürung Reduction of area Striction RA %	Resilienza Kerbschlagarbeit Impact Value Resilience	Durezza Härte Hardness Dureté HB
Valori richiesti Anforderungen/Required values Valeurs demandées		min max		485	-	660 860	- 25	- 45	-	-
D	12,5	20	L	655		789	39	78		260

Test on delivery condition				
TEST		min	max	
D	HRC		28,0	23,4

Corrosion test per ASTM G48 method A [25C/24h]

Corrosion test per ASTM G48 method A [25C/24h]

TEST		min	max	
B	Weight loss		4,0000	0,1800 g/m2

Ferrite content tested according to ASTM E562.

Analisi chimica

Chemische Zusammensetzung/Chemical Analysis/Analyse chimique

Colata /Heat Schmelze/Coulée	min	31,0	-	-	-	22,00	3,00	-	4,50	-	-	0,150	-	-	-
	max	38,0	0,030	1,00	2,00	23,00	3,50	-	6,50	-	0,030	0,015	0,200	-	-
	PRE	C %	Si %	Mn %	Cr %	Mo %	Cu %	Ni %	W %	P %	S %	N %			
427440	35,3	0,021	0,41	1,50	22,24	3,12	0,38	5,72	0,051	0,030	0,003	0,168			

Material is free from intermetallic phases and precipitates
 examined at 500x magnification.

Corrosion test per ASTM G48 PRACTICE A(25C/24hrs):
 no pitting at 20x magnification.

Annealing temperature 1080°C for 1 h/water cooling.

I.Korrosion nach EN ISO 3651-2A Sensibilisierung : T1 : OK

Vicenza, 28/10/15 VCC008 (Mod. MCE2) WSP668E/FBFD184474886AAA3E5455	Il collaudatore di stabilimento / der Werkssachverständige / Works inspector / L'agent d'usine M.Rizzotto	Pagina - 2 di 4
---	---	-----------------

Acciaierie Valbruna S.p.A.



CERTIFICATO DI COLLAUDO
ABNAHMEPRUEFZEUGNIS
INSPECTION CERTIFICATE
CERTIFICAT DE RECEPTION
EN 10204 (2004) , 3.1

QUALITY MANAGEMENT SYSTEM CERTIFIED BY LLOYD'S REGISTER

36100 VICENZA (Italia) - Viale della scienza, 25 z.i.
 Telefono 0444.968211 - Fax 0444.963836
 Stab.: 39100 BOLZANO (Italia) - Via A. Volta, 4/37
 Telefono 0471.924111 - Fax 0471.924497

Cliente / Besteller/Purchaser/Client

VALBRUNA NORDIC AB
 LOVARTSGATAN 7
 65221 - KARLSTAD - SWEDEN - SE

Produttore : **ACCIAIERIE VALBRUNA S.P.A.**
 Hersteller/Item/Usine productrice

Stato di fornitura : Hot rolled Descaled Annealed Hot
 Lieferzustand / Delivery state rolled
 Etat de livraison

Avviso di Spedizione:
 Lieferanzeige/Packing list/B.L. D-VI15027802

Ordine nr: R31641 R31641
 Bestell Your order
 Commande

Tipo di Elaborazione: E+AOD
 Erschmelzungsart/Melting process/Mode d'elaboration

Certificato nr: MEST768512/2015/
 Prüfung/Test/Essai

Conferma ordine nr: EI15000377
 Werks/Our Order/Ref. nr.

Marchio di Fabbrica:
 Zeichen des Lieferwerkes
 Trade mark
 Sigle de l'usine productrice



Punzone del Collaudatore:
 Stempel des Werkssachverständigen
 Inspector's stamp/Pointon de l'essayeur

MR

Corrosion test per EN ISO 3651-2A sensitized T1 : OK
 Reduction ratio = 111,4 : 1

Allegati / Anlagen / Enclosure / Attachments :
 ME15000780

Sono state soddisfatte tutte le condizioni richieste
 Die gestellten Anforderungen sind i. Anlage erfüllt
 The material has been furnished in accordance with the requirements
 Le materiel à été trouvé conforme aux exigences

Controllo antimescolanza: OK
 Verwechslungsprüfung: spectralanalytisch durchgeführt
 Antimixing testing performed: OK
 Contrôle antimélange fait: r.a.s.

Controllo visivo e dimensionale: soddisfa le esigenze
 Besichtigung und Ausmessung: ohne Beanstandung
 Visual inspection and dimensional checks: satisfactory
 Contrôle visuel et dimensions: satisfaisant

Melted and manufactured in Italy No welding or weld repair Material free from Mercury contamination

We declare that the finished product is checked for radioactive contamination through Portal System when it leaves the production plant.

The Quality Management System is Certified acc. Pressure Equipment Directive '97/23/EC' Annex 1, s. 4.3 by TUEV and LLOYD'S

Any act of tampering, modification, alteration, counterfeiting and/or falsification and/or any other action which modifies the contents of this test certificate shall constitute a violation of applicable civil and criminal laws. Acciaierie Valbruna shall protect its rights and interests before any competent court, authority and jurisdiction.

Maximal and/or Valplus grades/products are manufactured with ladle techniques to control composition, distribution, size and shape of non-metallic inclusions for improved machinability.

The supplied product conforms to requirements expressly requested by the purchaser and conforms to requirements specified by certified norms and standards. Should the product be used for more severe, critical and/ or in any case different applications than those the material is generally intended for, any different and/or supplementary requirements shall be specifically demanded, at least, upon order of the Product by the Purchaser. Acciaierie Valbruna SpA shall not be responsible for any improper use of the Products.

<p>Vicenza, 28/10/15 VCQ008 (Mod. MCE2) <small>WSP668E/F/FPD184474886AAA3E35455</small></p>	<p>Il collaudatore di stabilimento / der Werkssachverständige / Works inspector / L'agent d'usine M. Rizzotto </p>	<p>Pagina - 3 di 4</p>
---	---	------------------------



**Acciaierie
Valbruna S.p.A.**

36100 VICENZA (Italia) - Viale della scienza, 25 z.l.
Stab.: 39100 BOLZANO (Italia) - Via A. Volta, 4

CERTIFICATO Certificate - Zeugnis - Certificat N° ME15000780 Pag 4 di 4

ESAME METALLOGRAFICO

Metallographic examination - Mikroschliff Prüfung - Metallographic

mod. ME02

Secondo :

According to - Nach - Selon

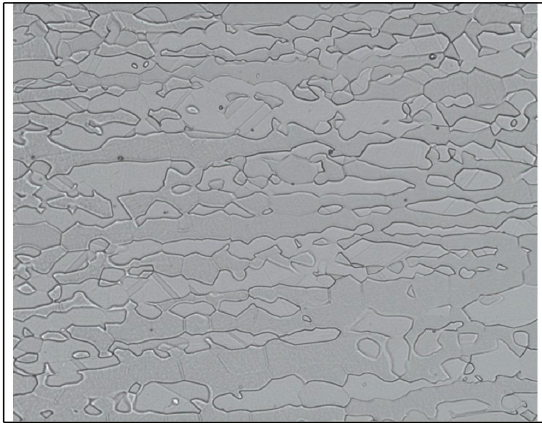
Cliente : VALBRUNA NORDIC AB

Customer - Besteller - Client

Conferma : EI15000377/0070/001

Confirmation - Bestätigung - Confirmation

MARCA	DIMENSIONI	COLATA	BARRE	PESO	LUNGHEZZA
Grade Qualität Nuance	Size Abmessungen Dimensions	Heat Schmelze Coulée	Bars Stäbe Barres	Weight Gewicht Poids	Length Länge Longueur
V225MN	Round 16,000 KG	427440		KG : 877,0	3300 3300
T. TERMICO H.Treatment Wärmebehandlung T.Termique	ESECUZIONE Condition Ausführung Execution	Condizioni Superficiali Surface Oberfläche Surface Conditions		TOLLERANZA Tolerance Toleranz Tolerance	
Annealed	Hot rolled	Descaled		Tol. as requested	



500x

ESAME MACROGRAFICO :

macrographical examination - macrographical-prüfung - examen de macrographical

NOME P.Ramina

Name - Nom

DATA : 21/10/15

Date - Date

FIRMA

Ramina P.b

COLLAUDATORE

Inspector - Abnahmesachsverst -
Inspecteur

D Material Certificate - 25Cr

Seite 1 / 2
Page



BGH Edelstahl Freital GmbH

BGH Edelstahl Freital GmbH Am Stahlwerk 1 01705 Freital

Sverdrup Steel A/S

Strandsvingen 2

4032 Stavanger
Norwegen

Kunden-Bestell-Nr. 814633
Customer order no.
Cde. no. du client

BGH-Auftrags-Nr. 34835301/193706
BGH works no.
BGH référence

Zeugnis-Nr. 409989
Certificate no.
No. de certificat

Bescheinigung über Werkstoffprüfung nach DIN EN 10204
Certificate of material tests according to DIN EN 10204 3.1
Certificat des essais des matériaux selon DIN EN 10204

Die Lieferung entspricht den vereinbarten Lieferbedingungen.
Delivery in accordance with the agreed terms of delivery.
La livraison correspond aux conditions de livraison convenues.

Zeichen des Lieferwerkes Stempel des Werksachverständigen
Trade mark Inspector's stamp
Signe du fournisseur Poinçon de l'inspecteur



Erzeugnisform Product	Stab, rund, geschält Round bars, peeled											
Werkstoff / Quality	UNS S32750											
Anforderungen Requirements	Doc.-No. 43.200.027 Rev.0 04/02 UNS S32750 ASTM A 276 - 13a UNS S32750 ASTM A 479 /A479M - 14 UNS S32750 NORSOK M 630 Edition 6 10/13 UNS S32750 NORSOK MDS - D 57 Rev. 5 10/13 UNS S32750 NACE MR 0175 ISO15156-3 2009+Cir.1:2011 UNS S32750 TR 2000 Sec. 6 MDS: D35 Rev. G 02/07 1.4410 - X2 CrNiMoN 25-7-4 DGRL 97/23/EG Anhang I, 4.3 durch NOBO 0036 F53 (UNS S32750) ASTM A182/A182M - aktuelle Ausgabe (nur Chemische Zusammensetzung und mechanische Eigenschaften) Gefertigt nach QTR_F_E_32750 nach Norsok M-650 Edition 4 PED 97/23/EG Annex I, 4.3 by NOBO 0036 F53 (UNS S32750) ASTM A182/A182M - Lat. Rev. (Chemical Composition and mechanical properties only) Manufactured acc. to QTR_F_E_32750 acc. to Norsok M-650 Edition 4											
Besichtigung und Maßnachprüfung Inspection and dimensional control Inspection et contrôle de dimension ohne Beanstandung without objection	Erschmelzung/Nachbehandlung Meltingprocess/secondary refining Mode d'élaboration/traitement ultérieure E- VOD					Verwechslungsprüfung (spectroanalytisch) Identification test (spectral-analysis) examenation d'identification(analyse spectrale) ohne Beanstandung without objection						
Pos. Item	Anzahl Quantity	Abmessung Dimension			Gewicht Weight		Schmelz-Nr. Heat-No.					
1	Bd.	16,00 RD			1616 kg		388475					
Schmelze Heat %	C	Si	Mn	P	S	Cr	Mo	Ni	Cu	N	PRE	
388475	0,024	0,25	0,80	0,024	0,0006	25,35	3,79	6,90	0,19	0,2750	42,257	
Wärmebehandlungszustand Condition of heat treat Traitement thermique	lösungsgeglüht gemäß ASTM A182 solution annealed 1127°C 87" Wasser/ water (<260°C)											
Probe-Nr. Test-No.	Lage loc.	Temp. °C	Rp0,2 N/mm ²		Rm N/mm ²	A4 %	Z %	Kerbschlagarbeit Impact value J			Probenform Shape of test piece Charpy-V °C	Hardness HRC
Soll/Req.	L	RT	>=550		>=800	>=25		>=45			-46	<=32
030HV1	L	RT	668		870	43	81	323	348	360	-46	28
Prob-Nr Test-No	Temp °C	later.Breitung mm later.expansion			Scherbruchant. % shear fracture							
030HV1	-46	2,1	2,2	2,3	100	100	100	(längs/longitudinal)				
Fertigung nach QM-System ISO 9001: 2008/ QM system in effect is ISO 9001: 2008												
Anlagen Encl. Annexe	US-Protokoll/ UT report Gefügeaufnahme/ micrograph				Freital den Place and date Lieu et date 01.09.2015				Abnahmebeauftragter Inspector representative Inspecteur de réception Kadner			
Das Zeugnis wurde maschinell erstellt und ist auch ohne Unterschrift gültig. Ce certificat a été établi sur système informatique et est valable sans signature aussi.												



BGH Edelstahl Freital GmbH

BGH Edelstahl Freital GmbH Am Stahlwerk 1 01705 Freital

Sverdrup Steel A/S

Strandsvingen 2

4032 Stavanger
Norwegen

Kunden-Bestell-Nr. 814633
Customer order no.
Cde. no. du client

BGH-Auftrags-Nr. 34835301/193706
BGH works no.
BGH référence

Zeugnis-Nr. 409989
Certificate no.
No. de certificat

Bescheinigung über Werkstoffprüfung nach DIN EN 10204
Certificate of material tests according to DIN EN 10204 3.1
Certificat des essais des matériaux selon DIN EN 10204

Die Lieferung entspricht den vereinbarten Lieferbedingungen.
Delivery in accordance with the agreed terms of delivery.
La livraison correspond aux conditions de livraison convenues.

Zeichen des Lieferwerkes Stempel des Werkssachverständigen
Trade mark Inspector's stamp
Signe du fournisseur Poinçon de l'inspecteur



Kontrolle auf Radioaktivität ohne Befund, der Messwert liegt unter der Nachweisgrenze von 0,1 Bq/g.
Radioactivity inspection without objection, the measured value is below the detection limit of 0.1 Bq/g.

Deltaferrit/ ferrite delta ASTM E562 (quer): D/2 = 51% relative Genauigkeit = 10%
Prüfung: 30 Felder/16 Punkt (30 fields of 16 points)
Ätzmittel/ Etchant: V2A + 30 % NaOH

Korros.-Test ASTM G48 Meth.A: 50°C/24h: kein Lochfraß- no pitting is observed
corrosion test Meth.A: Gewichtsverlust/weight loss: 0,027 g/m²

Längsproben/ longitudinal test specimen Prüfort-test location: D/2

Material wurde nicht reparaturgeschweißt/ Material no weld repaired.

Das Material ist frei von Quecksilber, Radium oder Alphateilchenverunreinigungen.
This material is free from mercury, radium or alpha particle contamination.

Gefüge frei von intermetallischen und anderen schädlichen Phasen.
Microstructure free from intermetallic or other detrimental phases.

Proben wurden von der Stabverlängerung entnommen x 6" Länge, gemäß ASTM A 370.
Test pieces taken from actual bar prolongation x 6" length according to ASTM A 370.

Stahlhersteller des Ausgangsmaterials: BGH Edelstahl Freital GmbH.
Steel manufacturer of starting material: BGH Edelstahl Freital GmbH.

Anlagen US-Protokoll/ UT report
Encl.
Annexe

Gefügeaufnahme/ micrograph

Freital, den
Place and date
Lieu et date
01.09.2015

Abnahmebeauftragter
Inspector representative
Inspecteur de réception
Kadner

Das Zeugnis wurde maschinell erstellt und ist auch ohne Unterschrift gültig.

This certificate was generated by data system and it is valid without signature as well.
Ce certificat a été établi sur système informatique et est valable sans signature aussi.

Ultraschallprüfung
Ultrasonic testing

DIN EN 10204 3.1

**BGH Edelstahl Freital GmbH**Kunden-Bestell-Nr. **814633**
Customer order no.
Cde. no. du clientBGH-Auftrags-Nr. **348353-01**
BGH works no.
BGH référenceZeugnis-Nr. **409989**
Certificate no.
No. de certificat

Erzeugnisform	: Stab, rund, geschält
Product	: Round bars, peeled
Werkstoff/Quality	: UNS S32750 Schmelze: 388475
Abmessung/Dimension:	16,00 RD
Anzahl/Quantity	: Bd. Gewicht /Weight : 1616 kg
Wärmebehandlungszustand	: lösungsgeglüht gemäß ASTM A182
Condition of heat treat	: solution annealed
Traitement thermique	: 1127°C 87" Wasser/ water (<260°C)
Prüfrichtlinie	
Specification	
API 6A, 20.Ed. 10/10	
PSL 3 Pkt. 7.4.2.3.15 (b)	
Bearbeitungszustand	: geschält
Machining condition	peeled
Prüfgerät	: GE ROWA B4
Test equipment	
Prüfkopf	: 4 Arrays á 90° - Radius:35 mm
	je 20 Elemente - 10 MHz
Probe	
Kopplungsmittel	: Wasser
Coupling medium	water
Prüfumfang	: vollständig
Extent of examination	completely
Einschallrichtung	: senkrecht und in Winkeleinschallung 40°
Direction of incidence	perpendicular and angle beam 40°
Registrierergrenze	: Prüfung und Justierung erfolgten gemäß obiger Spezifikation.
	50% Bezugslinie von 1,6 mm FBB
Registration level	Test and adjustment acc. to a. m. specification.
	50% of the reference line of 1.6 mm FBH
Befund	: keine registrierpflichtigen Anzeigen
Result	no reportable indications
Prüfdatum	: 28.08.2015
Examination date	

Freital, den
Place and date
Lieu et date
01.09.15Prüfer
Testing operator
Opérateur
Günther
Stufe 2 DIN EN 473 / ISO9712Abnahmebeauftragter
Inspector representative
Inspecteur de réception
JUNGKUNZ
Level III SNT-TC 1AÜberwacher
Supervisor
Surveilleur

Das Zeugnis wurde maschinell erstellt und ist auch ohne Unterschrift gültig.

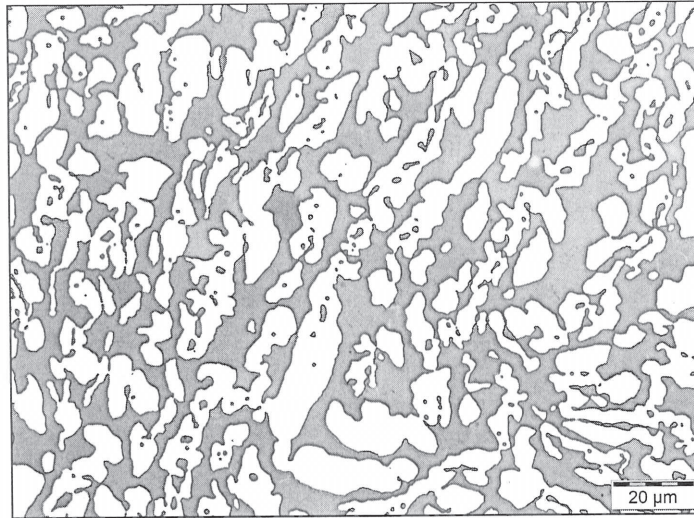
This certificate was generated by data system and it is valid without signature as well.
Ce certificat a été établi sur système informatique et est valable sans signature aussi.

Gefügeaufnahmen zum Zertifikat Nr. / Microstructure to certificate No.:

409989

Besteller/Purchaser: **Sverdrup Steel A/S**
Bestell-nr./Order-No.: **814633**
Werkstoff/Quality: **UNS S32750**
Chargen-nr./Cast-No.: **388475**
Erzeugnisform/Product: **Stab, rund, geschält / Round bars, peeled**
Abmessung/Dimension: **16,00 RD**
Komm.-nr./Work-No.: **34835301**

Proben-nr./Test-No.: **030HV1**



500:1

E Material Certificate - ATI830

 4374 Lancaster Highway, Richburg, SC 29729 US	CERTIFICATE OF TEST Cert No.99364 Rev.1	Batch - 141106
	 Terry R. Hopper/les Certification Auditor Date : February 02, 2017	Heat - C5B85 Ingot - 1

Purchase Order No	Sales Order No	Sales Order Line No
ATI 830 Alloy - Samples		

Size (in)	Size (mm)	Cross section	No Pcs	Weight (lbs)	Weight (kgs)	Alloy
0.7874	20.0000	Round	1	9	4	ATI 830TM Alloy

Specifications

Spec Name	Rev	Compliance Condition
CHEMISTRY REPORT ONLY	001	Chemistry Only

Remarks:

ATI 830TM Alloy

As Shipped Condition

Heat Treat	Heat Treat Cycles	Hot Work Type
Annealed and Cold Drawn	Heat To 2150 F (1177 °C) Hold 30 Min(s) Water Quench	Rolled

Surface Finish

Centerless Ground

Melt Method Details

Primary Melt	Facility	Address
Electric Arc Furnace/Argon Oxygen Decarburization	ATI Latrobe Operations	ATI Flat Rolled Products 242 Allvac Lane, Latrobe, PA 15650 US
Remelt	Facility	Address
Electroslag Remelt	ATI Lockport Operations	695 Ohio Street, Lockport, NY 14094 US

Conversion Method Details

Conversion Type	Facility	Address
Rolling	ATI Richburg Operations	4374 Lancaster Highway, Richburg, 29729 US

Batch - 141106

Heat - C5B85

Ingot - 1

CHEMISTRY

Test Facility			ATI Monroe Operations
Sample Source			Heat Avg
Elements	UOM	Method	Average
Al	%	XRF	0.020
Co	%	XRF	2.648
Cr	%	XRF	21.608
Cu	%	XRF	1.181
Mn	%	XRF	4.384
Mo	%	XRF	5.106
Nb	%	XRF	<0.01
Ni	%	XRF	29.993
P	%	XRF	0.0157
Si	%	XRF	0.238
Ti	%	XRF	<0.01
V	%	XRF	0.036
W	%	XRF	0.698
Fe	%	XRF	34.0658
Al+Ti	%	XRF	0.020
Ni+Co	%	XRF	32.642
Al+Ti+W	%	XRF	0.718
C	%	CS	0.004
S	%	CS	<0.0003
N	%	GAS	0.393
B	%	OES	0.0021

Remarks:

CS = Combustion/IR Detection
 GAS = Inert Gas Fusion
 OES = Spark Optical Emission
 XRF = X-Ray Fluorescence
 WET = Inductively Coupled Plasma Emission

Test Facility			ATI Monroe Operations
Sample Source			Ladle
Elements	UOM	Method	
Pb	PPM	WET	<1
Sn	PPM	WET	12

Remarks:

WET = Mass Spectroscopy

MECHANICAL

As Shipped

Tensile

Piece ID	Sample Direction	Test Temperature	Ultimate Strength	Ultimate Strength	.2% Yield Strength	.2% Yield Strength	4D-Elongation (%)	Reduction of Area (%)	Initial Gage Length	Initial Diameter	Crosshead Speed	Strain Rate (in/in/min)	Test Facility
1	L	ROOM	183.6 ksi 1265.9 MPa	183,597 psi 1266 MPa	168.2 ksi 1159.7 MPa	168,177 psi 1160 MPa	21.6	72.8	2 in 51 mm	0.504 in 12.802 mm	.05	.003	ATI Monroe Operations
1X	L	ROOM	180.9 ksi 1247.1 MPa	180,879 psi 1247 MPa	165.3 ksi 1139.7 MPa	165,304 psi 1140 MPa	21.9	72.9	2 in 51 mm	0.504 in 12.802 mm	.05	.003	ATI Monroe Operations

Remarks:

L = Longitudinal
 ASTM EB/E8M (2016a)
 Results reported for information only.

Hardness

Piece ID	Sample Location	Hardness Value (Rockwell)	Hardness Type	Test Facility
1	NS	41	HRC	ATI Monroe Operations
1	NS	40	HRC	ATI Monroe Operations
1	MR	40	HRC	ATI Monroe Operations
1	C	39	HRC	ATI Monroe Operations
1X	NS	41	HRC	ATI Monroe Operations

continued...

Batch - 141106 Heat - C5B85 Ingot - 1

Piece ID	Sample Location	Hardness Value (Rockwell)	Hardness Type	Test Facility
1X	NS	40	HRC	ATI Monroe Operations
1X	MR	40	HRC	ATI Monroe Operations
1X	C	37	HRC	ATI Monroe Operations

Remarks:

NS=Near-Surface
 MR = Mid-Radius
 C = Center
 ASTM E18 (2016)
 Results reported for information only.

Charpy

Piece ID	Sample Direction	Sample Location	Test Temperature	Sample Size (None)	Ft/Lbs Energy (ft/lbs)	Specimen Type	Striker Size	Test Facility
1	L	C	ROOM	Standard (10mm X 10mm)	218	V	8 mm	ATI Monroe Operations
1	L	C	ROOM	Standard (10mm X 10mm)	207	V	8 mm	ATI Monroe Operations
1	L	C	ROOM	Standard (10mm X 10mm)	187	V	8 mm	ATI Monroe Operations

Remarks:

L = Longitudinal
 C = Center
 ASTM E23 (2016b)
 Results reported for information only.

Outside Source Addresses

Outside Testing Laboratory

Facility	Address
ATI Monroe Operations	2020 Ashcraft Avenue, Monroe, NC 28110 USA

Remarks

Material has been produced, sampled, inspected and tested in accordance with the acknowledged customer purchase order and referenced specifications and conforms to the requirements unless otherwise noted in this Certificate of Test or in other communications regarding purchase order clarifications, specification exceptions, or long term agreements.

If customer purchase order does not specifically reference a revision to a specification, ATI Specialty Materials will work to the latest revision on file and in effect at the time of order placement.

ATI Specialty Materials has complied with all producer requirements of AS6279.

Any chemical elements analyzed and found to have values below the actual limits of detection may be reported as < less than or reported at the detection level.

When values are reported to the significant places called for in the specifications, rounding will be done in accordance with ASTM E29.

This is to certify that during the manufacturing, handling, testing and inspection, this material did not come in direct contact with mercury or any device employing a single boundary of containment.

ATI Specialty Materials products have not come in contact with radioactive materials during manufacturing or processing.

No weld repair has been performed on this material.

Material melted and manufactured in the United States of America unless otherwise noted in this Certificate of Test.

Material Safety Data Sheets (MSDS) - View or print from our site: www.atimetals.com
 Printed copies are available upon request from the ATI Specialty Materials Sales Department.

ATI Specialty Materials certifies that it has procedures in place to provide reasonable assurance that any non-scrap/non-recycled Conflict Minerals (Columbite-Tantalite/Coltan and its derivative metal Tantalum; Cassiterite and its derivative metal Tin; Wolframite and its derivative metal Tungsten; and Gold) included in the materials supplied under this purchase order do not originate from the Democratic Republic of Congo or specified adjoining countries (Covered Countries) as defined by and in accordance with Section 1502 of the Dodd-Frank Wall Street Reform and Consumer Protection Act of 2012. ATI Specialty Materials will provide a CMRT form annually upon request.

The recording of false, fictitious, or fraudulent statements or entries on this document may violate Federal statutes, including but not limited to Title 18, Chapter 47 of the United States Code and may be punishable as a felony.

This Certificate of Test shall not be reproduced, except in full, without the written approval of ATI Specialty Materials Quality.